The effect of IMC bus charging behavior on the trolleygrid

Rik Eggermont

MSc Thesis

TU Delft

The effect of IMC bus charging behavior on the trolleygrid

by

Rik Eggermont

to obtain the degree of Master of Science
at the Delft University of Technology,
to be defended on Thursday February 25, 2021 at 14:00.

Student number:	4013727
Project duration:	December 1, 2019 – February 18, 2021
Thesis committee:	Prof. dr. ir. P. Bauer
	Dr. ir. G. R. Chandra Mouli
	Dr. M. Cvetkovic
	Ir. I. Diab

Cover picture taken from `https://www.knorr-bremse.com/en/magazine/forever-young-trolleybuses-offer-a-green-solution-for-public-transport.json`.

An electronic version of this thesis is available at `http://repository.tudelft.nl/`.

TU Delft

Preface

My journey at TU Delft started with a bachelor in Aerospace Engineering as I always had a burning passion for technology. My other passion is to build a more sustainable future. With the master Sustainable Energy Technology I was able to combine both.

When searching for a thesis topic I found out about this emerging technology called IMC. After a first discussion with Ibrahim about this topic I knew I wanted to write my thesis about it. Writing this thesis felt like a giant leap for me personally and professionally. With this work I hope to give the implementation of IMC buses one small step in the right direction. Towards a more sustainable future.

I want to thank Prof.dr.ir. Pavol Bauer and Dr. Milos Cvetkovic as committee members for providing me with this opportunity to graduate. I want to thank my supervisor, dr. ir. Gautham Ram Chandra Mouli, for guiding me through the process of creating my thesis by defining the outline and endpoint of my thesis. I want to thank dr. ir. Aditya Shekhar who helped me out with defining my thesis as well as providing valuable feedback on the first part of my thesis. A special thanks goes to my daily supervisor Ibrahim Diab. A great mentor that kept me motivated all throughout this journey by showing me what to focus on and always making time for technical discussions. I want to thank my friends and family and of course my girlfriend Wieke who supported me along the way. To all who I mentioned, to all readers, and to anyone I might have forgotten to mention: Thank you for your support.

Rik Eggermont
Leiden, February 2021

Abstract

We are in the middle of a transition to zero-emission mobility. The European Union has set high targets for zero-emission bus sales. Many European local governments and public-transit operators are looking to replace their GHG-emitting diesel/gas bus fleets with clean alternatives. One such alternative is In Motion Charging (IMC) technology for trolleybuses. With this technology trolleybuses are able to charge an on-board traction battery whilst in motion and connected to the overhead wires. This makes it possible for these buses to extend their range outside the trolleygrid infrastructure. These IMC buses can replace diesel/gas buses.

IMC is of particular interest for municipalities that currently have a functioning trolleybus fleet and infrastructure. Existing infrastructures are however not built with the increased power demand of IMC buses in mind. A good understanding of the power demand of IMC buses and the limits of a trolleygrid is necessary before implementing IMC buses.

The explanatory research that is presented in this report aims to give insight in the design factors that influence the feasibility of adding in-motion charging buses to an existing trolleybus network. It does so by first explaining the difference in energy consumption between IMC buses and regular trolleybuses through simulations. Next, by performing a case study on the Arnhem trolleygrid the effect of IMC buses on the trolleygrid is discovered.

The results of the energy consumption comparison indicate that there is promising potential for IMC implementation. It shows that there is a large margin in which IMC buses can make more efficient use of their regenerative energy compared to their regular trolleybus counterparts. It also shows that there are large degrees of freedom in IMC bus implementation leaving room for errors. The Arnhem case study uncovers where exactly these errors lie by looking at potential power demand, minimum voltage and maximum current limit breaches on the network. As long as these breaches can be mitigated through smart charging strategies there is a lot of promise for IMC bus implementation on existing trolleygrid infrastructures.

Contents

List of Tables

List of Figures

1 Introduction

This chapter gives an introduction to trolleybuses, the Trolley:2.0 project and the In Motion Charging concept for trolleybuses. The chapter also provides an explanation of the problem statement and research questions of this thesis. At the end of the chapter a layout of the thesis is shown.

1.1. A brief trolleybus history

The market for electric buses is rapidly growing [23]. Public-transit operators and local governments all over Europe are looking to replace diesel/CNG buses and other polluting alternatives in favour of the e-bus. Figure 1.1 shows an example of an e-bus. These replacements can be seen as the result of member states of the European Union setting high targets for zero-emission bus sales. These targets are set at 75% by 2030 for 13 (including the UK which has since left the EU) of the 28 countries with other member states targeting between 43% and 71% of total bus sales [19]. By setting these targets an annual increase of 18% is expected for e-buses in Europe.

Figure 1.1: An e-bus with on-board battery. It is connected to the grid with its pantograph in order to charge the battery. It has to remain stationary in order to charge. [1]

One of the reasons that make this growth possible is the availability of affordable on-board traction batteries. In recent years a lot of European municipalities are transition their traditional ICE bus fleet to e-buses (i.e.

buses with on-board batteries which are charged overnight or throughout the day). That being said, the electric city bus has already had its first number of successful implementations almost a century ago [14] without on-board storage. At that time trams in the UK were blamed for increasing city congestion and were replaced by trolleybuses which quickly got the reputation of being reliable and comfortable compared to buses with internal combustion engines (ICEs). In the century that followed the utilisation of electric trolleybuses has seen its ups and downs with some countries abandoning them entirely (e.g. UK and Spain) while others embracing them (e.g. Russia and China). Large reasons for UK cities to abandon trolleybuses in favour of ICE buses were the cost of implementation and the lack of flexibility.

By combining the concept of a trolleybus and e-bus this lack of flexibility can be circumvented. This combination, which is called In Motion Charging, could emerge as a good alternative to other zero-emission bus concepts. This is especially the case for cities that currently have a trolleygrid infrastructure in place. Just as the name implies this concept combines a trolleybus with an on-board battery which makes it possible for the battery to charge while the bus is in motion. This combination allows for smaller batteries compared to regular e-buses which can only charge while stopped.

1.2. Trolley:2.0 project

This thesis is part of the Trolley:2.0 project's objectives. A lot of European countries have policies in place to continually evolve their cities' transportation networks, choosing the best option for each route [15]. Research initiatives funded by European governments help in deciding which emerging technologies are suited for implementation. The recent availability of on-board batteries could quickly result in European cities adopting a new and improved version of trolleybuses. The trolley:2.0 project is such an initiative that will investigate the usefulness of this IMC concept.

The trolley:2.0 project ran from April 2018 until September 2020 with a €3 million budget. The project aim was to prove the extent with which this new type of bus can be key in providing zero-emission public transport for public areas [18]. The trolley:2.0 team consists of nine partners. Two of those are industry partners PRE[32] and evopro Group[20]. Another two are public transport operators BBG[6] and SZKT[34]. One of the partners is international action group trolley:motion[38]. The remaining four are research partners TU Dresden [40], University of Gdansk[41], University of Szeged[42] and TU Delft[39].

Besides IMC the trolley:2.0 project also looks at other technologies to integrate with the trolley grid infrastructure. The other areas are: integration of renewable energy sources, innovative energy storage systems and multi-purpose charging infrastructure [38]. The trolley:2.0 project includes several key areas: increasing energy efficiency, range extension, economical evaluation and public acceptance of battery supported trolleybuses and integrating other electric mobility services as part of the smart trolley grid. Figure 1.2 shows the specific subprojects that are part of the trolley 2.0 project. These subprojects will be demonstrated inside existing trolley grid networks of the cities of Arnhem, Szeged, Gdynia and Eberswalde.

1.3. The concept of In Motion Charging

This thesis will investigate the viability of replacing CNG and diesel buses buses by zero-emission IMC buses. IMC is a relatively new type of technology in the family of electric bus technologies. Bartłomiejczyk [9] presents the concept of In Motion Charging (or Dynamic Charging) as one of the classifications for charging electric vehicles. The classifications can be divided based on charging strategies as well as charging methods. Four charging strategies that are considered feasible for electric buses are[9]:

1. Night charging at low power
2. Night charging at low power with recharging during the day at medium to high power charging stations
3. Fast charging at end stations with high power
4. Dynamic charging (or In Motion Charging, IMC)

Four charging methods are shown in Figure 1.3. They are [9]:

1. Plug-in connector

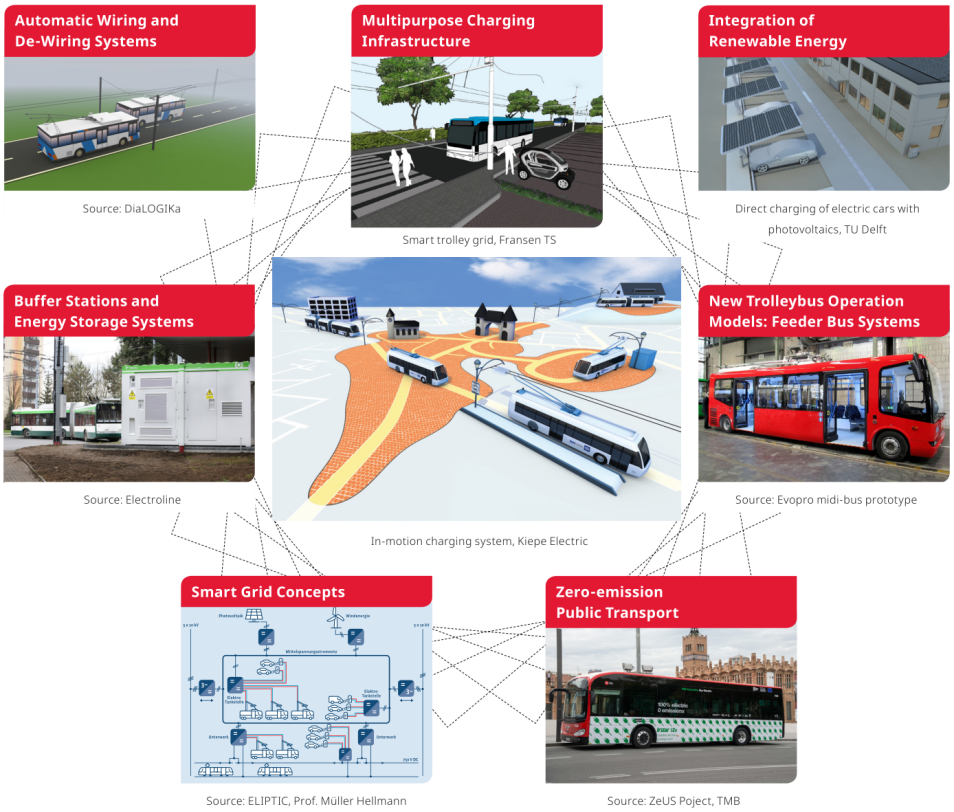

Figure 1.2: A visual overview of the subprojects of the trolley:2.0 project [38]

2. Four-pole system
3. Two-pole system
4. In motion charging (IMC)

The charging strategy of dynamic charging can only be implemented by the use of the IMC method. This method uses a combination of two-pole charging with trolleybus technology. As such the traction battery of the bus can be charged on parts of the route which are covered with an overhead line (Figure 1.4). The other parts of the route can then be covered in battery mode.

This strategy combines advantages of both trolleybuses and battery buses. The bus does not have to stop in order to be charged while the capacity of the battery can be decreased by increasing the section of the route covered by overhead lines. The on-board traction battery provides flexibility in multiple ways. Range extension provides huge flexibility in routes outside the trolley grid, as well as the possibility to remove overhead lines from architectural critical areas [38]. Emergency detours that would otherwise be performed with an auxiliary diesel power unit can also be performed emission-free. The flexibility also extends to city planning. Placement of overhead lines does not define the bus route for many years to come. Instead, placing overhead lines strategically on high bus traffic charging corridors makes it possible to flexibly change bus routes for many years to come.

The use of a trolley grid infrastructure (compared to overnight or opportunity charging) provides several efficiency benefits. IMC has the advantage of not interfering with the bus schedule. While opportunity charging buses will have to stand still at charging stations the IMC bus can stay on the move which prevents delays. Charging overnight also has this benefit but has the downside of a heavier battery to compensate for it. This increase in mass results in a higher energy consumption. A counterpoint to this argument is that the on-board energy storage can be used to store regenerative braking energy so potentially less energy is wasted. The increase in charging power that is necessary for opportunity charging often also results in mass increases as a larger dc/dc battery converter is needed.

Figure 1.3: Examples of different charging methods. (Top left) Plug-in connectors are typically used for overnight charging. (Top right) Four-pole systems are typically used for fast/opportunity charging. (Bottom left) Two-pole systems are typically used for low to medium charging speeds. (Bottom right) A regular trolleybus connected to the grid. With the right internal adjustments (i.e. adding a traction battery) trolleybuses can be converted to IMC buses. [9]

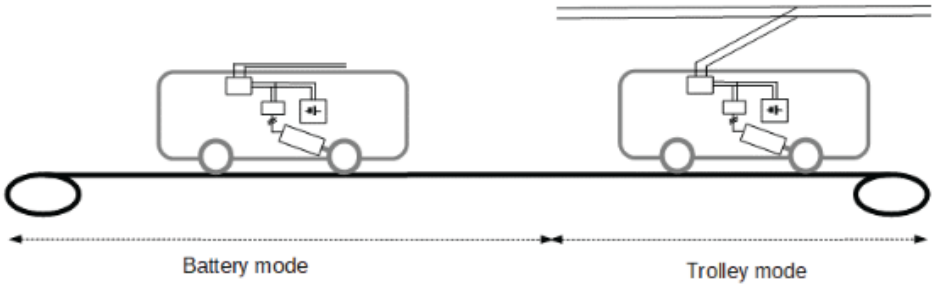

Figure 1.4: Dynamic charging system concept [9]

1.4. The trolleygrid

A large part of the research performed for this thesis revolves around the impact of IMC buses on the (Arnhem) trolleygrid infrastructure. These trolleygrids were to supply power to regular trolleybuses which can have power demand peaks of 300 kW while accelerating and will on average demand 70 kW. With IMC buses a battery charging power that can range from around 100 kW to 300 kW is added to that. Research should indicate where current trolleygrids fall short in supplying this additional power. A good understanding of the trolleygrid is required for this.

A trolleygrid consists of a large amount of separated sections of overhead lines. An individual section or Small group of sections is connected to a substation through separate feed-in cables. These substations convert AC power from the power grid to DC power for the trolleygrid. The length of each individual section typically ranges from 500 to 1000 [m]. Most sections consist of a set of parallel lines as buses need to pass each other from either direction.

Trolleybuses are able to share any power generated through regenerative braking with other buses on the same section that need it. To benefit more from this trolleygrids can make use of bilateral connections. Contrary to a stand-alone unilateral section this concept connects sections with each other. This new longer section now also has two feed-in points, hence the name bilateral connection.

1.5. Problem statement

Being able to replace all GHG emitting buses in a city with trolley grid infrastructure by zero-emission IMC buses through range extension can reduce the amount of CO_2. CNG buses are taken as an example as these are the GHG emitting buses used in Arnhem. CNG buses emit an average of 1.3 [kg/km] of CO_2 [31]. The average public transit bus in the Netherlands travels 72704 [km] per year (2019 value taken from [3]). This means that a CNG bus in the Netherlands approximately emits 95 tonnes of CO_2 per year. So for every CNG bus in Arnhem replaced by an IMC bus this is the approximate amount of yearly CO_2 emission reduction assuming the electricity is generated in a renewable way.

Implementation of this replacement of CNG buses with IMC buses is not so straightforward. For this thesis six parameters have been defined that have an effect on IMC bus performance. The six parameters can be divided in three bus parameters:

- Average velocity: the average velocity the bus is moving at in [m/s].
- Battery size: the capacity of the battery in [kWh].
- Energy consumption: the amount of energy consumed by the bus in [kWh/km].

And three city parameters:

- City topography: the topography of the city specifically measured by looking at road slope.
- Coverage length: the (relative) length of the charging corridor (i.e. the part of the trip where the IMC bus is covered by overhead wires) which can be measured in [km] or as a percentage of total trip length.
- Charging power: the amount of [kW] at which the on-board battery is charged.

These parameters can all have an influence on each other. Finding an energy and cost efficient combination of these parameters can only be done with a thorough understanding of these influences.

For a successful implementation of IMC buses for range extension two main issues have to be kept in mind. First, the bus batteries should not deplete before completing a full day of round trips even in worst case conditions. Next to that, the high power demand of IMC buses should not interfere with the power demand of other buses on the trolley grid. Research into the effects of the aforementioned parameters and resulting charging strategies is necessary to appoint these issues. This makes it so that the problem statement is two-fold:

> *Problem statement: Determine the feasibility of the introduction of IMC trolleybuses as a replacement of diesel/CNG buses.*

1.6. Research Questions

The explanatory research that is presented in this report aims to give the reader insight in the design factors that influence energy efficiency when adding IMC buses to an existing trolleybus network. The first parameter discussed is the average velocity of the bus while under the overhead lines. This is done by performing simulations on a MATLAB bus model. To further investigate the charging power, coverage length and energy consumption a MATLAB model of the Arnhem trolleygrid was used. This can be seen as the main part of the thesis. This Arnhem trolleygrid model is used to perform a case study. In this case study, bus routes that are currently covered by fossil fuel (compressed natural gas) consuming buses are replaced by IMC buses that draw their power from the trolleybus supply system.
Compared to regular trolleybuses it is hypothesised that the power and energy demand will increase so much that the supply system will have to be upgraded. These upgrades should make sure that transmission losses stay within limits and the overall capacity of the overhead lines and supply infrastructure will be enough to meet the increased demand. To test this hypothesis a good understanding of the IMC bus power/energy consumption, of its charge behaviour, and of the trolleybus supply system is needed.

In order to simulate the power demand of these buses an IMC bus model should be developed. This model can then be used for dynamic simulations to see the power demand of the bus at any point in time. Compared to regular trolley buses these IMC buses will draw more power individually to charge the on-board energy storage. On top of that, the on-board energy storage will add weight to the bus which negatively affects transport efficiency. This means that compared to a regular trolleybus the power and energy consumption will most likely increase. For modelling the bus it is therefore important to know what these consumption patterns will look like.

Apart from these consumption patterns it is also important to understand the limitations that IMC buses have. The degree of coverage by overhead lines will be different for every route. If this coverage ratio is too small the battery will not charge sufficiently to power the bus on the autonomous section of the route. The size of the battery and the maximum charging power are factors in determining the minimum coverage ratio.

All these considerations are summed up in the first research question, which is:

RQ1: What is the difference in energy consumption between IMC buses and regular trolleybuses?

RQ2 looks at the effect of IMC bus charging behaviour on the trolleygrid by simulating a full year of operation on the Arnhem trolleygrid. Parameters that will only be discussed without further investigations are average velocity and city topography. City topography can be simplified to road slope. The amount of power necessary to go uphill will naturally be higher than going downhill, but the effect this has on charging is still undiscovered. Although these two parameters do have influences on the others and can be of interest, they are no design parameters. What is meant by that is that when considering a certain city for IMC implementation the topography and average velocity (which is based on the city traffic) are fixed. This in direct contrast with the other parameters: battery size, energy consumption, coverage length and charging power.

The battery size will have an impact on the mass of the bus and the amount of energy that the bus can store. Energy consumption is a variable that is based on multiple factors. However, primary factors are the mass of the bus and its passengers which has a direct impact on the traction power demand and the amount of heating that the HVAC system of the bus demands. To account for the variation of mass and HVAC the bus models will include variations of traction power and HVAC demand based on battery and passenger mass and ambient temperature respectively.

The coverage length is limited by the amount of energy that is needed for each round trip. If the amount of energy that can be picked up while inside the charging corridor is lower than the amount of energy that is used while not connected to the overhead lines the amount of round trips that can be performed each day would be limited. Therefore, the coverage length should be large enough to make sure that a bus can perform its round trips for a full day after which it can charge back to full in the bus depot. There might however be other reasons for increasing the length. In this case study the coverage length is fixed. However, by performing simulations for various charging powers on each separate section it can be found out if charging can be turned off for some of the sections, effectively decreasing the coverage ratio.

The charging power which is arguably the most interesting parameter. The first thing to note here is that the charging power limit in practice will most often not be limited by the battery, but by the grid and more importantly the contact point of overhead line and catenary. As the contact point can overheat when subjected to high currents, a strict limit should be maintained. This limit should be lower while the bus is stopped as the conditions for cooling while stopped are less ideal. Next, the amount of power that the supply system can offer is limited which might mean that two buses on the same supply section charging or accelerating at the same time can hinder each other. This is already a problem with two regular trolleybuses accelerating at the same time. In the case study several different combinations of charging power while stopped and while moving will be discussed and investigated.

Together these four parameters will be the subjects in this case study on the Arnhem trolleygrid. Furthermore the effect on the trolleygrid is evaluated by looking at the power demand, minimum voltage and maximum current on each substation and/or section. A MATLAB model of the Arnhem trolleygrid is used for this. The case study will also serve as a means of verification of the results from research performed on the IMC bus model. As an expansion on the research performed this case study will give more insight on what happens when other trolleybuses are on the same charging section as an IMC bus.

The question posed for this second research question is:

RQ2: What is the effect of IMC buses on the trolleygrid? (Arnhem case study)

1.7. Thesis Layout

The chapters of the thesis are as follows:

- **Chapter 1**

  Introduction to IMC trolleybus technology and the research objective of this thesis.

- **Chapter 2**

  Literature review which discusses past research performed on IMC technology.

- **Chapter 3**

  Methodology of the thesis which includes a general overview, explanations of the tools (i.e. models) used and descriptions of the experiments performed.

- **Chapter 4**

  Results and discussion of the individual bus model simulations.

- **Chapter 5**

  Result and discussion of the Arnhem case study.

- **Chapter 6**

  Conclusion and recommendations for future works.

2

Literature review

This chapter discusses relevant literature on this thesis' research topics. The first two sections are more general takes on the current position of IMC in the electric bus landscape. These sections will mention the energy efficiency and cost comparison. The third section is about modelling electric vehicles. The fourth and final section goes more in depth on the specific research of this thesis. The section discusses literature about the six bus and city parameters that are mentioned in this thesis.

2.1. Energy efficiency

As the application of IMC buses is relatively new, a lot of research is done on its viability. Both energy and cost viability are therefore often found in recent literature about IMC buses. Bartłomiejczyk and Połom [10] describe the spatial aspects of trolleybus supply systems regarding energy saving. Transmission losses in overhead lines of trolleybus systems can reach values of 30%. Energy recuperation through regenerative braking can be ineffective when recuperated energy is unable to reach another bus that needs this energy at the same time. Two ways of saving energy are therefore reducing transmission losses in the supply system and making better use of regenerative braking by supplying this energy to other buses on the same overhead line section. An example of regenerative braking can be seen in Figure 2.1.

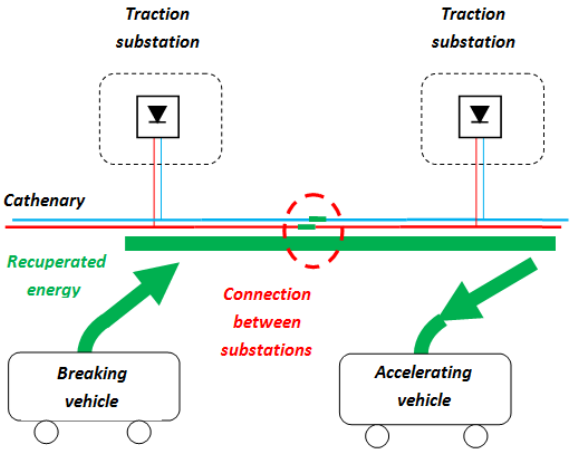

Figure 2.1: A diagram of a braking bus and accelerating bus on the same section. By using the electric motor for braking the braking bus is regenerating energy which flows to the accelerating bus. The electric motor of the accelerating bus converts this energy back to traction power. [8]

The paper bases its results on voltage and current measurements taken at the traction substations and inside the vehicles of the Gdynia trolleybus network. The results show that recuperation effectiveness increases with the amount of vehicles in the same supply area. Furthermore the results correctly indicate that higher transmission losses occur with longer feeder lines and higher traffic intensity. This is the result of these losses being proportional to the resistance and the square of the current according to Joule's first law (Equation 2.1).

$$P_{\text{losses}} \propto I^2 R \tag{2.1}$$

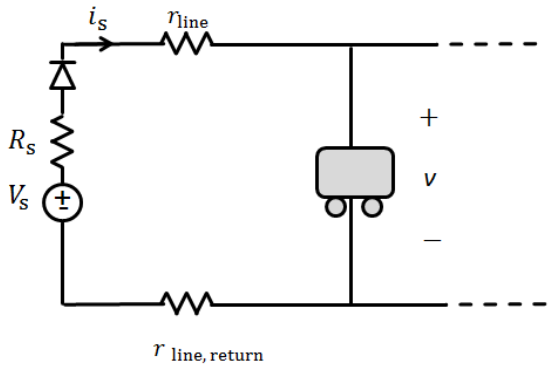

Figure 2.2: A diagram of a trolleybus connected to the substation (voltage source) through the overhead line. The line resistance increases with distance and current increases with load. The transmission losses. Transmission losses can be calculated based on the line resistance and current.

In the case of IMC buses the on-board battery can make near-optimal use of the buses own regenerative braking power which makes that part of the paper irrelevant. Transmission losses on the other hand will have an even higher impact for IMC buses given that they will draw a higher average current compared to regular trolleybuses in order to charge the battery.

In another paper by Bartłomiejczyk [8] the bilateral supply system is presented. With this form of supply system the power is supplied at two places for each section compared to one in a unilateral supply system. This is either performed by connecting two substations to one section or by using cable feeders to connect one substation to two points of the section. This splits up the vehicle current in two smaller load currents so theoretically transmission losses should decrease based on their proportionality (Equation 2.1).

Both configurations were tested at the Gdynia trolleybus network on three different sections. It resulted in increased recovery effectiveness, decreased transmission losses, and a decrease in voltage drops. This proves that conversion to a bilateral supply system is an effective method of saving energy. Again, the higher current that IMC buses will draw might urge the necessity of this type of improvement.

2.2. Cost comparison and efficiency

The economic rundown of Bedell [11] of a rapid charging hybrid (RCH) bus does not mention dynamic charging as an alternative. A rapid charging hybrid bus is however similar to it as instead of having sections of the route for charging it just has rapid charging at the end of the route. The paper compares this proposed RCH technology to other bus types. It most notably mentions the smaller battery size necessary compared to a 100% electric bus as it is charged each round trip instead of at the end of the day. This same benefit is the case for IMC buses. Next, comparing it to trolleybuses and trams the obvious benefit is not having to invest in the expensive overhead lines and electrical infrastructure.

Another not completely similar, but related, technology is wireless dynamic charging. Jeong et al. [25] gives a comparison of stationary charging at the end of the route and dynamic charging on multiple sections of the route with an economic model. They hypothesise that the shallow and frequent charging that is performed in dynamic charging is very beneficial to battery lifetime. A case study in Gumi, a city in South Korea, showed an expected 20.8% cost reduction when choosing dynamic charging. While the charging infrastructure 'power tracks' would be an extra investment, the reduction in battery cost can more than make up for it.

As one of the potential uses of IMC buses is the replacement of diesel and gas buses by utilizing the IMC range extension property it is interesting to take a look at a case study of the cost effectiveness of this. The paper Keskin [26] gives an economic comparison of (current) diesel buses and (possible replacement) trolleybuses in the city of Istanbul for a Bus Rapid Transit (BRT) system. What is meant by BRT system is one or multiple

Table 2.1: Comparison of vehicle costs per km between trolley and diesel buses in 2006 in Solingen, Germany [28]

	Trolleybus (no recuperative braking)	Trolleybus (with recuperative braking)	Diesel bus
Specific costs per km			
Personnel (driver)	Neutral	Neutral	Neutral
Operation costs	€ 0.23	€ 0.15	€ 0.59
Maintenance	€ 0.27	€ 0.27	€ 0.31
Capital costs	€ 0.22	€ 0.22	€ 0.15
Other costs			
Vehicle costs per km (sum of specific costs)	€ 0.72	€ 0.64	€ 1.04
Infrastructure	€ 0.36	€ 0.36	€ 0.00
Vehicle costs incl. Infrastructure	€ 1.08	€ 1.00	€ 1.04
	100%	93%	96%

bus lines which has/have the same capacity and speed of transit as a subway or tram connection. It was found that the trolleybuses benefit from the high energy efficiency and low electricity costs when compared to diesel buses even when factoring in the investment costs for charging infrastructure. They also of course have the added benefit of lower environmental impact even when factoring in the life cycle emissions that are mostly from manufacturing the trolleybuses.

The paper by Kühne [28] compares vehicle costs including infrastructure between three types of buses that all operate in the same city of Solingen in 2006. The comparison was made between the diesel bus, and trolleybuses with or without braking energy recuperation. In this comparison the buses with braking energy recuperation make use of on-board super-capacitors. Table 2.1 reveals that specific vehicle costs of diesel buses are higher.

Firstly this is because of higher operation costs because diesel fuel is a more expensive energy source than electrical energy. Maintenance on diesel buses is also more expensive which is largely because of the increased wear on the (gears of) the combustion engine compared to the gear-less electric engine and because electric engine braking diminishes the wear on conventional brakes. However, capital costs for the trolleybus vehicle is higher and adding the cost of infrastructure to the trolleybus the costs swing back in favour of diesel. The bottom line of this comparison shows that costs of diesel buses can be 4% lower than costs traditional trolleybuses. Costs of trolleybuses with recuperative braking are lower and are only 93% of traditional trolleybus costs.

2.3. Electric vehicle modelling

As this thesis revolves around performing simulations with an IMC bus model it is important to maintain accuracy while also being able to perform the simulations in a timely manner. The paper of Chymera et al. [16] introduces a modelling method for light rail traction systems. The conventional technique for simulating power flow, shown in Figure 2.3, is considered inadequate for comparing the efficiency of different light rail transit systems. External factors (e.g. traffic) have an effect on vehicle movement in street running systems which makes mathematical modelling of the movement difficult. This can be diverted by using vehicle movement as an input. Movement data measured on existing vehicles can then be used for comparing different transit systems. In Figure 2.4 this modelling technique is visualised. The article states that this new modelling method is suitable for comparing upgrades to existing networks regarding the energy efficiency when measured drive-cycle data is provided.

Furthermore, the paper looks at both the modelling of the vehicle dynamics as well as the electrical network. The power requirements of the engine are calculated by considering that the force required to drive the vehicle is given by adding frictional forces and changes to potential and kinetic energy. From this the mechanical torque is obtained which together with the angular velocity of the wheels gives the drive-line power. Adding gear, friction and windage losses then gives the total motor power. Inverter power loss and auxiliary load are added to this to obtain the total power requirement of the vehicle. The current of the vehicle can then be determined by dividing the total power by the vehicle voltage. The electrical network that consists of sub-

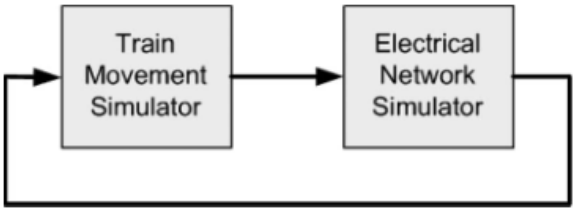

Figure 2.3: Conventional modelling technique for the power flow of light rail transit systems [16]

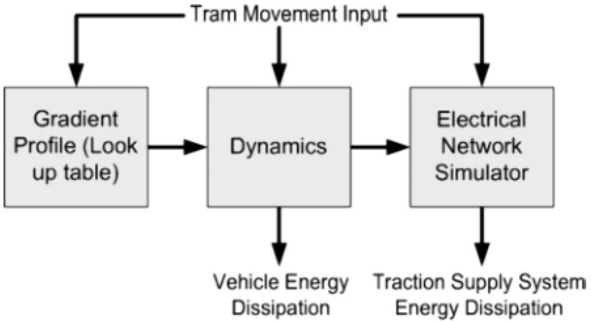

Figure 2.4: Adapted modelling technique for the power flow of light rail transit systems [16]

stations, supply and return resistances, and vehicles has to be reconfigured at each simulation time step as the location and power demand of vehicles changes. The paper also analyses the use of on-board storage for regenerative braking by adding an ultra-capacitor to the vehicles. This can result in significant power consumption decreases especially in the case of frequent start-stop cycles.

Combining IMC bus model with a supply system model is necessary in order to simulate the effects on the trolleygrid. The book Bartłomiejczyk [9] mentions this type of modelling and combines it with the Monte Carlo method to see what happens with multiple buses on one supply section. In Figure 2.5 this model is visualised with the use of a diagram. The diagram most importantly shows that although the buses have some current as input, the model at a later point might have to lower the current that goes to each bus if the supply section reaches its limits. This lowering of currents is an iterative process for each time step that halts when the voltage level is lower than the maximum allowed value.

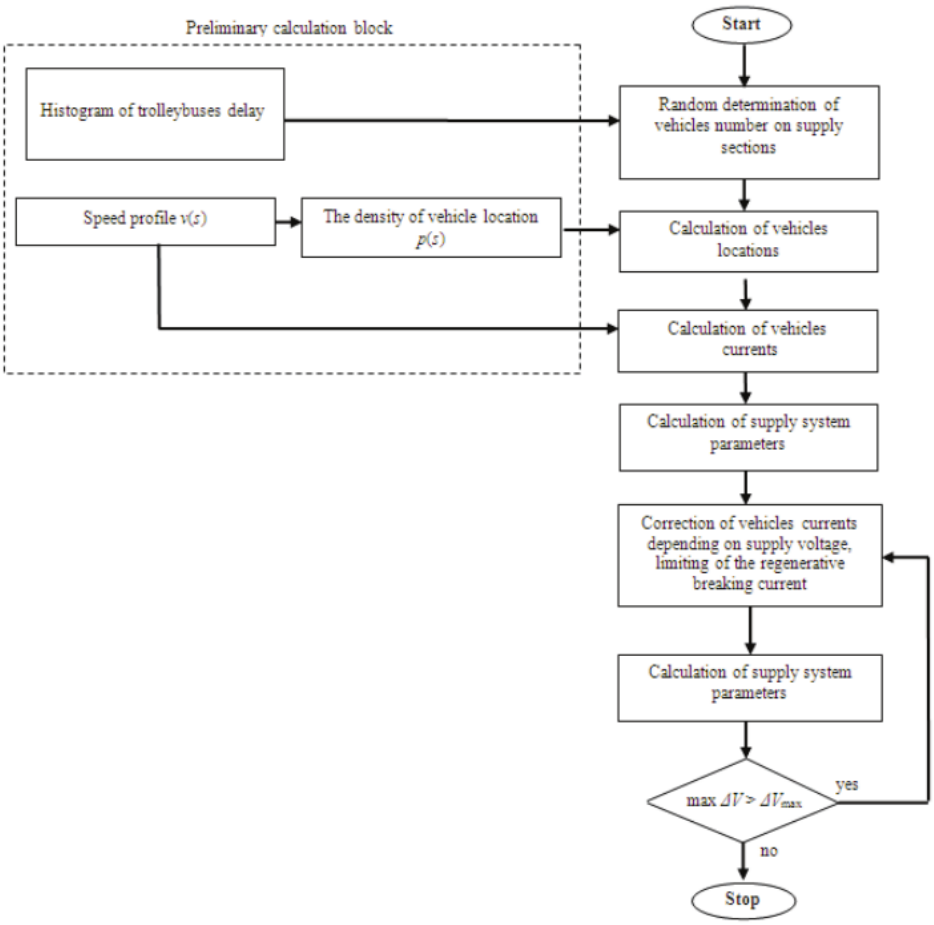

Figure 2.5: A diagram of a supply system model in combination with multiple modelled buses [9]

2.4. Bus and city parameters

This final section looks at literature on the bus and city parameters that will be investigated. Performing a literature review on these parameters is important to get a good idea of the potential effects they each have. Another benefit of this literature review is to get a grasp on the average as well as minimum and maximum values for each parameter. This section will mention relevant research that has been performed recently. By doing this a research gap can be established which this thesis attempts to cover. The parameters are:

- Average velocity
- Battery size
- Energy consumption
- City topography
- Coverage length
- Charging power

2.4.1. Average velocity

The average velocity has a direct influence on a lot of factors. First and foremost it dictates the traction power demand of the bus. The next biggest influence is the amount of charging power that can be drawn. Whenever the bus stops the maximum charging power can diminish to five times less than while moving because of cooling issues with the contact point [7].

The effect of average velocity on charging behaviour is a point of discussion in Bartłomiejczyk [9] in the form of a statistical analysis. In Figure 2.6 this can already clearly be seen. A lower average velocity results in a higher probability of successful charging for the same coverage percentage (x-axis).

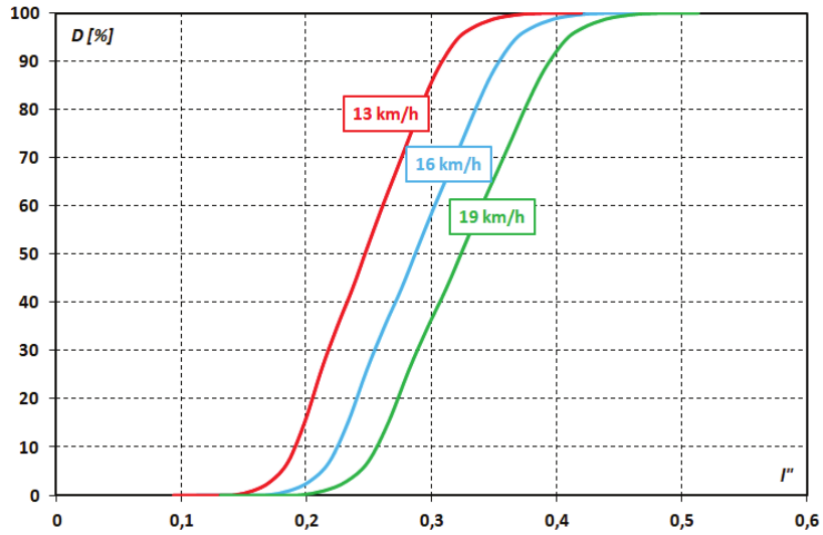

Figure 2.6: The successful charging probability as a function of coverage percentage for a charging power of 70 kW and for three average velocities of 13 (red), 16 (blue), 19 (green) km/h [9]

Using a velocity profile as an input for modelling gives the opportunity to create a custom velocity profile. This way a specific average velocity for just the charging corridor as well as the whole trip can be created. Some examples are given in Giakoumis [22]. Two of these are the Braunschweig cycle (Figure 2.7) and SORT cycle (Figure 2.8). The Braunschweig cycle is a more realistic profile while the SORT profiles are trapezoidal. What is interesting about the SORT cycles is that there are three similar cycles but one simulates heavy urban, the second easy urban and the third simulates suburban. The ways in which these three are distinguished are by an increase of maximum and average velocity for each step while the idling time is decreased.

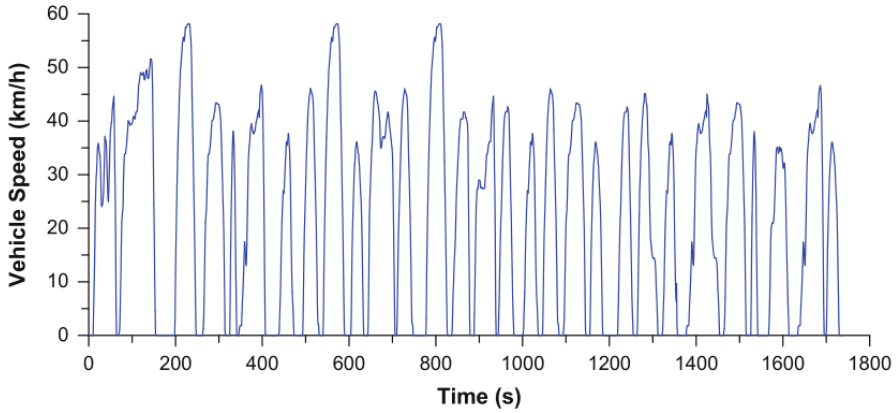

Figure 2.7: The Braunschweig cycle velocity profile [22]

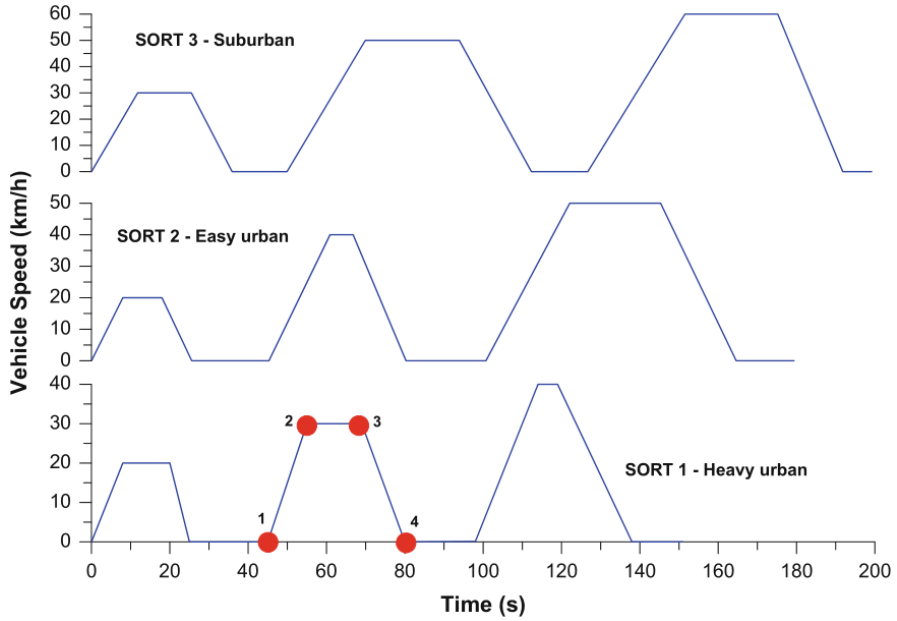

Figure 2.8: The three SORT cycle velocity profiles [22]

2.4.2. Battery size

The same paper that studied the effect of average velocity also studied the effects of battery size [9]. One relation that was found is the amount of charging power that is needed with a specific battery capacity for a coverage percentage of 30%. This can be seen in Figure 2.9.

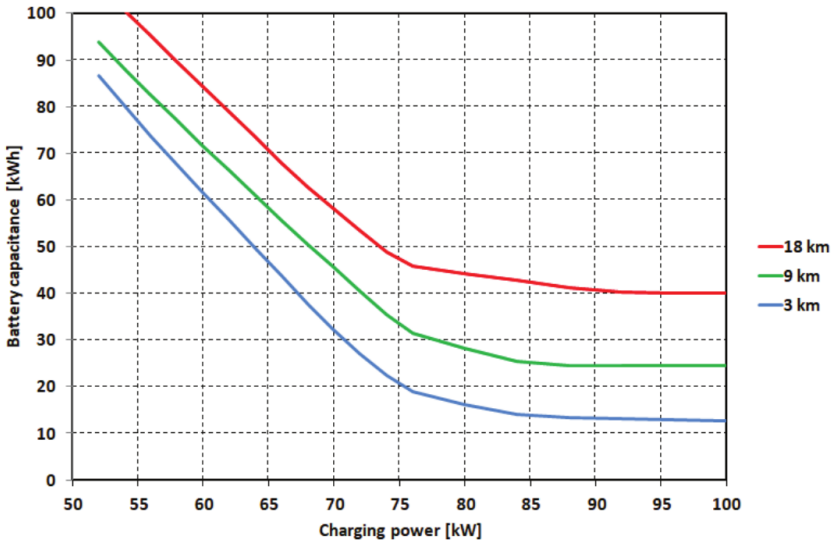

Figure 2.9: The relation between charging power and the required battery capacity (not capacitance as the y-axis label erroneously states) for different route lengths all with a coverage percentage of 30% [9]

2.4.3. Energy consumption

The energy consumption is mainly attributed to the traction power and heating of the interior of the bus. This is further elaborated in Bartłomiejczyk [9] where it is mentioned that the low efficiency of internal combustion engines comes with the upside that it provides large amounts of waste heat that can go into heating the bus interior. With the high efficiency electric motors this upside is no longer there. Figure 2.10 shows the amount of energy that is used for each driven kilometre for different days in the year. The main thing to take away from this graph is the increase in the winter months where heating is used more frequently. It shows that up

to half of the energy is used for heating in those months.

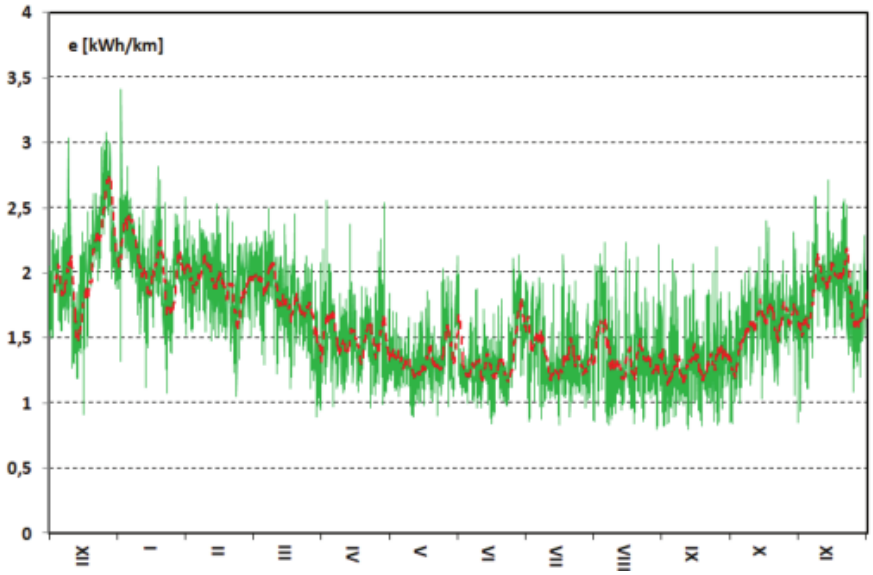

Figure 2.10: The energy consumption of a Trolleybus in Gdynia throughout a year from December (left) to November (right) [9]

2.4.4. City topography

Another study shows the relation between road slope and energy consumption [35]. Figure 2.11 shows that three of the six lines have a large height difference between beginning and end of trip. These are the lines 1, 3 and 7. Looking at the amount of energy consumption the trips going downhill (left side) have a significantly lower energy consumption than the ones going uphill.

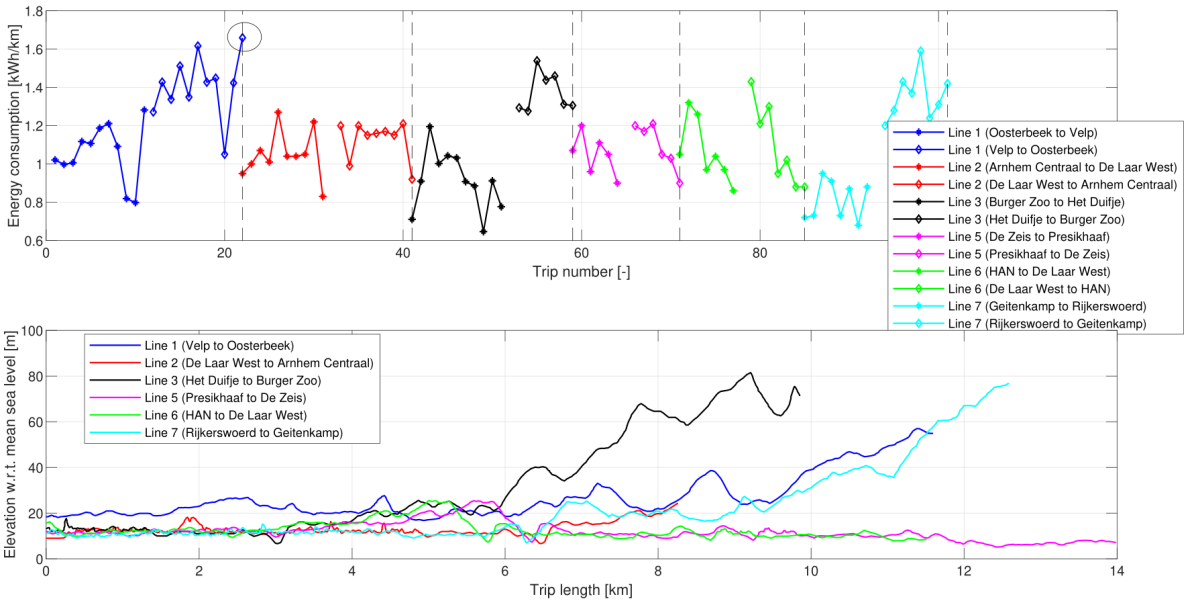

Figure 2.11: (Top) Energy consumption for different test trips of the different trolleybus lines in Arnhem, (bottom) the corresponding height profiles of the bus lines [35]

2.4.5. Coverage length

Bartłomiejczyk also looked at the coverage percentage necessary for successful charging in his study [9]. In Figure 2.12 the relation is shown of the amount of coverage that is needed with respect to the maximum charging power available for different vehicle masses and amount of heating. For ideal cases only 10% of coverage is enough while extreme cases could go higher than 50%.

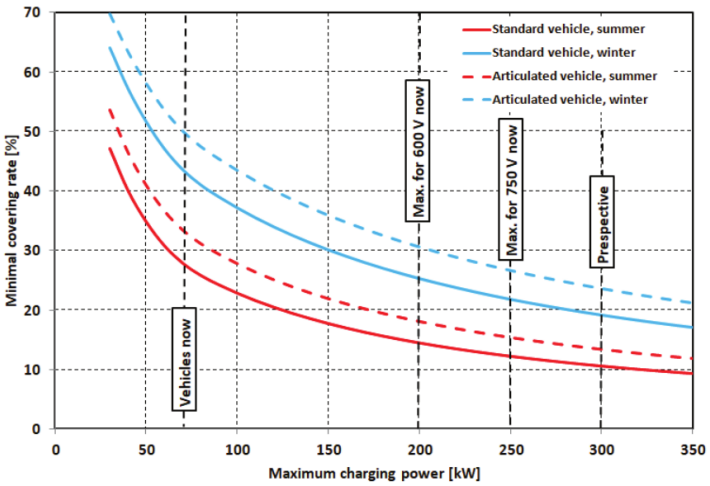

Figure 2.12: The minimum coverage percentage necessary as a function of maximum charging power for different vehicle masses (standard vs. articulated) and heating (summer vs. winter) [9]

2.4.6. Charging power

The charging power limitations are based on three separate components. First there is the battery which has C-rates for both charging and discharging. In Tomar et al. [35] this C-rate is discussed as one of the main performance characteristics of the battery. A high charging power limit is so important for IMC buses that the paper mentions that among several lithium ion battery technologies the LTO technology should be chosen for its high C-rate among other advantages.

The second limitation in the current collector component. The three parts that limit the current that goes through it are: the skid, the cable inside the tube and the connection between cable and spoon [9]. A thermal image in Figure 2.13 shows the temperature of a stationary bus in Gdynia which has a load current of 210 A. At this amount of current the temperature of the skid reaches over 200 °C. A higher current while stationary for a prolonged period would result in permanent damage to the current collector. A significantly higher current of around 600 A is possible whenever the vehicle is moving.

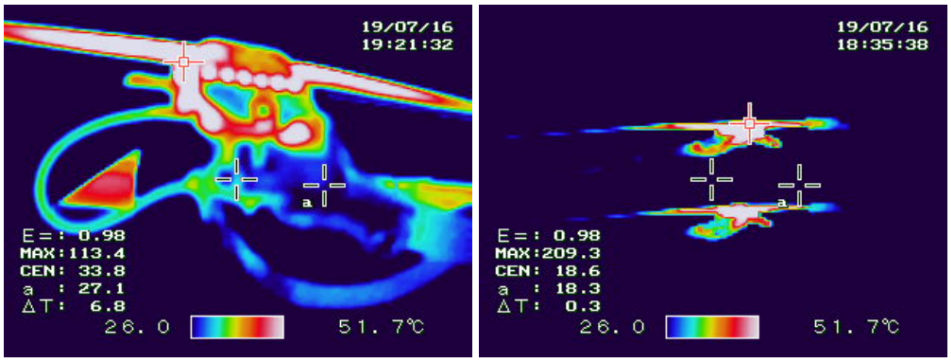

Figure 2.13: A thermal image taken of the current collector of a stationary IMC bus in Gdynia [7]

The third limitation is on the supply system itself. Multiple buses on the same section can pose a problem as the amount of current drawn can become too high. Not a lot of research has been performed on this particular limitation. One instance is Bartłomiejczyk [8] in which a study is performed on the benefits of bilateral supply.

In this study the interaction between two buses is shortly discussed. Furthermore, in Bartłomiejczyk [9] a set-up for modelling the effects of multiple buses on the same section was provided. Further research on this limitation will be performed in this thesis.

2.5. Research gap

Bartłomiejczyk [9] covers a large portion of technical limitations of IMC buses. Particular attention is put into the limitations of charging power. Apart from topography, all six parameters that are considered for this thesis, are also considered in this work. Through statistical analysis it was found that a lower average velocity results in a higher charging probability. However, the difference between average velocity inside the charging corridor and outside is not considered. Instead the research considers the average velocity of the whole trip. Furthermore, the connection with charging power and coverage length is taken into account. Lowering the charging power correlates with higher coverage lengths for the same successful charging probability.

Another example is that the work also considers different charging powers, talking about the difference it makes if different charging powers are considered for stopping and moving. Through a statistical experiment in which the Gdynia trolleygrid was simulated it was shown that the addition of IMC buses results in average current loads on the supply sections up to five times higher than standard trolleybus operation. It does not cover the relative increases in transmission losses as a result of this. This will be covered extensively in the answering of RQ4 of this thesis through a simulation of the Arnhem trolleygrid.

In general, the research gap that this thesis attempts to cross is the amalgamation of all six parameters under consideration. Some dependencies have been correctly identified and analysed in earlier works. In order to speed up the decision making process in identifying priority parameters in the design of a functioning system of IMC buses for range extension for any city this work will provide an overview of parameter dependencies not earlier discussed in previous literature.

3

Methodology

In this chapter the methodology used for performing this thesis is explained. The chapter starts off with a general section which includes the type of research, data collection method, data analysis method, the tools used to perform the research, and the rationale for using the chosen methods. Next a look is taken at different parameters that can have an impact on IMC charging performance and at two different charging strategies. After that the IMC bus model used for simulating bus power demand is explained. Next, the two different approaches to the research are explained as they each have their own methodology sections: the energy approach and the power approach in combination with an Arnhem case study.

3.1. General methodology

The thesis consists of two parts with the first part answering RQ1 and the second part answering RQ2. Another perspective on the two research questions is that RQ2 is needed to answer RQ1 more thoroughly. In other words, the first research question serves a broader purpose while the second research question has increased complexity and depth.

The first part can be seen as a set-up to the actual research performed. It consists of a literature review about the power/energy consumption of IMC buses and regular trolleybuses. It also includes the analysis of a Simulink model made by HAN university of the trolleybuses in Arnhem and the modelling of electric vehicle models in general. The understanding gathered from this analysis was used to expand upon the Simulink trolleybus model and make it an IMC bus model by adding a traction battery model to it. The first research question is:

> *RQ1: What is the difference in energy consumption between IMC buses and regular trolleybuses?*

The second part is the main research performed as it aims to give most of the actual academic context to the thesis. It does so by illustrating the effect of the charging behaviour of IMC buses and the effect this has on the trolleygrid. This is done by performing experimental simulations of IMC buses charging along their charging corridors for different coverage ratios, charging powers, battery sizes and energy consumption. The second part also introduces the use of a case study performed on the Arnhem trolleybus grid and makes use of measured drive cycles of the trolleybuses in Arnhem. Its results can for instance be used to strategically determine which overhead line sections are better for charging IMC buses than others. The second research question is:

> *RQ2: What is the effect of IMC buses on the trolleygrid? (Arnhem case study)*

3.1.1. Type of research

The goal of the research performed for this thesis is to help develop a procedure for determining the positioning of charging corridors for IMC buses for different bus and city parameters. In this sense it can be defined

Table 3.1: Parameters for IMC bus model. The type of trolleybus is Hess Swisstrolley 4 (BGT-N1D). Most parameter values are taken from the trolleybus model made by HAN [35]. Vehicle mass is taken from [2].

Parameter	Value	Unit
Vehicle mass	18890	[kg]
Frontal area	8.925	[m²]
Drag coefficient	0.9	[-]
Rolling coefficient	0.01	[-]
Rotational inertia factor	1.04	[-]
Battery capacity	78	[kWh]
Initial SOC	0.6	[-]
Maximum SOC	0.95	[-]
Minimum SOC	0.2	[-]
Gravitational acceleration	9.81	[m/s²]
Air density	1.225	[kg/m³]

as applied research as it can solve a practical problem for engineers looking into IMC buses for a certain city. The research is also exploratory instead of explanatory as it attempts to discover the answer to something that is under-researched. Furthermore, the research is deductive in that it tries to test a hypothesis by collecting data and analysing the results.

The type of research data can be described as mostly primary as the data that the hypothesis is tested with is gathered by experiments. However, some of the variables are gathered through a literature review (chapter 2) and measurement data (Appendix A) from Arnhem trolleybuses is used for validation. What is more clear is that the research data is quantitative and experimental. This is because the main research looks at numbers collected through experimentation in which some variables are controlled to see what the effect of the variables is.

3.1.2. Data collection method

As described earlier some of the data was collected through literature review (research question 1) and measurement data (research question 2), both of which are outside sources. However, for both research questions the data that is further analysed to prove the hypothesis is collected through experimentation.

The experimental simulations were performed using MATLAB and the MATLAB-based visual programming language Simulink. Models of regular trolleybuses, IMC buses, and the charging grid infrastructure have been made in these environments and used to gather the data. For research question 2 the individual IMC bus MATLAB model was used with an added grid model that performs simple DC power flow calculations. An overview of the IMC bus model can be found in Figure 3.1 and parameters used can be found in Table 3.1. The reference bus parameters are based on the two Arnhem trolleybuses that were changed to IMC buses by replacing the diesel APU with a battery.

The model of the bus is the Hess Swisstrolley 4 (BGT-N1D). In essence the model takes a velocity profile and extracts both the acceleration and distance travelled from it. The model retrieves the slope through a lookup table with distance travelled as input. The model gets the traction power required through the use of a dynamic model, mechanical transmission model, and induction motor model. For this it only needs constants with the exception of mass, which can be changed based on the passenger count. The other power usage of the bus comes from an auxiliary power model which models the heater, AC, ventilator, and compressor (used for lowering the bus at bus stops). The inputs of this model consist of the rated power of each of the components (which are constants) and a signal that determines whether the component is on or off. This signal can either be based on a duty cycle or measurement data.

The traction battery simply stores the energy and at each time step will either charge or discharge depending on the situation. This depends on the power demand from both the motor and auxiliaries as well as the amount of current that can flow through the current collector. The latter is because when the bus is standing still the current through the current collector should be limited as the overhead line otherwise would locally heat up resulting in failure.

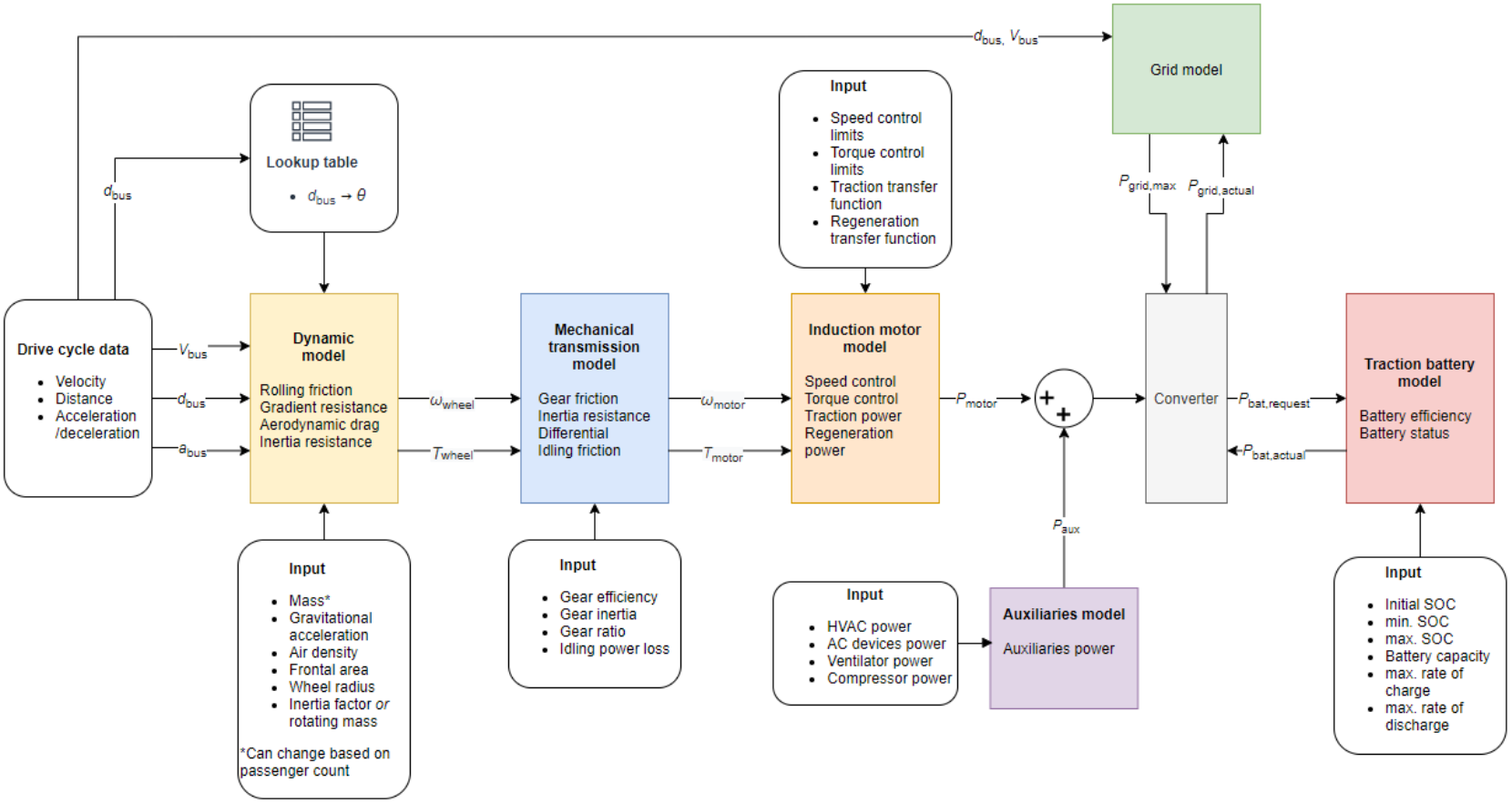

Figure 3.1: IMC bus model overview. It is based on a trolleybus model made by HAN [35]. The grid model and battery model are added to this trolleybus model.

3.2. Parameter dependencies

The four parameters that will be discussed are: energy consumption outside the charging corridor, battery size, charging power, and coverage length. Two other parameters, road slope and average velocity inside the charging corridor, are also mentioned. However, these two parameters are not as interesting from a design perspective. When designing IMC infrastructure for a specific case both the velocity and topography are reliant on outside influences, being traffic and topography of the city respectively. Although these parameters should not be ignored there is no real trade-off to be made as they can be considered fixed when considering a specific (city) case. This is not true for the other four parameters.

For a thorough investigation into the effects of these parameters the dependencies should be identified. Figure 3.2 and 3.3 are charts that show which dependencies are hypothesised. First all positive effects and possible benefits are shown in Figure 3.2 (e.g. coverage length can be lowered when battery size is increased). Figure 3.3 shows the possible remedies for negative effects (e.g. a higher energy consumption can be remedied by increasing the battery size, but also by increasing the charging power). It can be seen that all parameters affect each other in some way.

Figure 3.2: Chart that shows the hypothesised positive dependencies of the six bus and city parameters on each other. The possible benefits are shown in green. The most notable dependencies are further clarified beneath these charts.

		Energy consumption	Battery size	Charging power	Coverage length	Average velocity	Topography
Energy consumption outside charging corridor [kWh]	Lower consumption ->		smaller battery	lower power	lower coverage	higher velocity	higher slope
Battery size [kWh]	Higher capacity ->	higher consumption		lower power	lower coverage	higher velocity	higher slope
Charging power [kW]	Higher power ->	higher consumption	smaller battery		lower coverage	higher velocity	higher slope
Coverage length [km]	Higher coverage ->	higher consumption	smaller battery	lower power		higher velocity	higher slope
Average velocity inside charging corridor [km/h]	Lower velocity ->	higher consumption	smaller battery	lower power	lower coverage		higher slope
Slope inside charging corridor [rad]	Lower slope ->	higher consumption	smaller battery	lower power	lower coverage	higher velocity	

Figure 3.3: Chart that shows the hypothesised negative dependencies of the six bus and city parameters on each other. The possible remedies are shown in red. The most notable dependencies are further clarified beneath these charts.

		Energy consumption	Battery size	Charging power	Coverage length	Average velocity	Topography
Energy consumption outside charging corridor [kWh]	Higher consumption ->		larger battery	higher power	higher coverage	lower velocity	lower slope
Battery size [kWh]	Lower capacity ->	lower consumption		higher power	higher coverage	lower velocity	lower slope
Charging power [kW]	Lower power ->	lower consumption	larger battery		higher coverage	lower velocity	lower slope
Coverage length [km]	Lower coverage ->	lower consumption	larger battery	higher power		lower velocity	lower slope
Average velocity inside charging corridor [km/h]	Higher velocity ->	lower consumption	larger battery	higher power	higher coverage		lower slope
Slope inside charging corridor [rad]	Higher slope ->	lower consumption	larger battery	higher power	higher coverage	lower velocity	

The most notable dependencies with explanations are listed below for each of them. It is first stated if the effect of an increase is positive or negative.

- Energy consumption outside the charging corridor
  - Battery size: negative effect. Increasing the battery size also means an increase in mass which results in a higher energy consumption.
  - Coverage length: positive effect. Increasing the coverage length is the same as decreasing the distance that the bus drives autonomously (i.e. on battery power) which results in a lower energy consumption outside the charging corridor.
- Minimum battery size
  - Energy consumption outside the charging corridor: negative effect. Increasing consumption means that a larger battery is necessary to store it.
  - Charging power: possible positive effect. Increasing the charging power can make it possible to decrease battery size. This is the case up until the point where the amount of energy that is picked up for each round trip is higher than the amount of energy consumed outside the charging corridor at which point the minimum battery size is dictated by the energy consumption outside the charging corridor.
  - Coverage length: positive effect. As increasing the coverage length has a positive effect on energy consumption outside the charging corridor it inadvertently results in a decrease in minimum battery size.
- Minimum charging power
  - Energy consumption outside the charging corridor: negative effect. If more energy is needed, one option is to increase the charging power.
  - Battery size: positive or slightly negative effect. This can go both ways. Increasing the battery size will result in a slight energy consumption increase because of the mass increase which means that charging power should increase. However, increasing the battery size means that the bus starts off the day with a larger amount of energy on board so the amount of energy that is picked up per round trip can be decreased ergo the charging power can be decreased.

  - Coverage length: positive effect. An increase in coverage length will result in both a decrease in energy consumption outside the charging corridor and an increase in energy picked up inside the charging corridor. The charging power can be decreased as a result of both of these effects.
  - Average velocity inside the charging corridor: negative effect. Increasing the average velocity means that fewer time is spent connected to the overhead lines which means that charging power should be increased.
  - Slope inside charging corridor: negative or positive effect, it depends on the situation and might even be negligible. If the bus is driving on a positive slope there will be less power going into the battery from regenerative braking so more power should come from the supply system. The opposite is true as well: a negative slope means that more power comes from regenerative braking so less power is needed from the supply grid. For most bus routes (i.e. the bus moves back and forth through the same streets) the bus will experience both cases in one round trip. This could mean that for a round trip the two cancel each other out. The answer is straightforward if only one direction is considered. So when the slope is positive it will mean a higher charging power is necessary and vice versa.

- Minimum coverage length
  - Energy consumption outside the charging corridor: negative effect. If more energy is needed, another option (apart from increasing charging power) is to increase the coverage length.
  - Battery size: positive effect. The coverage length can be decreased for the same reasons that charging power can be decreased with a larger battery size.
  - Charging power: positive effect. Charging power and coverage length are interchangeable for obtaining energy from the grid.
  - Average velocity inside the charging corridor: negative effect. The time connected to the grid is decreased if average velocity is increased. This can be compensated by increasing the coverage length.
  - Slope inside charging corridor: see explanation for minimum charging power. As a higher slope can be either positive or negative, it depends on the situation whether this results in a larger or smaller minimum coverage length.

3.3. Battery charging strategies

In general two battery charging strategies can be considered for an IMC bus. Either the battery size is minimised to the point where the amount of energy needed for one round trip ($E_{\text{pick,req}}$) can only just be covered (excluding some reserve energy for emergencies E_{reserve}). In this case the amount of energy picked up in one round trip (E_{pick}) should exceed $E_{\text{pick,req}}$. Equation 3.1 shows how the minimum battery capacity can be calculated for this strategy.

Another strategy is suitable for when the amount of E_{pick} is lowered to a point where the bus charges less than is required for each round trip. The battery then has to be charged back to full overnight. In this strategy the battery should hold enough energy to cover $\Delta E_{\text{roundtrip}}$ which is the amount of energy that is depleted after each round trip for a whole day on top of $E_{\text{pick,req}}$. Equation 3.3 explains how this energy depletion per round trip is calculated. The maximum amount of energy picked up per round trip ($E_{\text{pick,max}}$) is calculated by adding the regenerative energy and energy from the grid (see Equation 3.4. $E_{\text{pick,req}}$ is calculated by multiplying the specific energy consumption (E_{specific}) with the driving range outside the charging corridor (DR) like in Equation 3.5. With Equation 3.2 the minimum battery capacity for this second strategy can be calculated.

$$E_{\text{bat,strategy1}} = E_{\text{pick,req}} + E_{\text{reserve}} \tag{3.1}$$

$$E_{\text{bat,strategy2}} = (n_{\text{roundtrip}} - 1) \cdot \Delta E_{\text{roundtrip}} + E_{\text{pick,req}} + E_{\text{reserve}} \tag{3.2}$$

$$\Delta E_{\text{roundtrip}} = E_{\text{pick,req}} - E_{\text{pick}} \tag{3.3}$$

$$E_{\text{pick,max}} = E_{\text{regen,cc}} + E_{\text{grid}} \tag{3.4}$$

$$E_{\text{pick,req}} = \text{DR} \cdot E_{\text{specific}} \tag{3.5}$$

To illustrate these two strategies, two simplified simulations were performed in Excel. Figure 3.4 and 3.5 show the results of these simulations. The energy consumption of the bus was fixed at 3 [kWh/km]. The amount of regenerative energy put back into the battery was set at 0.8 [kWh/km]. The amount of energy taken from the grid while inside the charging corridor was fixed at 7.5 [kWh/km] which means an average charging power of 150 [kW] at a velocity of 20 [km/h]. The battery capacity was set depending on the energy needs, 31 [kWh] for the first simulation and 64 [kWh] for the second one. This information can also be found in the top left of the two figures. The other fixed variable is the length of each section. It is fixed at 1 [km].

The picture on the right side of the two figures depicts a sketch of the bus route. Ten sections equal in length of which the green sections are charging corridors. For the first simulation sections 1, 2 and 3 are charging corridors. For the second simulation only section 1 and 2 are charging corridors. This decrease in total charging corridor length results in a decrease of E_{pick} but an increase in $E_{\text{pick,req}}$. In these simulations each section can be seen as one time step.

The middle table of the figures shows the (maximum) amount of energy going in and out of the battery for each section in each round trip. Figure 3.4 shows that $E_{\text{pick,max}}$ for 6 sections is 49.8 [kWh] using Equation 3.4. $E_{\text{pick,req}}$ is shown in the cell with red borders and is 30.8 [kWh] for 14 sections using Equation 3.5. As this is lower than $E_{\text{pick,max}}$ battery strategy 1 can be used (see Equation 3.1). For demonstration purposes a small value of 0.2 [kWh] was taken for E_{reserve}.

The bottom table of Figure 3.4 shows the battery charge after each section for a total of 15 round trips. It can be seen that the battery is nearly depleted after section 4 on the return trip just before it enters the charging corridor again at section 3 to start charging again.

Figure 3.4: Simulation of a battery charging strategy where a small battery is charged back to full after each round trip. (see full text for explanation)

	kWh/km
Energy use (motor+auxiliaries)	-3
Regen energy	0.8
Grid charge	7.5
Battery capacity	31

Section #	Length of section [km]	Energy taken from battery [kWh]	Regen energy in section [kWh]		Section is charging corridor	Energy from grid in section [kWh]	
1	1	0	0.8	0	1	7.5	8.3
2	1	0	0.8	0	1	7.5	8.3
3	1	0	0.8	0	1	7.5	8.3
4	1	-3	0.8	-2.2	0	0	-2.2
5	1	-3	0.8	-2.2	0	0	-2.2
6	1	-3	0.8	-2.2	0	0	-2.2
7	1	-3	0.8	-2.2	0	0	-2.2
8	1	-3	0.8	-2.2	0	0	-2.2
9	1	-3	0.8	-2.2	0	0	-2.2
10	1	-3	0.8	-2.2	0	0	-2.2
10	1	-3	0.8	-2.2	0	0	-2.2
9	1	-3	0.8	-2.2	0	0	-2.2
8	1	-3	0.8	-2.2	0	0	-2.2
7	1	-3	0.8	-2.2	0	0	-2.2
6	1	-3	0.8	-2.2	0	0	-2.2
5	1	-3	0.8	-2.2	0	0	-2.2
4	1	-3	0.8	-2.2	0	0	-2.2
3	1	0	0.8	0	1	7.5	8.3
2	1	0	0.8	0	1	7.5	8.3
1	1	0	0.8	0	1	7.5	8.3
		-42	16	-30.8		45	19

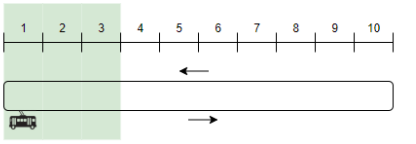

Roundtrip number:	1	2	3	4	5	6	7	8	9	10	11	12	13	14	15
Battery charge at beginning of roundtrip:	31	25.1	25.1	25.1	25.1	25.1	25.1	25.1	25.1	25.1	25.1	25.1	25.1	25.1	25.1
Battery charge after section: 1	31	31	31	31	31	31	31	31	31	31	31	31	31	31	31
2	31	31	31	31	31	31	31	31	31	31	31	31	31	31	31
3	31	31	31	31	31	31	31	31	31	31	31	31	31	31	31
4	28.8	28.8	28.8	28.8	28.8	28.8	28.8	28.8	28.8	28.8	28.8	28.8	28.8	28.8	28.8
5	26.6	26.6	26.6	26.6	26.6	26.6	26.6	26.6	26.6	26.6	26.6	26.6	26.6	26.6	26.6
6	24.4	24.4	24.4	24.4	24.4	24.4	24.4	24.4	24.4	24.4	24.4	24.4	24.4	24.4	24.4
7	22.2	22.2	22.2	22.2	22.2	22.2	22.2	22.2	22.2	22.2	22.2	22.2	22.2	22.2	22.2
8	20	20	20	20	20	20	20	20	20	20	20	20	20	20	20
9	17.8	17.8	17.8	17.8	17.8	17.8	17.8	17.8	17.8	17.8	17.8	17.8	17.8	17.8	17.8
10	15.6	15.6	15.6	15.6	15.6	15.6	15.6	15.6	15.6	15.6	15.6	15.6	15.6	15.6	15.6
10	13.4	13.4	13.4	13.4	13.4	13.4	13.4	13.4	13.4	13.4	13.4	13.4	13.4	13.4	13.4
9	11.2	11.2	11.2	11.2	11.2	11.2	11.2	11.2	11.2	11.2	11.2	11.2	11.2	11.2	11.2
8	9	9	9	9	9	9	9	9	9	9	9	9	9	9	9
7	6.8	6.8	6.8	6.8	6.8	6.8	6.8	6.8	6.8	6.8	6.8	6.8	6.8	6.8	6.8
6	4.6	4.6	4.6	4.6	4.6	4.6	4.6	4.6	4.6	4.6	4.6	4.6	4.6	4.6	4.6
5	2.4	2.4	2.4	2.4	2.4	2.4	2.4	2.4	2.4	2.4	2.4	2.4	2.4	2.4	2.4
4	0.2	0.2	0.2	0.2	0.2	0.2	0.2	0.2	0.2	0.2	0.2	0.2	0.2	0.2	0.2
3	8.5	8.5	8.5	8.5	8.5	8.5	8.5	8.5	8.5	8.5	8.5	8.5	8.5	8.5	8.5
2	16.8	16.8	16.8	16.8	16.8	16.8	16.8	16.8	16.8	16.8	16.8	16.8	16.8	16.8	16.8
1	25.1	25.1	25.1	25.1	25.1	25.1	25.1	25.1	25.1	25.1	25.1	25.1	25.1	25.1	25.1

Figure 3.5: Simulation of a battery charging strategy where a larger battery is slowly depleted over the course of a day. (see full text for explanation)

	kWh/km
Energy use (motor+auxiliaries)	-3
Regen energy	0.8
Grid charge	7.5
Battery capacity	64

Section #	Length of section [km]	Energy taken from battery [kWh]	Regen energy in section [kWh]		Section is charging corridor	Energy from grid in section [kWh]	
1	1	0	0.8	0	1	7.5	8.3
2	1	0	0.8	0	1	7.5	8.3
3	1	-3	0.8	-2.2	0	0	-2.2
4	1	-3	0.8	-2.2	0	0	-2.2
5	1	-3	0.8	-2.2	0	0	-2.2
6	1	-3	0.8	-2.2	0	0	-2.2
7	1	-3	0.8	-2.2	0	0	-2.2
8	1	-3	0.8	-2.2	0	0	-2.2
9	1	-3	0.8	-2.2	0	0	-2.2
10	1	-3	0.8	-2.2	0	0	-2.2
10	1	-3	0.8	-2.2	0	0	-2.2
9	1	-3	0.8	-2.2	0	0	-2.2
8	1	-3	0.8	-2.2	0	0	-2.2
7	1	-3	0.8	-2.2	0	0	-2.2
6	1	-3	0.8	-2.2	0	0	-2.2
5	1	-3	0.8	-2.2	0	0	-2.2
4	1	-3	0.8	-2.2	0	0	-2.2
3	1	-3	0.8	-2.2	0	0	-2.2
2	1	0	0.8	0	1	7.5	8.3
1	1	0	0.8	0	1	7.5	8.3
		-48	16	-35.2		30	-2

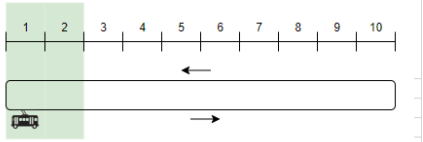

Roundtrip number:		1	2	3	4	5	6	7	8	9	10	11	12	13	14	15
Battery charge at beginning of roundtrip:		64	45.4	43.4	41.4	39.4	37.4	35.4	33.4	31.4	29.4	27.4	25.4	23.4	21.4	19.4
Battery charge after section:	1	64	53.7	51.7	49.7	47.7	45.7	43.7	41.7	39.7	37.7	35.7	33.7	31.7	29.7	27.7
	2	64	62	60	58	56	54	52	50	48	46	44	42	40	38	36
	3	61.8	59.8	57.8	55.8	53.8	51.8	49.8	47.8	45.8	43.8	41.8	39.8	37.8	35.8	33.8
	4	59.6	57.6	55.6	53.6	51.6	49.6	47.6	45.6	43.6	41.6	39.6	37.6	35.6	33.6	31.6
	5	57.4	55.4	53.4	51.4	49.4	47.4	45.4	43.4	41.4	39.4	37.4	35.4	33.4	31.4	29.4
	6	55.2	53.2	51.2	49.2	47.2	45.2	43.2	41.2	39.2	37.2	35.2	33.2	31.2	29.2	27.2
	7	53	51	49	47	45	43	41	39	37	35	33	31	29	27	25
	8	50.8	48.8	46.8	44.8	42.8	40.8	38.8	36.8	34.8	32.8	30.8	28.8	26.8	24.8	22.8
	9	48.6	46.6	44.6	42.6	40.6	38.6	36.6	34.6	32.6	30.6	28.6	26.6	24.6	22.6	20.6
	10	46.4	44.4	42.4	40.4	38.4	36.4	34.4	32.4	30.4	28.4	26.4	24.4	22.4	20.4	18.4
	10	44.2	42.2	40.2	38.2	36.2	34.2	32.2	30.2	28.2	26.2	24.2	22.2	20.2	18.2	16.2
	9	42	40	38	36	34	32	30	28	26	24	22	20	18	16	14
	8	39.8	37.8	35.8	33.8	31.8	29.8	27.8	25.8	23.8	21.8	19.8	17.8	15.8	13.8	11.8
	7	37.6	35.6	33.6	31.6	29.6	27.6	25.6	23.6	21.6	19.6	17.6	15.6	13.6	11.6	9.6
	6	35.4	33.4	31.4	29.4	27.4	25.4	23.4	21.4	19.4	17.4	15.4	13.4	11.4	9.4	7.4
	5	33.2	31.2	29.2	27.2	25.2	23.2	21.2	19.2	17.2	15.2	13.2	11.2	9.2	7.2	5.2
	4	31	29	27	25	23	21	19	17	15	13	11	9	7	5	3
	3	28.8	26.8	24.8	22.8	20.8	18.8	16.8	14.8	12.8	10.8	8.8	6.8	4.8	2.8	0.8
	2	37.1	35.1	33.1	31.1	29.1	27.1	25.1	23.1	21.1	19.1	17.1	15.1	13.1	11.1	9.1
	1	45.4	43.4	41.4	39.4	37.4	35.4	33.4	31.4	29.4	27.4	25.4	23.4	21.4	19.4	17.4

Figure 3.5 shows that section 3 is not a charging corridor anymore for the second simulation. This results in $E_{\text{pick,max}}$ decreasing 33.2 [kWh] on the remaining 4 charging sections. $E_{\text{pick,req}}$ is instead increased to 35.2 [kWh] as the autonomous part is increased to 16 sections. This means that $\Delta E_{\text{roundtrip}}$ becomes 2 [kWh] at which point battery strategy 2 should be applied. Using Equation 3.2 the battery capacity becomes 64 [kWh]. A 0.8 [kWh] reserve energy is chosen in this case again just for demonstration purposes. Now the bottom table in Figure 3.5 shows a different pattern. The amount of energy in the battery can be seen slowly depleting after each round trip with the lowest charge after section 3 of the final round trip of 0.8 [kWh].

These simplified simulations showed two strategies for choosing the correct battery size. It can be seen that if strategy 1 (minimise the battery size) is preferred then either the length of the charging corridor or the charging power should be increased. Decreasing the average velocity inside the charging corridor also has a positive impact on $E_{\text{pick,max}}$. A difference in road slope/topography can also have an impact on the amount of energy picked up. E_{regen} can be seen as the variable for road slope. In these simulations the road slope was assumed constant (at zero) so regenerative energy was a constant 0.8 [kWh]. If this road slope was instead positive, the regenerative energy would decrease as less braking occurs. If the road slope is negative then more braking would result in a higher value for E_{regen}.

For the case study it was chosen to go with the first strategy. The batteries of each of the IMC bus lines are sized based on one round trip. A further explanation of the sizing can be found in subsection 3.6.2.

3.4. HAN trolleybus model

A trolleybus model was developed in Simulink by the Hogeschool van Arnhem en Nijmegen (HAN) [35]. Figure 3.6 contains an overview of this model. Power from the overhead grid is distributed in the bus into three parts: the electric motor, the heater, and the other auxiliary components. The model includes regenerative braking of the electric motor and as such the indicated "Motor Power" can be positive as well as negative. The model takes bus velocity as the main input to simulate motor power. The other power flows in the bus are simulated based on the on/off statuses of each power consuming device. These inputs are obtained from measurement data of driving buses which is provided as backup files from Kiepe Electric, the manufacturer of electrical components of the trolleybuses in Arnhem. As this measurement data also contains the power demand of each bus component the simulated power flow can easily be validated by comparison.

This section will describe every part of the Simulink model. For this thesis the model was copied into MATLAB code format. Some parts of the model were changed or added to this new version. These changes are explained for the relevant subsystems. Every following subsection corresponds with one of the subsystems in Figure 3.6.

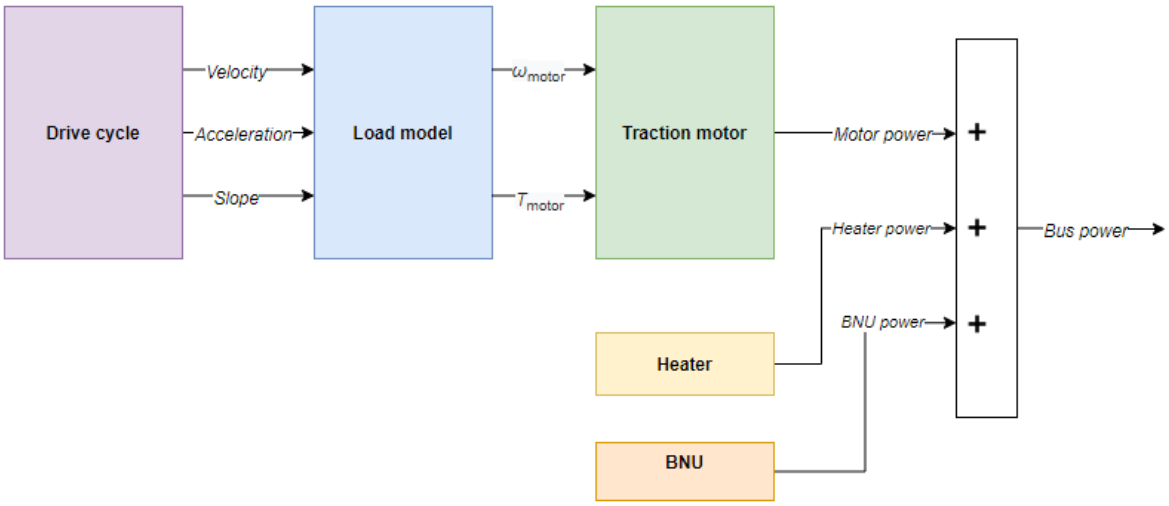

Figure 3.6: An overview of the HAN trolleybus model. The original model, made in Simulink contains the five parts depicted here (i.e. drive cycle, load model, traction motor, heater and BNU). [35]

3.4.1. Drive Cycle

A (measured) drive cycle should be used as an input for the model. In this model the drive cycle input is bus velocity V_{bus} in km/h which is converted to m/s. The distance the bus has travelled (d_{bus}) is then given by Equation 3.6. With this distance a lookup table is used to obtain the inclination/slope θ at that point on the route. The acceleration of the bus (a_{bus}) is given by Equation 3.7.

$$d_{\text{bus}} = \int V_{\text{bus}} dt \tag{3.6}$$

$$a_{\text{bus}} = \frac{dV_{\text{bus}}}{dt} \tag{3.7}$$

3.4.2. Load Model

The Load Model block takes this velocity, acceleration, and slope as inputs and has the angular velocity and torque of the motor as outputs. This is done by first determining the angular velocity of the wheels and the torque on the wheels which is needed to overcome resistance forces and then converting these by means of a differential of the motor.

The angular velocity of the wheel ω_{wheel} [rad/s] is given by Equation 3.8,

$$\omega_{\text{wheel}} = \frac{V_{\text{bus}}}{r_{\text{wheel}}} \tag{3.8}$$

Where, V_{bus} [ms^{-2}] is the bus velocity and r_{wheel} [m] is the wheel radius. The torque on the wheels T_{wheel} is given by Equation 3.9,

$$T_{\text{wheel}} = F_{\text{traction}} \cdot r_{\text{wheel}} \tag{3.9}$$

Where the traction force F_{traction} is the sum of all resistance forces. It is the sum of two to four different forces depending on the slope of the road and whether the bus has a constant velocity or is accelerating/decelerating (i.e. $\frac{dv}{dt} = 0$ or $\frac{dv}{dt} \neq 0$).

The equation for the traction force is given by Equation 3.10,

$$F_{\text{traction}} = F_{\text{roll}} + F_{\text{aero}} + F_{\text{gradient}} + F_{\text{inertia}} \tag{3.10}$$

Where, F_{roll} is rolling resistance, the force that a surface exerts on a body when the body rolls on the surface. F_{aero} is air drag (or aerodynamic resistance), the force exerted by a fluid onto the solid that moves through this fluid. F_{gradient} is gradient (or slope) resistance, the part of the gravitational force exerted on the bus that pulls the bus down along a slope. F_{inertia} is inertia (or acceleration) resistance, the force that resists any change in velocity. The rolling resistance is given by Equation 3.11,

$$F_{\text{roll}} = C_{\text{roll}} M_{\text{bus}} g \cdot cos(\theta) \tag{3.11}$$

Where, C_{roll} [-] is the coefficient of rolling resistance, M_{bus} [kg] is the total vehicle mass, g [ms^{-2}] is the gravitational acceleration, and θ [rad] is the slope of the road. The aerodynamic resistance is given by Equation 3.12,

$$F_{\text{aero}} = \frac{1}{2} \rho A_{\text{f}} C_{\text{d}} (V_{\text{bus}} + V_{\text{wind}})^2 \tag{3.12}$$

Where ρ [kgm^{-3}] is the air density; A_{f} [m^2] is the frontal area of the bus; C_{d} [$-$] is the drag coefficient. It also combines the bus velocity V_{bus} [ms^{-1}] and wind velocity V_{wind} [ms^{-1}] (with head wind being positive) into a relative velocity between bus and air. The gradient resistance is given by Equation 3.13,

$$F_{\text{gradient}} = M_{\text{bus}} \cdot g \cdot sin(\theta) \tag{3.13}$$

Which, just like the equation for rolling resistance, contains the bus mass M_{bus} [kg], the gravitational acceleration g [ms^{-2}], and the slope θ [rad].

The inertia resistance is given by Equation 3.14,

$$F_{\text{inertia}} = (M_{\text{bus}} + M_{\text{eq}}) \cdot a \tag{3.14}$$

Where M_{bus} [kg] is the mass of the bus, M_{eq} [kg] is the equivalent mass of rotating parts, and a is the acceleration of the bus. Instead of the equivalent mass of rotating parts, the model uses C_{inertia} a rotational inertia coefficient which factors in the rotational inertia based on the mass of the bus. The inertia resistance is then given by Equation 3.15,

$$F_{\text{inertia}} = M_{\text{bus}} \cdot C_{\text{inertia}} \cdot a \tag{3.15}$$

This coefficient is among several other constants and variables used as inputs for modelling the bus dynamics. An overview of these parameters and how their value is defined can be found in Table 3.2.

In Table 3.3 the relevant forces for different conditions of slope and velocity are depicted. Furthermore it should be noted that apart from the rolling resistance the forces can either resist or assist in traction. The conditions for this can be found in Table 3.4. The Simulink model handles all conditions by just following equations 3.11-3.15 except for one condition which is when the bus is standing still (i.e. $V_{\text{bus}} = 0$. The rolling

Table 3.2: Parameters for resistance force equations

Parameters	Description	Value	Unit	Definition
Constants				
C_r	Rolling coefficient	0.01	-	Assumed
C_d	Drag coefficient	0.9	-	Assumed
A_f	Frontal area of the bus	8.925	m^2	Based on bus dimensions
ρ	Density of air	1.15	kgm^{-3}	Standard value
g	Gravitational acceleration	9.81	ms^{-2}	Standard value
Variables				
M_{bus}	Bus mass	18495 + pass.	kg	Empty bus + passengers
θ	Inclination of the road		rad	Based on velocity input
a_{bus}	Acceleration		ms^{-2}	Based on velocity input
V_{bus}	Bus velocity		ms^{-1}	From drive cycle data
V_{wind}	Wind velocity	0	ms^{-1}	Not in use

Table 3.3: Resistance forces on the wheels for each combination of constant/non-constant velocity and zero/non-zero slope

Velocity	Slope	Rolling	Aerodynamic	Gradient	Inertia
zero	any	no	no	no	no
constant (dv/dt = 0)	zero	yes	yes	no	no
constant	non-zero	yes	yes	yes	no
accelerating/decelerating	zero	yes	yes	no	yes
accelerating/decelerating	non-zero	yes	yes	yes	yes

and gradient resistance equations do not use velocity or acceleration which means they will continue to simulate a force when the bus is standing still. To counter this in the model a conditional switch sets these forces to zero when the velocity is zero.

The next modelling step is to convert the wheel angular velocity and wheel torque to angular velocity and torque of the motor. The motor angular velocity ω_{motor} is given by Equation 3.16,

$$\omega_{motor} = \omega_{wheel} \cdot n_{gear} \tag{3.16}$$

Where, ω_{wheel} is the angular velocity of the wheel which is multiplied by the gearbox ratio n_{gear} which is a constant. In the case of the engine used in the Arnhem trolleybuses this constant is 9.817. For particular instances the torque is not calculated but fixed at -50 Nm. This is the case when velocity is not zero and two signals from the measurement data are equal to zero. It is not completely clear what these two signals mean, one of them is the acceleration pedal so it can be assumed that the other one is the brake pedal. This would mean that this would be the case whenever the vehicle is cruising and no input is given by the driver. In other cases to get from wheel torque to motor torque several losses have to be taken into account and torque should be converted from the gear to the motor. Motor torque T_{motor} is given by Equation 3.17 for driving and Equation 3.18 for braking,

$$T_{motor} = \frac{T_{gear}}{\eta_{gear}} \tag{3.17}$$

$$T_{motor} = \eta_{gear} \cdot T_{gear} \tag{3.18}$$

Where, η_{gear} is the gearbox efficiency which is 95% for these specific motors and T_{gear} is the gear torque. This gear torque is a sum of frictional losses ($T_{friction}$), losses due to inertia ($T_{inertia}$), and the wheel torque (T_{wheel}) itself and is given by Equation 3.19,

$$T_{gear} = T_{wheel} + T_{friction} + T_{inertia} \tag{3.19}$$

The frictional losses depend on the rotational velocity and are given by Equation 3.20,

Table 3.4: Conditions for either resisting or assisting traction for different resistance forces

	Aerodynamic	Gradient	Inertia
Resist traction	Head wind	Positive slope	Bus is accelerating
Assist traction	Tail wind	Negative slope	Bus is decelerating

$$T_{\text{friction}} = \frac{P_{\text{gear loss}}}{\omega_{\text{wheel}}} \tag{3.20}$$

Where, $P_{\text{gear loss}}$ is the idling power loss due to friction which is 500 W for these motors, and ω_{wheel} is the rotational velocity of the wheels. As these losses do not occur when the bus is standing still a conditional switch is added in the model that sets T_{friction} to zero for values of ω_{wheel} lower than 1. The losses due to inertia are given by Equation 3.21,

$$T_{\text{inertia}} = \alpha_{\text{gear}} \cdot I_{\text{gear}} \tag{3.21}$$

Where, α_{gear} (or $\frac{d\omega_{\text{gear}}}{dt}$) is the angular acceleration of the gear, and I_{gear} is the inertia of the gear which is set at 0.01 kgm^2.

3.4.3. Traction Motor

The last step is to obtain the motor power from its torque and angular velocity. The motor power P_{motor} is simply given by Equation 3.22,

$$P_{\text{motor}} = T_{\text{motor}} \cdot \omega_{\text{motor}} \tag{3.22}$$

Where, T_{motor} is the motor torque and ω_{motor} is the motor angular velocity. Both of these have been calculated in preceding steps but three additional steps are performed for accurate induction motor modelling. The first two steps are speed control and torque control. For speed control the maximum is set at 467.67 [rads^{-1}]. The torque control sets a maximum torque of 1305 [Nm]. Then, after torque and angular velocity are multiplied, the third and final step is a transfer function. There are two transfer functions, one for traction and one for regeneration. These have been empirically determined by HAN university. The output of that step is the simulated motor power.

3.4.4. HVAC and other auxiliaries

In the original HAN model the auxiliaries are subdivided in the heater and BNU. For the purpose of this thesis all auxiliaries are gathered into one model called HVAC. First the original two submodels (i.e. heater and BNU are explained). Next, the new HVAC model will be explained.

In cold winter months up to half of the energy usage can come from heating. Because of this significance it has its own subsystem in the model. The actual modelling of the heater is very simple. An on/off switch determines whether the heater is on and when it is on the heater runs at full power (36.5 kW) which is then divided by its efficiency (95%) to get the actual input power for the heater. This means that measurement data that corresponds with the drive cycle should be provided in order to model the heater.

BNU is a reference to the auxiliary components power supply converter. It consists of the air conditioner, the auxiliary batteries, ventilation, and compressor (that can be used for power steering and braking). The energy usage of these auxiliary systems is only a few percent of the total energy the bus uses. The power of the batteries is modelled by using voltage and current of the batteries from telemetry data as input. Multiplying these gives the power of the batteries. A negative current would mean that the batteries are supplying energy while a positive current suggests that the batteries are charging.

The other auxiliary power units all use the same modelling as the heater. They all have an on/off switch and a fixed power value when the unit is turned on, which is 750 W for the ventilator, 5 kW for the compressor, and 4 kW for the air conditioner. This means that, just as with the heater, in order to model these auxiliary electronics telemetry data should be provided. The combined auxiliary power is divided by the same efficiency as the heater (95%) in order to get the BNU power of the model.

Table 3.5: Look-up table connecting ambient temperature with average power. The duty ratio is derived from this average power. [33]

Temperature [°C]	Average power [kW]	Duty ratio [-]	Temperature [°C]	Average power [kW]	Duty ratio [-]	Temperature [°C]	Average power [kW]	Duty ratio [-]
-10	38.42	1.00	7	16	0.42	24	4	0.10
-9	38.42	1.00	8	15	0.39	25	5	0.13
-8	38.42	1.00	9	14	0.36	26	6	0.16
-7	38.42	1.00	10	12	0.31	27	7	0.18
-6	38.42	1.00	11	11	0.29	28	9	0.23
-5	37	0.96	12	10	0.26	29	10	0.26
-4	36	0.94	13	9	0.23	30	11	0.29
-3	34	0.88	14	8	0.21	31	12	0.31
-2	33	0.86	15	7	0.18	32	13	0.34
-1	31	0.81	16	5	0.13	33	14	0.36
0	30	0.78	17	4	0.10	34	16	0.42
1	29	0.75	18	3	0.08	35	17	0.44
2	27	0.70	19	2	0.05	36	18	0.47
3	26	0.68	20	1	0.03	37	19	0.49
4	24	0.62	21	1	0.03	38	20	0.52
5	23	0.60	22	2	0.05	39	21	0.55
6	17	0.44	23	3	0.08	40	22	0.57

The original model depended on measurement data as an input. This new HVAC model can be used to create custom HVAC power patterns based on ambient temperature as an input. Analysis of the measurement data of Arnhem trolleybus trips has shown that the HVAC power profile can be modelled as a duty cycle. Modelling this duty cycle was performed in Scheurwater [33]. The duty cycle has a fixed period of 300 seconds and the duty ratio is calculated based on the outside temperature. A look-up table was created based on measurement data [35]. The look-up table can be found in Table 3.5. It shows the corresponding average HVAC power and duty ratio for ambient temperatures from -10 [°C] to 40 [°C].

3.5. Energy approach

This first approach is in some way a simplification of the power approach. Instead of looking at the power demand at each timestep, this approach looks at the amount of energy picked up while in the charging corridor. For this, a simpler IMC bus model was used with some simplifying assumptions. In this section the model, assumptions and intended outcome will be explained. The performed simulation was used to show the effect that average velocity in the charging corridor has on the amount of energy picked up. It can be seen as proof of whether or not this has more research potential. The results of this can be found in section 4.2.

3.5.1. Simplified IMC bus model

The IMC bus model used in this energy approach used the same parameters as shown in Table 3.1 except for a fixed vehicle mass of 20000 kg. The model uses a drive cycle in the form of the vehicle velocity as an input. The simplified model shares a lot of the same equations as can be found in the HAN model, but replaces the induction motor model by a fixed motor efficiency.

Both the acceleration and distance at each time step are derived from this using Equation 3.23 and Equation 3.24,

$$d_{\text{bus}} = \int V_{\text{bus}} dt \tag{3.23}$$

$$a_{\text{bus}} = \frac{dV_{\text{bus}}}{dt} \tag{3.24}$$

The traction power can then be calculated with Equation 3.25,

$$P_{\text{traction}} = V_{\text{bus}} \cdot (F_{\text{roll}} + F_{\text{aero}} + F_{\text{gradient}} + F_{\text{inertia}}) \tag{3.25}$$

Where, F_{roll} is rolling resistance, the force that a surface exerts on a body when the body rolls on the surface. F_{aero} is air drag (or aerodynamic resistance), the force exerted by a fluid onto the solid that moves through this fluid. F_{gradient} is gradient (or slope) resistance, the part of the gravitational force exerted on the bus that pulls the bus down along a slope. F_{inertia} is inertia (or acceleration) resistance, the force that resists any change in velocity. The rolling resistance is given by Equation 3.26,

$$F_{\text{roll}} = C_{\text{roll}} M_{\text{bus}} g \cdot cos(\theta) \tag{3.26}$$

Where, C_{roll} [-] is the coefficient of rolling resistance, M_{bus} [kg] is the total vehicle mass, g [ms^{-2}] is the gravitational acceleration, and θ [rad] is the slope of the road. The aerodynamic resistance is given by Equation 3.27,

$$F_{\text{aero}} = \frac{1}{2} \rho A_{\text{f}} C_{\text{d}} (V_{\text{bus}} + V_{\text{wind}})^2 \tag{3.27}$$

Where ρ [kgm^{-3}] is the air density; A_{f} [m^2] is the frontal area of the bus; C_{d} [$-$] is the drag coefficient. It also combines the bus velocity V_{bus} [ms^{-1}] and wind velocity V_{wind} [ms^{-1}] (with head wind being positive) into a relative velocity between bus and air. The gradient resistance is given by Equation 3.28,

$$F_{\text{gradient}} = M_{\text{bus}} \cdot g \cdot sin(\theta) \tag{3.28}$$

Which, just like the equation for rolling resistance, contains the bus mass M_{bus} [kg], the gravitational acceleration g [ms^{-2}], and the slope θ [rad].

The inertia resistance is given by Equation 3.29,

$$F_{\text{inertia}} = (M_{\text{bus}} + M_{\text{eq}}) \cdot a \tag{3.29}$$

Where M_{bus} [kg] is the mass of the bus, M_{eq} [kg] is the equivalent mass of rotating parts, and a is the acceleration of the bus. Instead of the equivalent mass of rotating parts, the model uses C_{inertia} a rotational inertia factor which factors in the rotational inertia based on the mass of the bus. The inertia resistance is then given by Equation 3.30,

$$F_{\text{inertia}} = M_{\text{bus}} \cdot C_{\text{inertia}} \cdot a \tag{3.30}$$

3.5.2. Simulation set-up

The simulation makes use of a measured drive cycle from test drives in Arnhem. This and other assumptions that were used for the simulation are:

- The auxiliary power which includes all power usage except traction power is set at a constant of 20 [kW],
- The slope of the road is set to zero,
- The efficiency of the battery is set to 95%,
- The efficiency of the electrical motor including its converter is set to 80%,
- The power that can be taken from the grid is fixed at 60 [kW] during stops and 300 [kW] while driving,
- The maximum charging power of the battery has no limit such that even when maximum regenerative braking and maximum power from the grid apply it still takes in all power (see Equation 3.31e),
- The used drive cycle is taken from measurements of Arnhems trolleybus line 1 (Oosterbeek to Velp, Line1_O2V_min),
- The charging corridor length is set at 20% of the total travel distance.

The first four assumptions are rather straightforward. Fixing the auxiliary power and slope of the road as well as the battery and electrical motor efficiency is done as these factors are not the main point of concern for this simulation. The difference in charging power during stops and while driving is however important, as the effect of this will become clear in the results and the discussion that follows from it. The maximum charging power of the battery not being limited again is there as it is not of concern here. The drive cycle, although necessary to mention, can be interchanged if wanted. The same can be said of the charging corridor length,

but results will show that this value of 20% is a desirable value. The last two assumptions give a total travel distance of 11.86 [km] which means that the charging corridor will be 2.37 [km] in length.

The simulation set-up is based on equations 3.31a to 3.31e. With the first two equations the energy that is picked up (E_{pick}) and the energy that is required for a round trip ($E_{\text{pick,req}}$) can be determined. E_{pick} is calculated by adding the energy picked up while moving to the energy picked up while stopped. $P_{\text{pick,move}}$ and $P_{\text{pick,stop}}$ are the fixed charging powers while moving (300 [kW]) and while stopped (60 [kW]) respectively. These are multiplied by the respective amounts of time spent inside the charging corridor, which is t_{tot} minus t_{stop} for time moving, and simply t_{stop} for time stopped.

The amount of energy picked up required for a round trip ($E_{\text{pick,req}}$) is set equal to the driving range outside the charging corridor (DR) times the specific energy consumption per kilometre (E_{specific}). Picking up this amount of energy ensures that after each round trip the state of charge of the battery returns to the energy level prior to the round trip. This is a simplification and one of two battery charging strategies. In reality this value can also be lower depending on the size of the battery. A full battery at the start of the day with a larger capacity can slowly deplete after each round trip. Overnight this battery can then be charged back to full. These two strategies are further investigated in section 3.3.

SOC_{f} is the final SOC which can be found with Equation 3.31c. It takes the initial SOC and subtracts or adds the difference after the trip from it. The next equation, Equation 3.31d, is similar to the assumption that there is no charging power limit. It states that the charging power of the battery (P_{bat}) can be as high as the charging power while moving and regenerative power combined.

$$E_{\text{pick}} = P_{\text{pick,move}}(t_{\text{tot}} - t_{\text{stop}}) + P_{\text{pick,stop}}\, t_{\text{stop}} \tag{3.31a}$$

$$E_{\text{pick,req}} = \text{DR} * E_{\text{specific}} \tag{3.31b}$$

$$\text{SOC}_{\text{f}} = \text{SOC}_{\text{i}} - \frac{E_{\text{pick,req}} - E_{\text{pick}}}{E_{\text{bat}}} \tag{3.31c}$$

$$P_{\text{bat}} = P_{\text{pick,move}} + P_{\text{regen}} \tag{3.31d}$$

$$t_{\text{tot}} = \frac{x_{\text{cc}}}{V_{\text{avg}}} \tag{3.31e}$$

The final equation of this set, Equation 3.31e, is important for the simulation as it connects the amount of energy picked up with the average velocity (V_{avg}) through the total time inside the charging corridor (t_{tot}). x_{cc} is the length of the charging corridor, which is fixed at 2.37 km as earlier stated. The simulation will be performed a total of 95 times with the position of the charging corridor shifting by 100 meters for every iteration (i.e. the charging corridor in the first simulation is positioned from 0 [km] to 2.47 [km], in the second simulation the charging corridor is positioned from 0.1 [km] to 2.57 [km], etc.). This is illustrated in Figure 3.7. The charging corridor position of the first simulation is shown in the top graph with a red dashed line starting at 0 [km] (red dot) and ending at 2.47 [km] (red square). The bottom graph shows the starting points of all 95 iterations (red dots) and the final iteration charging corridor is depicted with a red dashed line starting at 9.4 km.

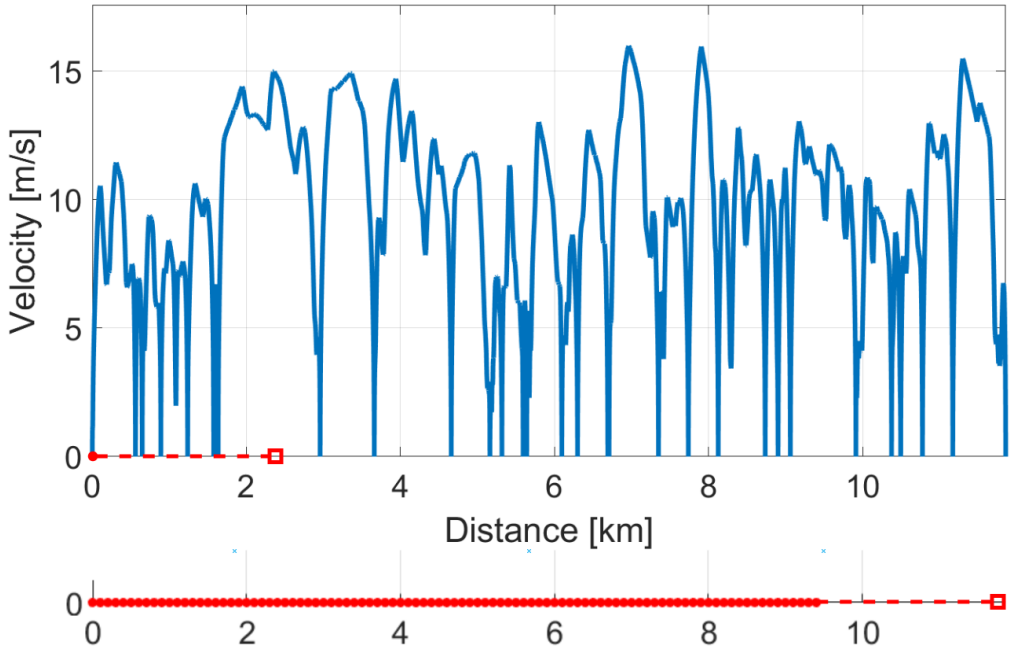

Figure 3.7: Top graph: velocity over distance of the Line1_O2V_min drive cycle in blue. In red the first iteration charging corridor position is illustrated. Bottom graph: the starting points of each of the 95 iterations are indicated with red dots. The final iteration charging corridor is depicted by the dotted line ending with a red square.

As the position of the charging corridor is different for each iteration of the simulation, both V_{avg} and E_{pick} will be different for each iteration. It can be expected that there is a correlation between the two as a decrease in t_{tot} as a result of an increase in V_{avg} will mean less time charging. However, because the ratio of time stopped versus time moving inside the charging corridor can be different as well the correlation will not be completely linear. This can be observed simply by comparing the velocity over distance profile in Figure 3.7 with Figure 3.8. For instance, the iterations which include the large stopping time from 900 to 1200 seconds will have a low average velocity. This is further elaborated in the results section of the energy approach (section 4.2).

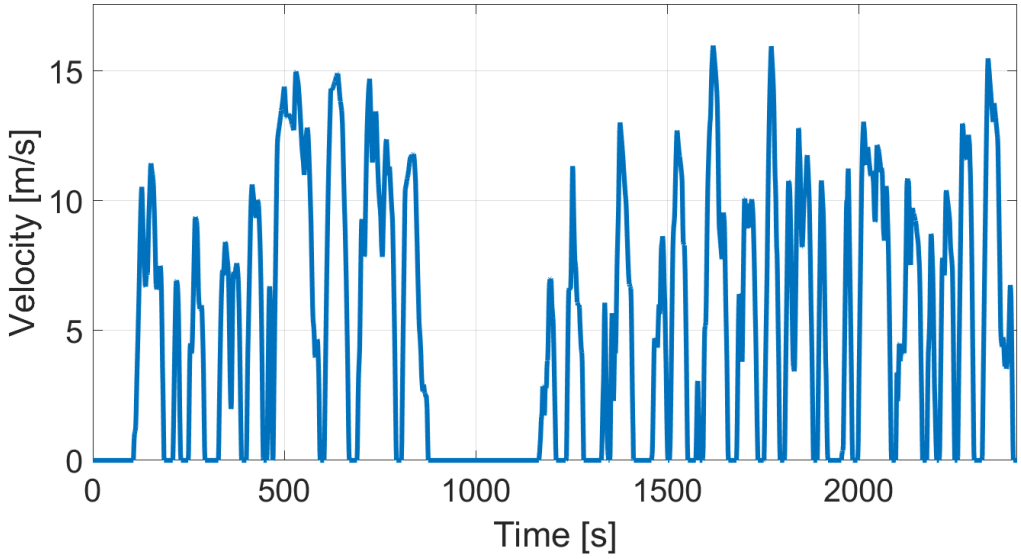

Figure 3.8: Velocity over time of the Line1_O2V_min drive cycle

3.6. Power approach and Arnhem case study

The power approach will be used for the main part of the research of this thesis. Instead of looking at the energy picked up in a whole trip this approach will look at the power flows at each time step. This is better suited specifically for looking into the effect of charging power limits. The simplified model used for the energy approach is expanded by more accurately portraying the motor behaviour. Instead of assuming an 80 percent efficiency of the engine the mechanical transmission model and induction motor model from section 3.4 are introduced.

In this case study the effect of an IMC bus implementation on the Arnhem trolleybus grid was simulated and investigated. This implementation is the replacement of gas bus lines by IMC range extension buses. The study was performed for bus lines 4, 13, 29, and 352, all of which are currently bus lines that make use of gas buses.

To model both the regular trolleybuses and IMC buses drawing power from the trolleygrid a complete representation of the grid was made. This was done by identifying 40 separate feed-in sections which are connected to 19 different substations. Modelling the position and power of each individual bus made it possible to perform power flow calculations for each timestep for each section. This way an accurate representation of both the total power and transmission losses for each substation could be made. A full map overview of these sections can be found in Figure 3.9.

A map with all bus lines in Arnhem including both regular trolleybus lines (i.e. lines 1, 2, 3, 5, 6, and 7) and proposed IMC range extension bus lines (i.e. lines 4, 13, 29, and 352) can be found in Figure 3.10. Each regular trolleybus line (of which there are six) has a different route which can be seen as a path along different feed-in sections. The suggested IMC bus lines all share some part of the route of a regular trolleybus line. Because of that the velocity profiles gathered from measurement data of the regular trolleybus lines can also be used for the trolley mode parts of the IMC bus lines. Trolley mode here means part of the IMC bus route on which it functions as a trolleybus (i.e. it is connected to the overhead lines). The other part of the route is considered the battery mode (i.e. the bus is not connected to overhead lines and drives autonomously). For all ten lines in total the simulation considers a full (work)day simulation. This is the most common schedule as it is performed on five days a week excluding holidays.

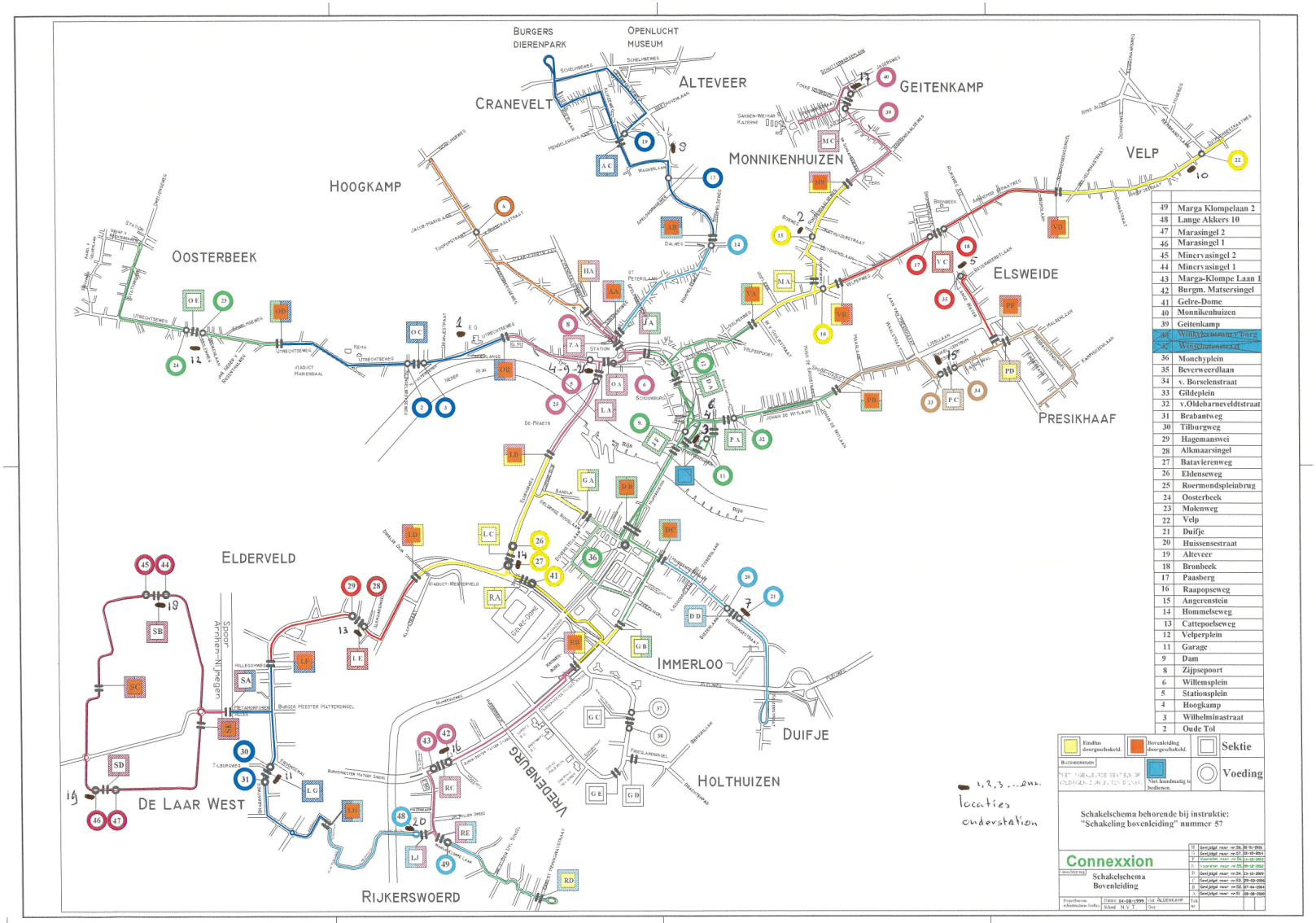

49	Marga Klompelaan 2
48	Lange Akkers 10
47	Marasingel 2
46	Marasingel 1
45	Minervasingel 2
44	Minervasingel 1
43	Marga-Klompe Laan 1
42	Burgm. Matsersingel
41	Gelre-Dome
40	Monnikenhuizen
39	Geitenkamp
38	Winkelsestraat
37	Winkelsestraat
36	Monchyplein
35	Beverweerdlaan
34	v. Borselenstraat
33	Gildeplein
32	v.Oldebarneveldtstraat
31	Brabantweg
30	Tilburgweg
29	Hagemanswei
28	Alkmaarsingel
27	Batavierenweg
26	Eldenseweg
25	Roermondspleinbrug
24	Oosterbeek
23	Molenweg
22	Velp
21	Duifje
20	Huissensestraat
19	Alteveer
18	Bronbeek
17	Paasberg
16	Raapopseweg
15	Angerenstein
14	Hommelseweg
13	Cattepoelseweg
12	Velperplein
11	Garage
9	Dam
8	Zijpsepoort
6	Willemsplein
5	Stationsplein
4	Hoogkamp
3	Wilhelminastraat
2	Oude Tol

Figure 3.9: Overview of feed-in sections and substation positions of the Arnhem trolleygrid. [17]

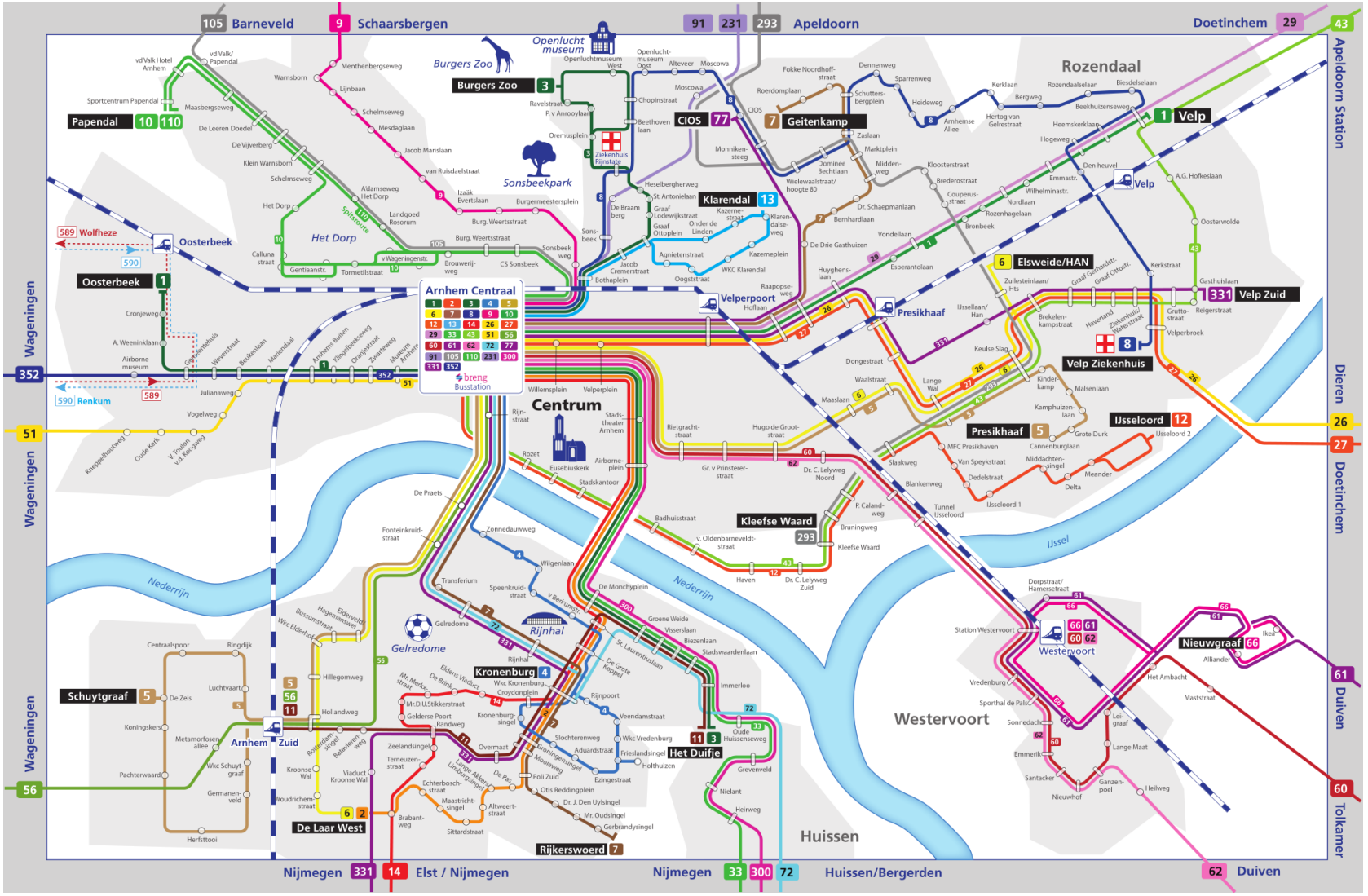

Figure 3.10: Map of bus lines in and around Arnhem. [13] (Full map can be downloaded from `https://www.breng.nl/nl/onze-routes/dienstregeling-en-halte-informatie/lijnennetkaarten-en-lijnfolders`. Choose 'Lijnennetkaart Arnhem stadlijnen'.)

3.6.1. Creating individual bus timetables

The simulation was performed by combining measured drive cycles (i.e. velocity profiles) of all six trolleybus lines with the timetables of both trolleybus lines (i.e. lines 1, 2, 3, 5, 6, and 7) and proposed IMC range extension bus lines (i.e. lines 4, 13, 29, and 352). Timetables were taken from the Breng website [13]. Breng is the bus operator in the Arnhem-Nijmegen metropolitan area.

In the first couple simulations a single (school holiday) workday schedule was required. By combining drive cycles and timetables a full regular workday of bus operation could be simulated. This set-up consisted of a total of 32 trolleybuses and 12 IMC buses. The numbers of buses per bus line for both regular trolleybuses and IMC buses is given in tables Table 3.6a and Table 3.6b respectively.

Table 3.6: Number of simulated trolleybuses and IMC buses for a full weekday simulation per bus line (*Buses of line 2 turn into line 6 and vice versa at terminus De Laar West so they share the same buses.)

(a) Regular trolleybus lines

Line	# of buses
1	6
2 and 6*	8
3	6
5	5
7	7

(b) IMC bus lines

Line	# of buses
4	2
13	1
29	3
352	6

Later on a more complete representation of a full year was simulated. It was created by adding in timetables for other types of schedules of which there are six in total. In Table 3.7 for each of the six types of schedules the number of buses used in the simulation is given. Next to that the type of schedule corresponding to each line is given. Most of these corresponding schedules are obvious (i.e. all lines use the regular schedule on a regular weekday). There are some exceptions like line 7 which has no separate Summer weekday schedule but shares this schedule for all school Holiday weekdays. The total number of buses for each type of day is given in the bottom row of the table.

The amount of buses per line was found by making logical individual bus timetables by looking at times of arrival and departure at final stops and Arnhem Central Station. Per example, a bus with an arrival time of 15:30 and a departure time of 15:40 at the same terminus is considered as the same bus in this simulation. This way the simulation does not just consist of individual bus trips but will also include buses that are waiting for a new trip to commence while still drawing power for HVAC. An example of the work performed for creating these individual timetables can be found in Figure 3.11.

Arnhem Central Station can be seen as the main hub of the trolleybus grid as each trolleybus line passes it. Each of the individual bus timetables was converted into an array of departure step numbers where each second is one step starting at 5:00 AM (i.e. step 1 is 5:00:00 AM, step 2 is 5:00:01 AM all the way to step 75600 for 1:59:59 AM the next night). These arrays were accompanied by string arrays containing descriptive strings of the trip that the bus would start performing at the corresponding step (e.g. "Vel2Cen" for a trip from Velp to Arnhem Central Station and "Cen2Vel" for a trip from Arnhem Central Station to Velp). A full list of trips and their trip names for the regular trolleybuses is given in table Table 3.8. An example of the creation of a list of 'steps and strings' for each individual bus can be found in Figure 3.12.

3.6.2. Generating bus traction and HVAC power vectors

For each of these trips a set of three vectors was made. The three vectors contain velocity, distance travelled and motor power at each time step. The velocity vectors were extracted from the lowest consumption measurement data files which are described in Appendix A. The distance travelled and motor power were both obtained by running the bus model which is described in section 3.4. A different (higher) empty mass was chosen for the IMC bus lines as the on-board traction battery can result in a considerably higher mass. This has a negative impact on the energy consumption of the bus as can be seen in Table 4.2.

The empty mass of all regular trolleybuses was set to 18270 [kg] as this is the known empty mass as seen in Table B.1. A different empty mass was chosen for each of the four IMC bus lines. It was based on the 18665 [kg] empty mass of the two IMC buses currently in use in Arnhem. This empty mass is with a 76 [kWh] battery. As all four of the IMC bus lines (except for line 13) require a larger battery capacity than that in order

Table 3.7: Number of buses per schedule type for each bus line. All six types of schedules are represented.

LINE	Regular weekday		Regular Saturday		Summer weekday		Summer Saturday		School Holiday weekday		Sun- and special holiday	
1	6	Regular	6	Saturday	3	Sum. Work	3	Sum. Sat.	6	Regular	3	Sun- Holiday
2/6	10	Regular	10	Saturday	5	Sum. Work	5	Sum. Sat.	8	Scho. Work	5	Sun- Holiday
3	6	Regular	7	Saturday	6	Sum. Work	6	Sum. Sat.	6	Regular	5	Sun- Holiday
5	6	Regular	6	Saturday	3	Sum. Work	3	Sum. Sat.	5	Scho. Work	3	Sun- Holiday
7	10	Regular	7	Saturday	7	Scho. Work	7	Saturday	7	Scho. Work	6	Sun- Holiday
4	2	Regular	2	Saturday	2	Regular	2	Saturday	2	Regular	2	Sun- Holiday
13	1	Regular	0	-	1	Regular	0	-	1	Regular	0	-
29	3	Regular	0	-	3	Regular	0	-	3	Regular	0	-
352	9	Regular	3	Saturday	6	Scho. Work	3	Saturday	6	Scho. Work	6	Sun- Holiday
TOTAL:	53		41		36		29		44		30	

Gegevens van breng.nl, donderdag 1 oktober 2020

O2V					V2O				
VAN		NAAR			VAN		NAAR		
Station Oosterbeek	Station Velperpoort	Centraal Station	Beekhuizenseweg		Beekhuizenseweg	Centraal Station	Centraal Station	Station Oosterbeek	BUS
5:59	-	06:34	0:35		5:44	-	05:57		1
6:35	-	06:49	6:49		6:04	-	06:17		2
6:19	-	06:54	0:35		6:19	-	06:32		3
6:34	-	07:09	0:35		6:34	-	06:47		4
6:49	-	07:27	0:38		6:21	-	06:55		5
7:03	-	07:44	0:41		6:36	-	07:12		6
7:18	-	08:00	0:42		6:51	-	07:28		
7:31	-	08:15	0:44		7:04	-	07:43		
7:46	-	08:30	0:44		7:19	-	07:58		
8:01	-	08:45	0:44		7:32	-	08:13		
8:16	-	09:00	0:44		7:47	-	08:28		
8:31	-	09:14	0:43		8:02	-	08:41		
8:46	-	09:28	0:42		8:18	-	08:56		
9:03	-	09:43	0:40		8:34	-	09:11		
9:18	-	09:58	0:40		8:49	-	09:26		
9:33	-	10:13	0:40		9:04	-	09:41		
9:48	-	10:28	0:40		9:19	-	09:56		
10:03	-	10:43	0:40		9:34	-	10:11		
10:18	-	10:58	0:40		9:49	-	10:26		
10:33	-	11:13	0:40		10:04	-	10:41		
10:48	-	11:28	0:40		10:19	-	10:56		
11:03	-	11:43	0:40		10:34	-	11:11		
11:18	-	11:58	0:40		10:49	-	11:26		
11:33	-	12:13	0:40		11:04	-	11:43		
11:48	-	12:28	0:40		11:18	-	11:58		
12:03	-	12:44	0:41		11:32	-	12:13		
12:18	-	12:59	0:41		11:47	-	12:28		
12:32	-	13:14	0:42		12:02	-	12:43		
12:47	-	13:29	0:42		12:17	-	12:58		

Figure 3.11: An example of individual timetable creation by colouring matching arrival and departure times of a full bus line timetable. This is for bus line 1.

BUS 1							BUS 2						
				step number							step number		
Power on	Centraal	5:34		2341	Turnon		Power on	Centraal	5:54		3541	Turnon	
Depart	Centraal	5:44	600	2941	Cen2Oos	0:15	Depart	Centraal	6:04	600	4141	Cen2Oos	0:15
Depart	Oosterbeek	5:59	1500	3841	Oos2Cen	0:16	Depart	Oosterbeek	6:19	1500	5041	Oos2Cen	0:16
Depart	Centraal	6:15	2460	4801	Cen2Vel	0:21	Depart	Centraal	6:35	2460	6001	Cen2Vel	0:29
Depart	Beekh'weg	6:36	3720	6061	Vel2Cen	0:21	Depart	Beekh'weg	7:04	4200	7741	Vel2Cen	0:23
Depart	Centraal	6:57	4980	7321	Cen2Oos	0:21	Depart	Centraal	7:27	5580	9121	Cen2Oos	0:19
Depart	Oosterbeek	7:18	6240	8581	Oos2Cen	0:17	Depart	Oosterbeek	7:46	6720	10261	Oos2Cen	0:19
Depart	Centraal	7:35	7260	9601	Cen2Vel	0:27	Depart	Centraal	8:05	7860	11401	Cen2Vel	0:29
Depart	Beekh'weg	8:02	8880	11221	Vel2Cen	0:25	Depart	Beekh'weg	8:34	9600	13141	Vel2Cen	0:23
Depart	Centraal	8:27	10380	12721	Cen2Oos	0:19	Depart	Centraal	8:57	10980	14521	Cen2Oos	0:21
Depart	Oosterbeek	8:46	11520	13861	Oos2Cen	0:19	Depart	Oosterbeek	9:18	12240	15781	Oos2Cen	0:17
Depart	Centraal	9:05	12660	15001	Cen2Vel	0:29	Depart	Centraal	9:35	13260	16801	Cen2Vel	0:29
Depart	Beekh'weg	9:34	14400	16741	Vel2Cen	0:23	Depart	Beekh'weg	10:04	15000	18541	Vel2Cen	0:23
Depart	Centraal	9:57	15780	18121	Cen2Oos	0:21	Depart	Centraal	10:27	16380	19921	Cen2Oos	0:21
Depart	Oosterbeek	10:18	17040	19381	Oos2Cen	0:17	Depart	Oosterbeek	10:48	17640	21181	Oos2Cen	0:17
Depart	Centraal	10:35	18060	20401	Cen2Vel	0:29	Depart	Centraal	11:05	18660	22201	Cen2Vel	0:27
Depart	Beekh'weg	11:04	19800	22141	Vel2Cen	0:23	Depart	Beekh'weg	11:32	20280	23821	Vel2Cen	0:25
Depart	Centraal	11:27	21180	23521	Cen2Oos	0:21	Depart	Centraal	11:57	21780	25321	Cen2Oos	0:21
Depart	Oosterbeek	11:48	22440	24781	Oos2Cen	0:17	Depart	Oosterbeek	12:18	23040	26581	Oos2Cen	0:17
Depart	Centraal	12:05	23460	25801	Cen2Vel	0:27	Depart	Centraal	12:35	24060	27601	Cen2Vel	0:27
Depart	Beekh'weg	12:32	25080	27421	Vel2Cen	0:25	Depart	Beekh'weg	13:02	25680	29221	Vel2Cen	0:25
Depart	Centraal	12:57	26580	28921	Cen2Oos	0:20	Depart	Centraal	13:27	27180	30721	Cen2Oos	0:20
Depart	Oosterbeek	13:17	27780	30121	Oos2Cen	0:18	Depart	Oosterbeek	13:47	28380	31921	Oos2Cen	0:18
Depart	Centraal	13:35	28860	31201	Cen2Vel	0:27	Depart	Centraal	14:05	29460	33001	Cen2Vel	0:27
Depart	Beekh'weg	14:02	30480	32821	Vel2Cen	0:25	Depart	Beekh'weg	14:32	31080	34621	Vel2Cen	0:25
Depart	Centraal	14:27	31980	34321	Cen2Oos	0:20	Depart	Centraal	14:57	32580	36121	Cen2Oos	0:19

Figure 3.12: An example of a list of 'steps and strings' for an individual bus timetable. This is for buses 1 and 2 of bus line 1.

Table 3.8: Trips for each of the six regular trolleybus lines. A descriptive string is used to distinguish them. The last column shows which feed-in sections are passed for each trip. *In reality the buses alternate direction in the loop

Line	String	Trip description	Feed-in sections (in trip order)
1	Cen2Oos	Arnhem CS to Oosterbeek	5, 3, 2, 23, 24
	Cen2Vel	Arnhem CS to Velp	5, 6, 12, 16, 17, 18, 22
	Oos2Cen	Oosterbeek to Arnhem CS	24, 23, 2, 3, 5
	Vel2Cen	Velp to Arnhem CS	22, 18, 17, 16, 12, 6, 5
2	Cen2Dlw	Arnhem CS to De Laar West	5, 6, 12, 9, 36, 41, 42, 43, 48, 31
	Dlw2Cen	De Laar West to Arnhem CS	31, 48, 43, 42, 41, 36, 9, 12, 6, 5
3	Cen2Dui	Arnhem CS to Het Duifje	5, 6, 12, 9, 36, 20, 21
	Cen2Zoo	Arnhem CS to Burgers' Zoo	5, 6, 8, 14, 13, 19
	Dui2Cen	Het Duifje to Arnhem CS	21, 20, 36, 9, 12, 6, 5
	Zoo2Cen	Burgers' Zoo to Arnhem CS	19, 13, 14, 8, 6, 5
5	Cen2Pre	Arnhem CS to Presikhaaf	5, 6, 12, 9, 32, 33, 34
	Cen2Zei	Arnhem CS to Schuytgraaf*	5, 25, 26, 27, 28, 29, 30, 44, 45
	Pre2Cen	Presikhaaf to Arnhem CS	34, 33, 32, 9, 12, 6, 5
	Zei2Cen	Schuytgraaf to Arnhem CS*	45, 44, 30, 29, 28, 27, 26, 25, 5
6	Cen2Han	Arnhem CS to Elsweide/HAN	5, 6, 12, 9, 32, 33, 34, 35
	Cen6Dlw**	Arnhem CS to De Laar West	5, 25, 26, 27, 28, 29, 30, 31
	Han2Cen	Elsweide/HAN to Arnhem CS	35, 34, 33, 32, 9, 12, 6, 5
	Dlw6Cen**	De Laar West to Arnhem CS	31, 30, 29, 28, 27, 26, 25, 5
7	Cen2Gei	Arnhem CS to Geitenbeek	5, 6, 12, 16, 15, 39, 40
	Cen2Rij	Arnhem CS to Rijkerswoerd	5, 25, 26, 27, 41, 42, 43, 49
	Gei2Cen	Geitenbeek to Arnhem CS	40, 39, 15, 16, 12, 6, 5
	Rij2Cen	Rijkerswoerd to Arnhem CS	49, 43, 42, 41, 27, 26, 25, 5

Table 3.9: Trips for each of the four IMC bus lines. A descriptive string is used to distinguish them. The second to last column shows which feed-in sections are passed for each trip. The last column indicates of which regular trolleybus trip the trip is part of.

Line	String	Trip description	Feed-in sections (in trip order)	Part of
4	Cen2Pra	Arnhem CS to De Praets	5, 25	Cen2Zei
	Pra2Cen	De Praets to Arnhem CS	25, 5	Zei2Cen
13	Cen2Ott	Arnhem CS to Graaf Ottoplein	5, 6, 8, 14	Cen2Zoo
	Ott2Cen	Graaf Ottoplein to Arnhem CS	14, 8, 6, 5	Zoo2Cen
29	Cen2Vel	Arnhem CS to Velp	5, 6, 12, 16, 17, 18, 22	Cen2Vel
	Vel2Cen	Velp to Arnhem CS	22, 18, 17, 16, 12, 6, 5	Vel2Cen
352	Cen2Gem	Arnhem CS to Gemeentehuis Oosterbeek	5, 3, 2, 23, 24	Cen2Oos
	Gem2Cen	Gemeentehuis Oosterbeek to Arnhem CS	24, 23, 2, 3, 5	Oos2Cen

Table 3.10: Masses of IMC buses for the four different bus lines. Each bus line has a different autonomous trip distance and therefore requires a different battery size. Mass is based on battery capacity at 5 kg/kWh and 3.5 kWh/km and a . *The minimum battery capacity is 76 kWh as this is the battery capacity of IMC buses currently in use of which empty vehicle mass is known.

Line	Autonomous trip distance [km]	With added 20% margin [km]	Total energy [kWh] (e = 3.5 kWh/km)	Battery capacity [kWh] (usable SOC 0.2-0.6)	Rounded battery capacity [kWh]	Empty bus mass [kg]
4	12.3	14.76	51.66	129.15	130	18935
13	3	3.6	12.6	31.5	*76	18665
29	55	66	231	577.5	580	21185
352	26.4	31.68	110.88	277.2	280	19685

to complete the autonomous part of the trip this empty mass is increased by 5 [kg/kWh]. The battery capacity necessary to complete the trips is for a 3.5 [kWh/km] energy consumption based on the measurement data on Arnhem trolleybuses described in Appendix A. This energy consumption is considered worst case (i.e. both high traction energy and high HVAC energy).

Table 3.10 shows the autonomous trip distance of each of the bus lines. A 20% margin is added to each of them and together with the fixed energy consumption of 3.5 [kWh/km] a total energy consumption for each autonomous trip can be found. As the battery used in the Arnhem IMC buses a usable SOC of 40% of its total SOC (i.e. from 20% to 60%) this energy consumption is multiplied by 2.5 to obtain a battery capacity in [kWh]. A final step of rounding up is performed which results in four different battery capacities. For bus line 13 this means that battery capacity is rounded up to the lowest amount possible (i.e. 76 [kWh]). This is the battery capacity of the IMC buses currently in use in Arnhem. The empty vehicle masses of these buses is known. This is considered the lower value of the battery including all other battery electronics (e.g. battery converter). As such it is safe to assume that capacity can be increased by 5 [kg/kWh] which is the average mass of batteries used in IMC buses. There is a higher uncertainty for decreasing the mass as it is not known how much of the 76 [kWh] battery mass is just the batteries and how much is other battery electronics.

All of these separate trips start or end at Arnhem Central Station. This means that for all regular trolleybus lines four of these trips were extracted (i.e. two trips coming in Arnhem Central Station from either terminus and another two going out from Arnhem Central Station towards either terminus). There is an exception for line 2 which only has two trips as Arnhem Central Station is one of the termini.

Separate trip vectors were made for most of the IMC range extension bus lines. This is because although these bus lines share part of the route, the buses have to (dis)connect at the bus stop closest to where the bus lines separate. No velocity profiles for the autonomous part of the routes were used. Instead a constant energy consumption of 2.5 [kWh/km] was assumed, based on the average of measurement data. See Appendix A. The velocity profiles on parts of the routes where the IMC buses are connected to the grid were obtained as follows.

- Bus line 4: Arnhem CS - Kronenburg. It shares the same route with trolleybus lines 5, 6 and 7 until bus stop De Praets. Its velocity profile was extracted from one of these lines. The velocity profile of line 5

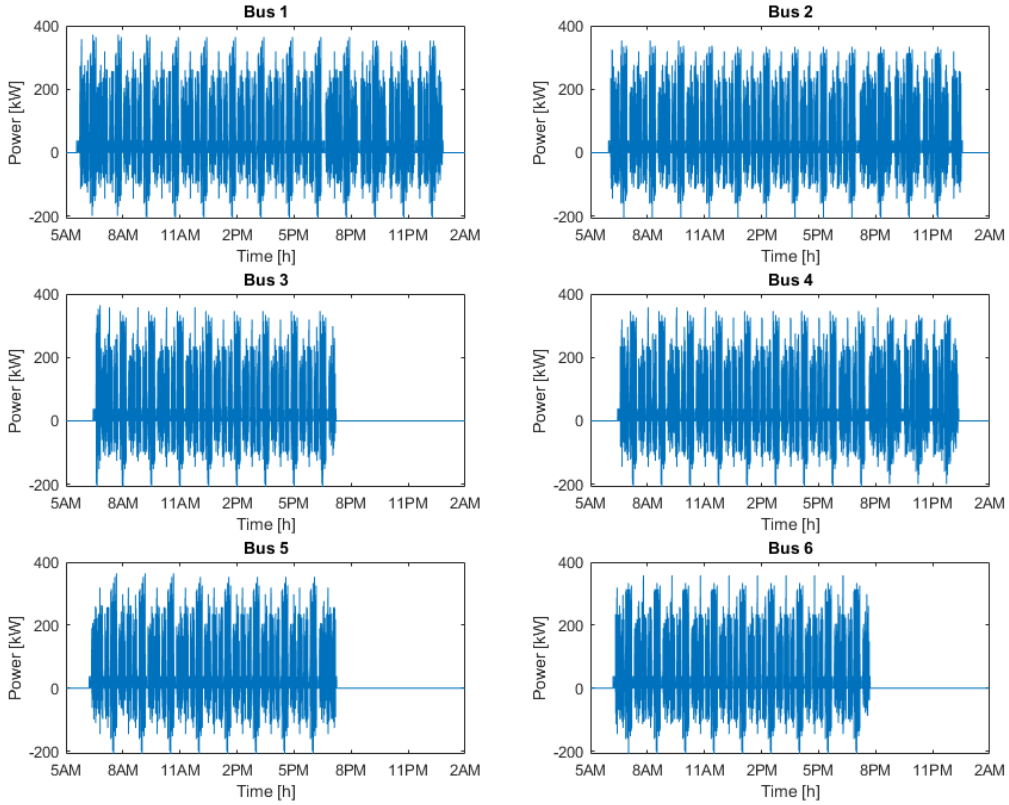

Figure 3.13: Simulated traction powers of six buses of line 1. It can be seen that some of the buses will only drive until around 7:30 PM. This is because the bus schedule requires less buses in the evening/night.

was chosen for this. This profile was slightly altered by including a 15 second acceleration/deceleration section at De Praets as no measurement data was found in which either bus line 5, 6 or 7 stopped at this bus stop.

- Bus line 13: Arnhem CS - Klarendal. The bus (dis)connects at bus stop Graaf Ottoplein. The route is part of the route of bus line 3 and therefore its velocity profiles are parts of the bus line 3 profiles.

- Bus line 29: Arnhem CS - Doetinchem. Line 29 follows the same route as the east part of bus line 1 all the way to its terminus at Velp. Therefore the same velocity profiles as for (the east part of) line 1 were used.

- Bus line 352: Arnhem CS - Wageningen Station. This bus line runs along the route of the west part of bus line 1 up until bus stop Gemeentehuis (Oosterbeek). The velocity profiles were gathered by taking the velocity profiles of line 1 up to that bus stop.

With this information a total of 30 velocity vectors were gathered. By running the trolleybus model with the velocity profiles and varying masses as input both the distance and traction power vectors could be created. These can later be used and combined to create bus position data and total bus power data for all days in a year for each individual bus. An example of simulated traction powers can be found in Figure 3.13.

The HVAC power should also be accounted for for each full day for each bus. By combining the look-up table information (Table 3.5) with a list of hourly ambient temperatures for a day in Arnhem a full day cycle of HVAC power can be made. This full day cycle is a long string of duty cycles. This full day cycle can be customised for each individual bus by looking at the times at which the bus powers on and shuts off.

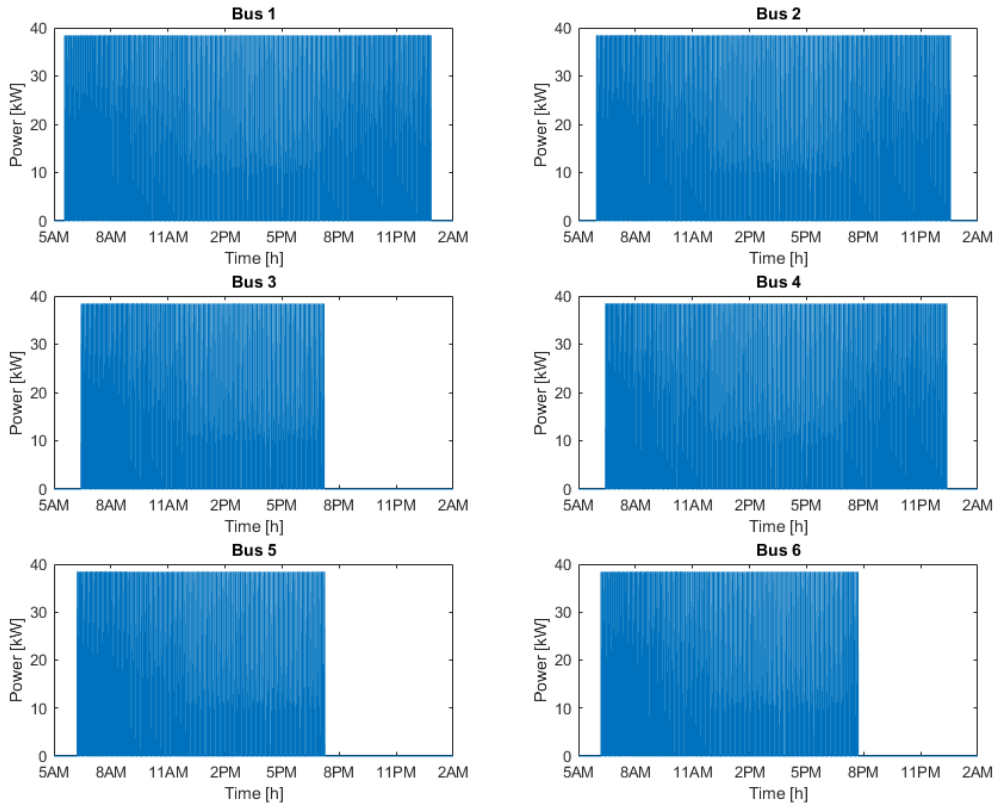

Figure 3.14: Simulated HVAC powers of the six buses of line 1.

Line 1 - Velp to Oosterbeek

RELATIVE			ABSOLUTE								
X0	Xs	X1	X0	Xs	X1	Bus location	Vs	Voeding	Substation	Points on route	
0	277	1579	0	277	1579	1579	716	22	10	starts	0
1580	2760	2819	0	1180	1239	2819	700	18	5		
2820	2860	3809	0	40	989	3809	700	17	5		
3810	3950	4679	0	140	869	4679	698	16	2		
4680	5760	5789	0	1080	1109	5789	630	12	3	Split at	900
5790	6220	6239	0	430	449	6239	660	6	4		
6240	6390	7179	0	150	939	7179	660	5	4		
7180	8030	8119	0	850	939	8119	698	3	1		
8120	8200	9389	0	80	1269	9389	698	2	1		
9390	10160	10199	0	770	809	10199	686	23	12		
10200	10260	11700	0	60	1499	11650	686	24	12	final stop	11650

Line 2 - Arnhem Central to Zuid-Laren

RELATIVE			ABSOLUTE								
X0	Xs	X1	X0	Xs	X1	Bus location	Vs	Voeding	Substation	Strange points on route	
0	60	260	0	60	260	260	685	5	4	starts	0
261	280	709	0	19	449	709	685	6	4		
710	1070	1109	0	360	400	1109	630	12	3		
1110	1608	1827	0	498	718	1827	660	9	6		
1828	2848	2687	0	1020	860	2687	630	36	3		
2688	2848	3907	0	160	1220	3907	630	36	3		
3908	5068	4408	0	1160	501	4408	628	41	14	split at	230
4409	5563	5602	0	1154	1194	5602	705	42	16		
5603	5643	6320	0	40	718	6320	705	43	16		
6321	6361	7998	0	40	1678	7998	?	48	?		
7999	9147	9186	0	1148	1188	8436	659	31	11	final stop	8436

Line 3 - Burgers' Zoo - Duifje

RELATIVE			ABSOLUTE								
X0	Xs	X1	X0	Xs	X1	Bus location	Vs	Voeding	Substation	Points on route	
0	1460	1580	0	1460	1580	1580	700	19	8	starts	0
1581	2470	3239	0	840	1659	3239	700	13	8		
3240	4500	4559	0	50	1320	4559	698	14	2		
4560	4610	4659	0	50	100	4659	698	8	4		
4660	4910	4979	0	250	320	4979	698	6	4		
4980	5310	5639	0	330	660	5639	698	5	4		
5640	5710	6079	0	70	440	6079	698	6	4		
6080	6440	6479	0	360	400	6479	630	12	3		
6480	6945	7156	0	465	677	7156	660	9	6		
7157	?	8016	0	1020	860	8016	630	36	3		
8017	8177	8526	0	160	510	8526	630	36	3		
8527	9327	9476	0	800	950	9476	724	20	7		
9477	9527	10536	0	50	1060	10537	724	21	7	final stop	10537

Figure 3.15: Part of table which contains the length, feed-in point position and distance relative to bus line trip distance for each feed-in section. X0 is at what trip distance the bus enters a section, Xs is where the feed-in point is and X1 is where the bus exits the section. [33]

3.6.3. Collecting and rectifying bus position data

For each of the 30 velocity vectors a distance vector was also created. This distance had to be converted into a position on the trolleygrid. A list of section lengths, feed-in point positions and distance relative to trip distance of each bus line was used in combination with the distance vectors for this [33]. Part of this list can be found in Figure 3.15. It shows the start and end point on the sections at either end of each line. It also shows the length of each section the bus passes in a full trip for each line and the feed-in point position on each section.

It was found that the combined cable length of sections passed for a whole trip is not exactly similar to the distance travelled. This can have multiple causes. For one, the cable length of a section might be over- or underestimated as this had to be estimated through the use of Google Maps. Apart from that, the bus might travel longer or shorter distance than the cable length as the bus can make wide or tight turns, the bus overtakes another vehicle or whenever the bus makes a slight detour as it stops at a bus stop. Figure 3.16 shows these differences. The final column shows the percentage difference for each trip. This was done for all original trips as mentioned in Table 3.8.

By multiplying each distance vector with the ratio of the original trip distance to the cable length the bus position was effectively scaled to the position on the cable. This was done to be sure that when the trip

		start	end	length	original	
Line 1	V2C	0	6389	6389	6414	**0.39%**
	C2O	6389	11650	5261	5345	**1.60%**
	O2C	0	5143	5143	5160	**0.34%**
	C2V	5143	11660	6517	6695	**2.73%**
Line 2	DL2C	755	9269	8514	8340	**-2.04%**
	C2DL	0	8436	8436	8564	**1.51%**
Line 3	BZ2C	0	5309	5309	5177	**-2.49%**
	C2HD	5309	10537	5228	5192	**-0.68%**
	HD2C	0	5131	5131	5074	**-1.11%**
	C2BZ	5131	10111	4980	4844	**-2.73%**
Line 5	DZ2C	370	8834	8464	8306	**-1.86%**
	C2P	8834	14777	5943	5832	**-1.87%**
	P2C	120	5826	5706	5676	**-0.53%**
	C2DZ	5826	14179	8353	8270	**-0.99%**
Line 6	DL6C	1270	8030	6760	6595	**-2.44%**
	C2H	8030	13543	5513	5396	**-2.12%**
	H2C	180	5316	5136	5017	**-2.32%**
	C6DL	5316	12278	6962	6965	**0.04%**
Line 7	GK2C	0	5593	5593	5426	**-2.99%**
	C2R	5593	12648	7055	6936	**-1.69%**
	R2C	0	7000	7000	7006	**0.09%**
	C2GK	7000	12716	5716	5701	**-0.26%**

Figure 3.16: Combined length of all sections a bus passes for a specific trip compared to the (original) distance travelled in measurement data. The last column shows the percentage difference which can be used to scale the distance vector of each trip.

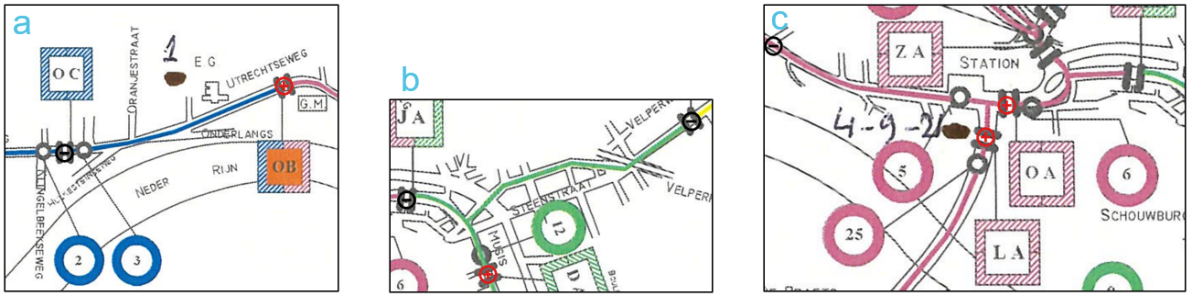

Figure 3.17: Three examples of the different feed-in section types that can be encountered. A) Straightforward sections. B) Forked sections (buses might not pass feed-in point in these sections). C) Arnhem CS section (buses turn around in this section).

distance vector was combined with the section lengths it would align properly. For instance, a bus might otherwise erroneously show up in the next section when it should be stopped at Arnhem CS.

This new distance vector could then be converted to position relative to the feed-in point of each section. To do this, three types of sections were first identified. The three types of sections can be found in Figure 3.17. Each straightforward section was assigned a positive and negative side and look-up tables were created to convert trip distance to position relative to feed-in point. This was a simple process for straightforward sections. In figure A of Figure 3.17 an example of a straightforward section is shown. The circle with a 3 indicates where the feed-in point is. At the short end a negative sign indicates the negative side while the red plus-sign indicates the positive side. By making sure that the sign is the same with buses coming in from both sides the position is always correct.

For the forked section, indicated with a B in Figure 3.17, the buses can enter at one sign and leave at the other (i.e. from positive to negative and vice versa). In that case, the look-up table is similar as used in straightforward sections. However, when the bus enters at one negative sign and leaves at the other negative sign the buses will never actually pass the feed-in point which in this example is located near the positive exit point. For these cases a look-up table in which the relative position increases at first and then decreases again after the cable intersection. This means that the two prongs of the fork are essentially combined as one for power flow purposes. This assumption should will cause the losses to appear slightly larger than in reality as currents that flow on two different pairs of parallel wires in reality are considered to flow on the same set of wires in the simulation. Transmission losses are however found to be a rather small part of total power demand (i.e. around 2.5% as per Figure 5.1 and Figure 5.2).

Next is section 5, which is the section containing Arnhem CS, indicated with a C in Figure 3.17. This section is a forked section as well with one big difference. For all bus lines (except bus line 1 which enters/leaves on the west side) the buses will enter from either south or east side and will leave again from either of those sides. Before leaving again the buses will stop at the terminus located a little bit beyond the feed-in point. For practical purposes the look-up table for these cases was made so that the bus reverses direction precisely at the point at which it stops.

3.6.4. Generating IMC battery power vectors

The traction battery model was used separately from the rest of the IMC bus model as traction power and HVAC power were modelled at an earlier stage already. Some extra conditions were added to the simple battery model for this specific case study. These are the section conditions and the reset condition.

The reset condition simply tells the model that the bus is reconnecting to the grid. At this point the SOC is reset to an initial condition which is a predefined value based on the autonomous trip distance [km] and the energy consumption [kWh/km]. Outside the grid, the model SOC will show as 0, while of course in reality it would slowly decrease towards the earlier mentioned initial condition while it travels along its route.

The section conditions are used in order to define the maximum charging powers for each section. This is done to be able to include variations in charging powers per section individually. The default maximum charging power values are 150 [kW] while moving and 100 [kW] while stopped.

Examples of the resulting battery SOC values and matching charging powers can be found in Figure 3.18 and Figure 3.19.

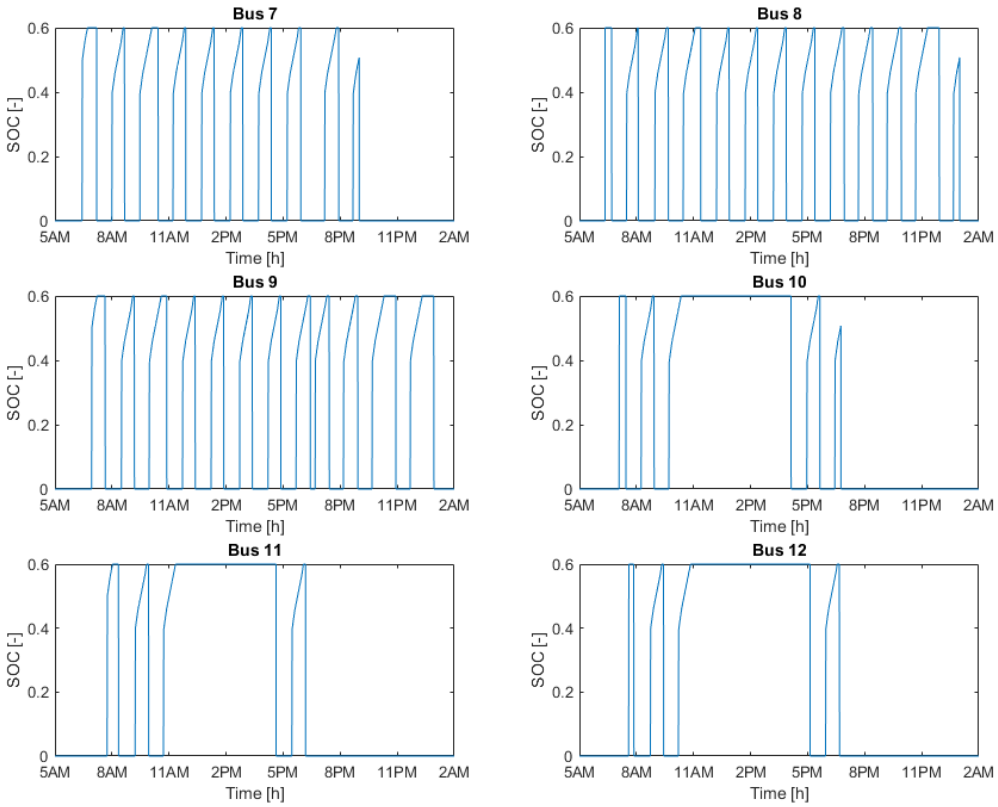

Figure 3.18: Simulated battery SOC levels for the six buses of line 352. Because SOC is only calculated when the bus is connected to the grid, its value is set to zero whenever the bus exits the grid. It can be seen that bus 10, 11 and 12 are not in use during the afternoon as the bus schedule requires less buses at that time. The bus SOCs therefore remain at 0.6 (i.e. full capacity).

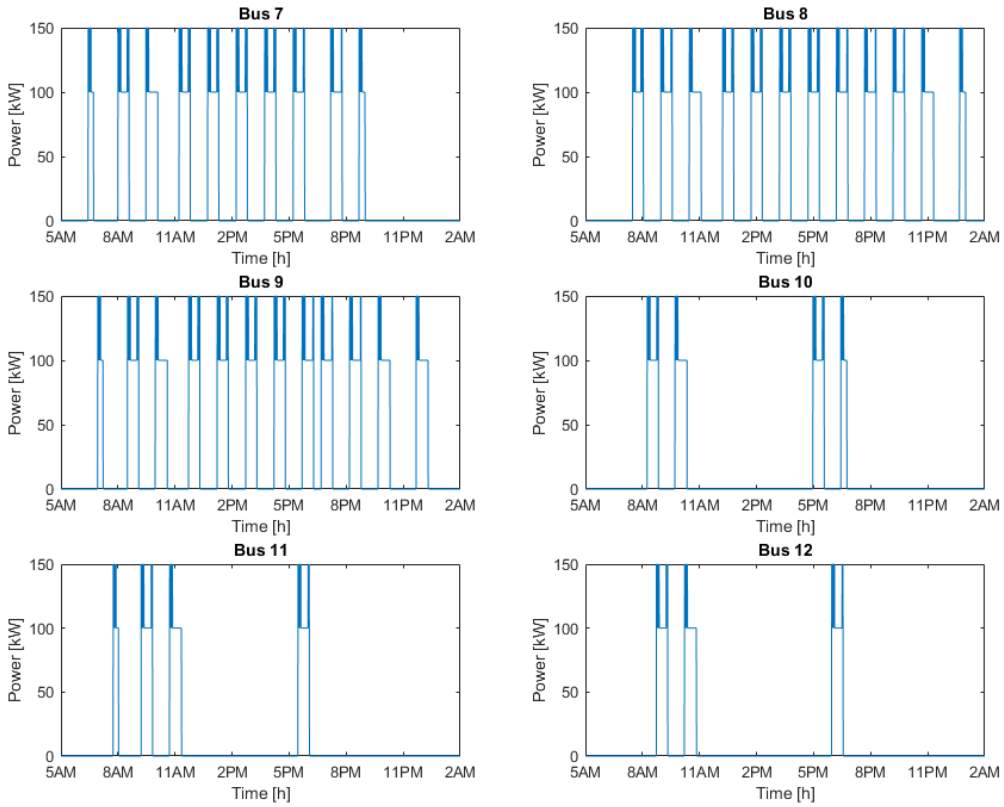

Figure 3.19: Simulated charging power values for the six buses of line 352. For these simulations the charging power was set to 100 [kW] while stopped and 150 [kW] while moving. It can be seen that bus 10, 11 and 12 are not in use during the afternoon as the bus schedule requires less buses at that time.

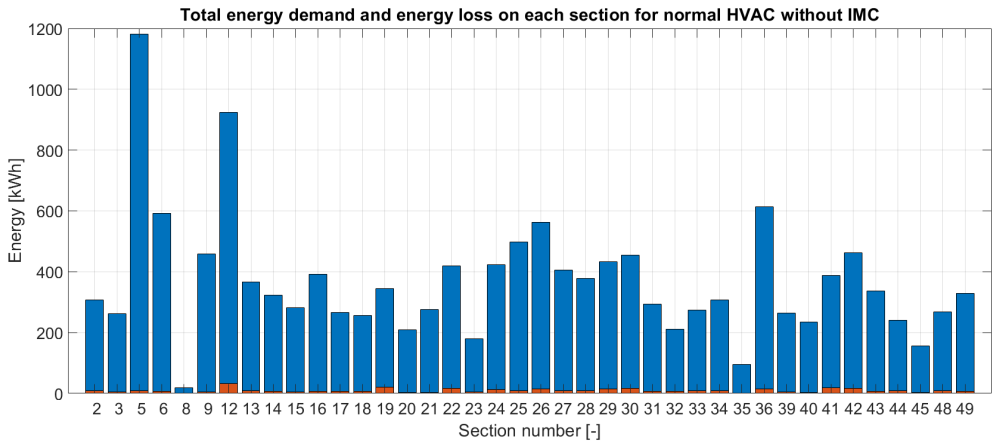

Figure 3.20: The total energy demand for a full workday per section. In this example a normal HVAC profile is used (i.e. temperatures around 15 [°C] and without IMC buses.

3.6.5. Input/output of Arnhem grid model

Now that all individual parts have been explained the the integration of parts that together form the input can be explained. Furthermore, it can now be explained how these inputs are used to calculate the outputs of the Arnhem trolleygrid model.

As the model considers full days (which together can form a year) of trolleybus operation each individual bus needs complete day cycle arrays of relevant data. This means that there are four sets per day of these arrays all 75600 steps (i.e. 21 hours in seconds) long for each of the 54 buses. The four sets are necessary for: the section the bus is on, relative position on each section, total bus power (excluding charging power) and the charging power.

The first two sets of arrays (section number and position on section) are created by combining the 'steps and strings' of each bus with the corresponding trip distance vectors. Before and after each trip the position and section number are added as well which means that the simulated bus will stay stationary between two trips.

Similarly, for the traction power part of the bus power the total bus power arrays are created by combining the 'steps and strings' of each bus with the corresponding bus power vectors. The HVAC power is added on top of that by only adding HVAC power when the bus is on. This is done by adding conditions which specify that HVAC power only applies during and 10 minutes before and after each trip. This attempts to simulate real behaviour as HVAC is kept on while the bus is waiting for its next trip to commence.

The charging power set of arrays is created with the total bus power arrays already known. This is done because a limitation of 500 [kW] total bus power demand is added. The charging power will be decreased whenever this limit would otherwise be exceeded. Next to that, the charging power also includes any regenerative braking power. Lastly, the velocity arrays are used to check whether the bus is moving or is stopped which has an impact on the maximum charging power.

The Arnhem trolleygrid model now needed two more inputs in order to calculate the power and transmission losses for each section. A list of substation number and substation voltages is added as inputs for the power flow calculation model. These two inputs connect the section numbers with the correct substations and for each power flow calculation the correct voltage at the feed-in point can now be selected. The list of substations, voltages and corresponding sections can be found in Table 3.11.

Now the power flow calculations could be performed which result in the total power and transmission losses per section as well as per substation. An example of this can be found in Figure 3.20. A final assumption for these calculations is that any regenerative power from regular trolleybuses that could be supplied to other trolleybuses on the same section is ignored. This was done as one of the main objectives of this case study was to identify any breaches of the maximum power demand of the substations.

Table 3.11: Substation numbers and voltages and their corresponding feed-in sections.

Substation	Voltage [V]	Section
1	698	2
		3
2	698	14
		15
		16
3	630	12
		36
4	685	5
		6
		8
5	700	17
		18
		35
6	660	9
		32
7	724	20
		21
8	700	13
		19
9	677	25
10	716	22
11	659	30
		31
12	686	23
		24
13	673	28
		29
14	628	26
		27
		41
15	684	33
		34
16	705	42
		43
17	728	39
		40
18	700	44
		45
20	700	48
		49

4

Trolley & IMC bus energy consumption comparison

This is the first of two chapters with results of the thesis. All results gathered from using the energy comparison, of which the methodology is described in chapter 3, can be found here. The first section discusses the difference in energy consumption of regular trolleybuses and IMC buses. The comparison suggests that the IMC buses could have a lower energy consumption as they make optimal use of regenerative braking power. The second section goes into picked up energy (i.e. battery charging of IMC buses) and how charging corridor positioning and average velocity can have an effect on it. It suggest that picked up energy is very reliant on charging corridor size and placement. Both of these suggestions are further investigated in the Arnhem case study in chapter 5.

4.1. Energy consumption comparison

As a first (general) research question and stepping-off point, it is important to quantify the difference in energy consumption between IMC buses and regular trolleybuses. To answer this question the differences in power demand have to be considered. A distinction is made in motor power (i.e. both the power consumed by the motor to provide traction as well as power generated through braking), auxiliary power (i.e. power consumption for all auxiliary electronics, most of which is consumed by the HVAC system) and charging power.

Table 4.1: Maximum values for the different power demand categories for both a regular trolleybus and IMC trolleybus. For both traction power (i.e. power needed to move the bus) and regenerative power (i.e. power generated through braking) the amount will be slightly higher for IMC trolleybuses as mass increases. The other addition when considering IMC is of course the charging power.

Maximum for:	Regular trolleybus	IMC trolleybus
Traction power [kW]	300	300 + x
Regenerative power [kW]	150	150 + y
Auxiliary power [kW]	40	40
Charging power [kW]	0	300

A first assumption made based on this breakdown is that the auxiliary power will not play a role in the comparison. The auxiliaries, of which the highest power demand comes from the HVAC system, are assumed to draw the same amount of power in both regular and IMC type trolleybuses. On the contrary, charging power is only part of the power consumption pattern of IMC buses. Apart from the efficiency loss due to charging it does not have an effect on the total energy consumption of the bus. This leaves the motor power which can be split into traction power and regenerative braking power. Comparing the amount of traction energy per [km] needed on average to the energy generated by regenerative braking per [km] defines comparison margins between regular trolleybuses and IMC buses. First up is the traction power consumption comparison. Next, the regenerative braking power and how the on-board battery can benefit from this is explained.

4.1.1. Traction energy consumption comparison

The higher mass of the IMC bus compared to the regular trolleybus should result in an increase in traction power demand. The simulated motor powers of four buses with different empty masses can be found in

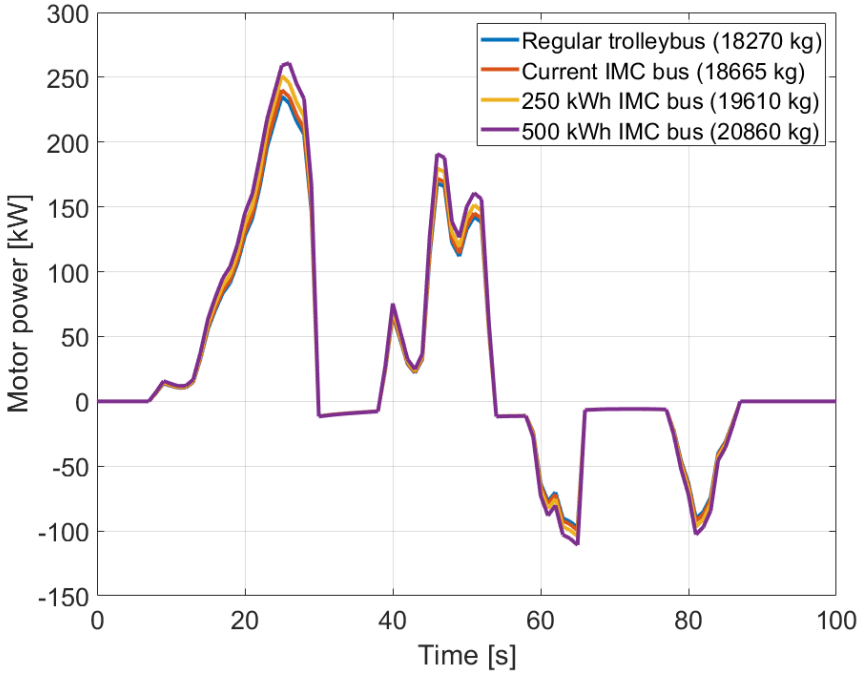

Figure 4.1: A comparison of simulated motor powers of four buses with varying masses of (part of) an Oosterbeek to Velp (Line 1) trip.

Table 4.2: The energy consumption of four buses with varying masses simulated with the HAN trolleybus model for the O2V_min velocity profile. *This is the IMC bus currently in use in Arnhem

Bus type	Empty mass [kg]	e_{trac} [kWh/km]	Mass increase	Energy increase
Regular trolleybus	18270	1.568		
76 kWh IMC bus*	18665	1.595	2.16%	1.69%
250 kWh IMC bus	19610	1.650	7.33%	5.23%
500 kWh IMC bus	20860	1.722	14.18%	9.85%

Figure 4.1. It can be seen that both the positive (traction) power and negative (regenerative braking) power increase for higher masses. The increase in traction power is necessary as a higher kinetic energy is needed to move the bus. Similarly, as a bus with a higher mass brakes there will be more kinetic braking energy that can be converted to electric energy. Table 4.2 shows the mass and energy consumption increase in percent based on a simulation. The energy consumption increase can be as high 10% for IMC buses with high battery capacity. This can in effect be countered by making better use of regenerative braking as IMC buses can store any amount of energy generated in the battery.

4.1.2. Regenerative braking energy generation

Regular trolleybuses generally send large amounts of regenerative braking energy directly into the braking resistor. Only when a trolleybus is braking while another trolleybus on the same section is drawing power can the resulting energy be used effectively as the braking power flows towards the other bus. A case study can provide the amount of regenerative braking energy that is generated in a whole day and what percentage of that energy can be used. First, the amount of regenerative braking energy that was generated as a function of the amount of traction energy that was consumed by trolleybuses in Arnhem is considered.

Table 4.3 shows the measured motor energy (both consumed and generated) of 24 trips of the Arnhem trolleybuses. The two values are also plotted against each other in Figure 4.2 By looking at the average energy per kilometre a ratio between regenerative braking energy and traction energy can be observed. This can be found as a percentage in the table. Values between 18.3% and 42.1% were found with an average of 31.4%. When used efficiently this regenerative energy can significantly decrease the total energy consumption of trolleybuses. To be clear, this percentage is not the percentage of energy recuperated from mechanical to

Table 4.3: Average traction energy consumed and regenerative energy generated by the induction motor of Arnhem trolleybuses taken from the measurement data of 24 trips. The ratio of regen-to-traction energy is displayed by stating the percentage of regenerative energy compared to traction energy.

Line	Direction	min/max	e_trac [kWh/km]	e_regen [kWh/km]	Regen percentage
1	O2V	max	2.136	-0.854	40.0%
		min	1.687	-0.607	36.0%
	V2O	max	2.283	-0.666	29.2%
		min	1.714	-0.414	24.1%
2	AC2DLW	max	1.954	-0.744	38.1%
		min	1.350	-0.417	30.9%
	DLW2AC	max	1.702	-0.508	29.8%
		min	1.304	-0.319	24.5%
3	BZ2HD	max	1.443	-0.278	19.3%
		min	1.154	-0.469	40.6%
	HD2BZ	max	2.106	-0.677	32.2%
		min	1.740	-0.464	26.7%
5	DZ2P	max	1.629	-0.566	34.7%
		min	1.497	-0.400	26.7%
	P2DZ	max	1.789	-0.577	32.3%
		min	1.149	-0.210	18.3%
6	DLW2HAN	max	2.222	-0.852	38.4%
		min	1.912	-0.650	34.0%
	HAN2DLW	max	1.541	-0.510	33.1%
		min	1.307	-0.326	25.0%
7	G2R	max	1.557	-0.656	42.1%
		min	1.165	-0.478	41.0%
	R2G	max	2.233	-0.671	30.0%
		min	1.661	-0.432	26.0%
	MEAN VALUES		**1.676**	**-0.531**	**31.4%**

electrical energy. Instead it states that for every 100 [kWh] used for traction (i.e. electrical to mechanical) an average of 31.4 [kWh] is recuperated (i.e. mechanical to electrical).

Now combining the 10% energy consumption increase when driving IMC buses to this 30% energy recuperated there is effectively a 20% margin. IMC buses, as long as the battery is not full will be able to make optimal use of this recuperated energy. IMC buses will therefore use 20% less energy compared to a trolleybus that wastes all energy generated by the induction motor. In reality most regular trolleybuses will not waste all this energy but instead share some of it with another trolleybus on the same section when possible. The amount of energy not wasted is therefore not only dependent on the traffic density. The amount of power recuperated at each moment in time should also be needed by another bus at that same moment. Both of these factors will be different for each city as differing bus schedules will have a large impact on this. This should be taken into consideration when cities are looking to replace their regular trolleybuses by IMC buses.

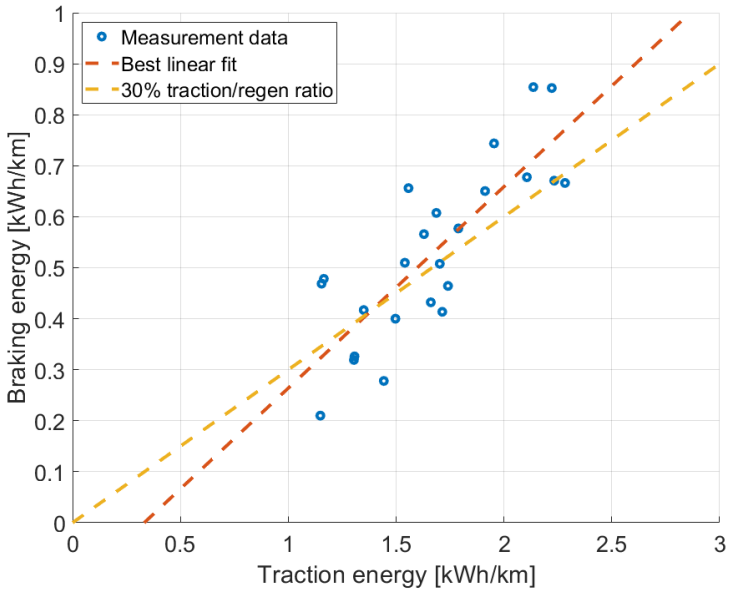

Figure 4.2: The energy generated through regenerative braking plotted versus the traction energy consumed by Arnhem trolleybuses based on measurement data of 24 trips. The average ratio of regen-to-traction energy was found to be 30%.

4.2. Picked up energy

The simulation set-up that was mentioned in section 3.5 is used to show the effect that charging corridor positioning and the subsequent change in average velocity while charging has on the amount of energy picked up. As a first orientation the total drive is divided in five equal sections (i.e. section I going from 0 [km] to 2.37 [km], section II from 2.37 [km] to 4.74 [km], all the way to the end). In Figure 4.3 a clear difference in the amount of charging can be seen. Section II is the worst section with a final SOC of 47% while the best, section III, has a final SOC of 68%. This makes section III also the only section in which more energy can be charged than is discharged throughout the trip.

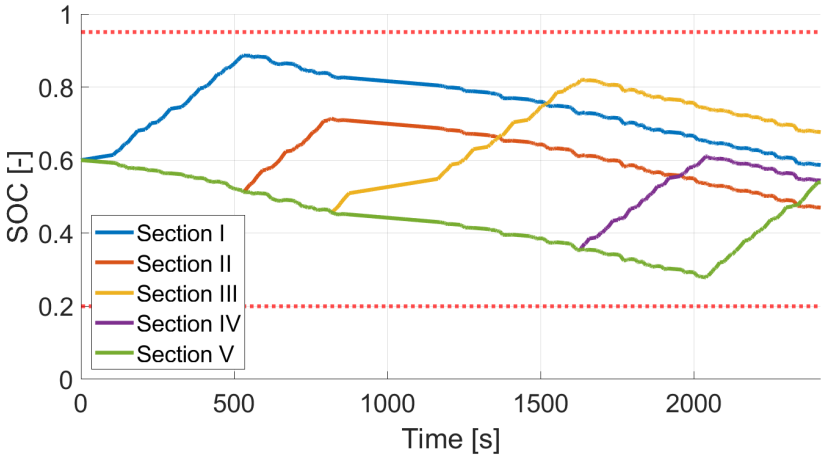

Figure 4.3: State of charge of the on-board battery during the trip for each of the five sections. The maximum and minimum SOC are indicated with red dotted lines.

By looking at the numbers in Table 4.4 these differences can be explained. Section III takes the longest time, both stopped and moving. It also is the section with the lowest average velocity. This results in the highest energy taken from the grid which shows that placement of overhead lines at sections with low average velocity can make a large difference in efficacy.

Table 4.4: Time and stopping time, amount of energy gathered from the grid, and average velocities in each of the five equal sections

	section I	**section II**	**section III**	**section IV**	**section V**
Time [s]	533	287	811	410	373
Stopping time [s]	210	46	449	110	71
Grid energy during stopping [kWh]	3.50	0.77	7.48	1.83	1.18
Grid energy during moving [kWh]	26.92	20.08	30.17	25.00	25.17
Total grid energy [kWh]	30.42	20.85	37.65	26.83	26.35
Average velocity [m/s]	4.45	8.26	2.92	5.78	6.36
Average velocity while moving [m/s]	7.34	9.84	6.55	7.90	7.85

4.2.1. Average velocity and charging power

This first orientation is elaborated by looking at the picked up energy of more charging corridors. The next simulation was performed for different charging corridor positions at a 100 meter increment. This was chosen to cover most combinations of time stopped and time moving as bus stops typically occur every 500 [m] excluding any stops due to heavy traffic and traffic lights. The 100 meter increment means that the charging corridor in the first simulation was positioned from 0 [km] to 2.37 [km], in the second simulation the charging corridor was positioned from 0.1 [km] to 2.47 [km]. This is done for a total of 95 simulations ending with a simulation with a charging corridor from 9.4 [km] to 11.86 [km] (the end of the route).

The result of this simulation can be found in Figure 4.4. Every blue circle is the result of one of the 95 simulations. Right away an inverse correlation can be seen between the average velocity and the amount of energy picked up in the charging corridor.

When looking closer two separate groups of data can be observed. The first group goes approximately from 10 [km/h] at 40 [kWh] (top left) to 14 [km/h] at 27 [kWh]. Its trend is indicated with the red line. The other group goes from 16 [km/h] at 32 [kWh] to 34 [km/h] at 18 [kWh]. This has to do with the inclusion/exclusion of a large stop at the Arnhem CS train station in the middle of the route. Its trend is indicated with the purple line. The large stopping time there gives a relatively high amount of picked up energy for a low average velocity. On top of that it shows that increasing this average velocity has a way larger effect for the first group than for the second group. What can be observed here is the result of the large difference in amount of charging power when stopped or moving.

To further illustrate this large difference, in Figure 4.5 the same graph is presented but now with two added values at 20 [km/h]. The yellow triangle illustrates the amount of picked up energy when the bus would be moving with an average velocity of 20 [km/h] for 100% of the time while in the charging corridor. This gives a picked up energy of 35.6 [kWh]. The red triangle shows the other extreme, which is being stopped for half of the time while driving at an average of 40 [km/h] for the remainder of time in the charging corridor. This gives a picked up energy of only 21.3 [kWh], a 40.2% decrease from the other extreme. This is a significant observation that shows how much of a difference the stopping behaviour of the bus can have because of alternating charging powers.

In these 95 simulations all with the same velocity profile a highest picked up energy of 39.3 [kWh] and a lowest picked up energy of 18.9 [kWh] was found. The average picked energy of all 95 simulations is 27.8 [kWh]. These large variations in picked up energy for a fixed coverage length of 20% show that it is not possible to define a coverage length and corridor position independently. They are dependent design choices.

This, together with the energy consumption comparison show that there is definitely potential in IMC bus implementation. The energy consumption comparison showed that there is a large margin in which IMC buses can make more efficient use of their regenerative energy. This goes as far as potentially decreasing total energy consumption because of it. The picked up energy results in Figure 4.5 showed that there is also a large amount of freedom in finding the right charging corridor for efficient battery charging. In the implementation of IMC buses this can have a large impact on the battery capacity needed. In this chapter it was also shown that the change in bus mass does not infer a big change in traction power while regenerative power can reduce the amount of energy consumption by a large factor of up to 30%.

Both these high degrees of freedom are promising but they also show that there is a lot of room for errors. Therefore in the next chapter simulations of IMC bus implementation on the Arnhem trolleygrid are discussed. By looking at power instead of energy details may come to light which are not clear from this preliminary analysis.

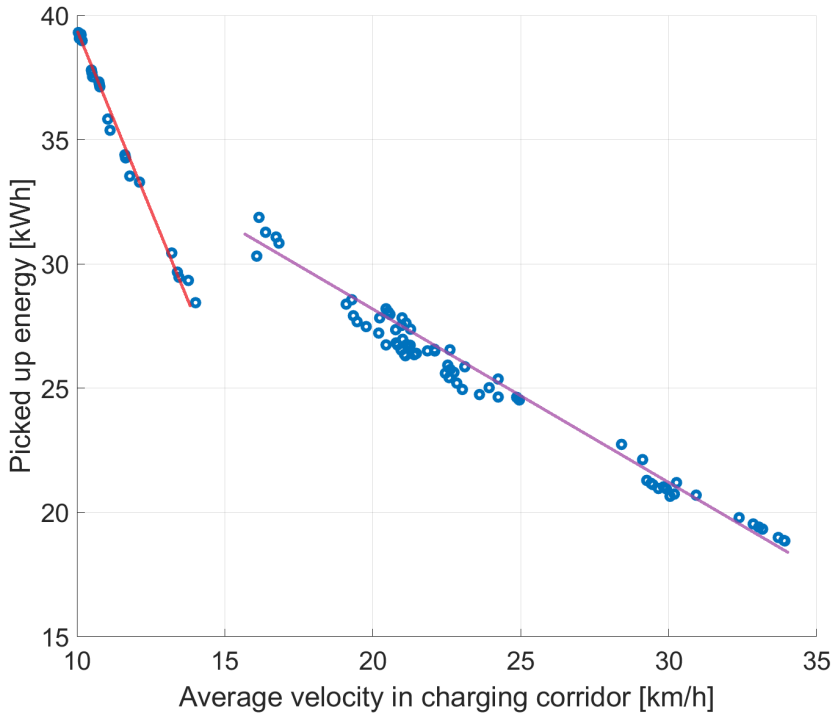

Figure 4.4: Picked up energy vs. average velocity in charging corridor. The graph shows the result of 95 simulations of the same route with a 20% coverage length and two different charging powers (300 [kW] while moving and 50 [kW] while stopped). In each simulation the position of the charging corridor is different resulting in a (high) variation of energy that can be picked up.

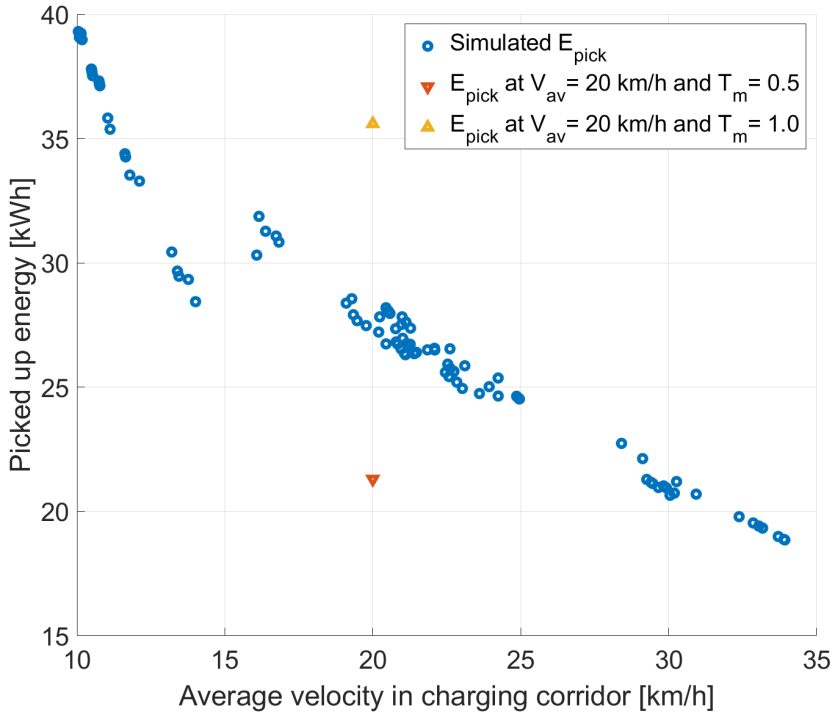

Figure 4.5: Picked up energy vs. average velocity in charging corridor with two extreme values added at 20 [km/h]. The two extremes show the amount of energy that can be picked up when the bus is stopped for half of the time (bottom triangle) and without stopping (top triangle).

5

Results and discussion: Arnhem case study

Results of the energy approach from last chapter have shown potential for IMC bus implementation based on Arnhem measurement data. To further investigate this potential a case study of IMC bus implementation on the Arnhem trolleygrid was performed. In this chapter the results from the different experiments performed with the Arnhem trolleygrid model can be observed. The first section shows how total energy demand increases and how transmission losses are impacted with IMC bus implementation. The following sections show which parts of the Arnhem trolleygrid have limit breaches based on power demand, minimum voltage and maximum current analysis of each section and substation. The final section of this chapter discusses the potential for peak shaving by showing the amount of charging powers each of the eight relevant substations can take.

5.1. Transmission losses and energy demand per section

In the previous chapter it was shown that IMC bus implementation can be fruitful considering the optimal use of regenerative braking power. The flip side to this is that there can be a lot of variability in the amount of picked up energy depending on charging corridor size and placement. The first simulations of this next chapter performed with the Arnhem trolleygrid model aimed to give an overview of the total energy demand and the amount of transmission losses for a full weekday of operation. The simulation was first performed with all regular trolleybus lines but without any IMC bus lines. Next the simulation was performed with all bus lines (i.e. both regular trolleybus and IMC bus lines). IMC buses were set to charge their batteries at 100 [kW] while stopped and 150 [kW] while moving. More information on the individual lines and the simulation set-up can be found in chapter 3. The total energy and energy transmission losses of these simulations can be found in Figure 5.1 and Figure 5.2.

First, in Figure 5.1 a list of all sections in order from section 2 to section 49 of total energy and energy losses is shown. The highest energy demand per day (1182 [kWh]) is found in section 5 which is the section with Arnhem CS. The high energy demand most probably comes from idle buses waiting at the central station with their HVAC system still drawing power. The lowest energy demand (19 [kWh]) can be found in section 8. This is because section 8 only covers a tiny fraction of just one bus route of line 3 (see Figure 3.9). In fact, the amount of energy demand in each section has no real surprises as it can be explained mostly by the section length, the number of buses passing the section and if it does or does not contain a terminus. Summing up the energy demand of all sections a total energy of 14688 [kWh] was found.

Just regular trolleybuses					
Section	Total energy	Percent of total energy	Energy loss	Percent of total loss	Percent loss
2	306.51	2.09%	9.62	2.64%	3.14%
3	262.29	1.79%	5.30	1.45%	2.02%
5	1181.83	8.05%	9.06	2.48%	0.77%
6	591.90	4.03%	7.59	2.08%	1.28%
8	19.15	0.13%	0.02	0.01%	0.10%
9	458.34	3.12%	5.38	1.47%	1.17%
12	924.20	6.29%	31.90	8.74%	3.45%
13	367.23	2.50%	8.45	2.32%	2.30%
14	322.17	2.19%	6.30	1.73%	1.96%
15	282.43	1.92%	5.04	1.38%	1.78%
16	391.98	2.67%	7.21	1.97%	1.84%
17	266.35	1.81%	6.72	1.84%	2.52%
18	256.53	1.75%	6.82	1.87%	2.66%
19	345.46	2.35%	20.87	5.72%	6.04%
20	209.67	1.43%	2.82	0.77%	1.35%
21	275.92	1.88%	3.58	0.98%	1.30%
22	418.99	2.85%	16.64	4.56%	3.97%
23	179.97	1.23%	3.93	1.08%	2.18%
24	424.21	2.89%	13.73	3.76%	3.24%
25	497.18	3.38%	9.47	2.59%	1.90%
26	562.15	3.83%	14.42	3.95%	2.57%
27	405.73	2.76%	9.20	2.52%	2.27%
28	378.34	2.58%	8.59	2.35%	2.27%
29	432.64	2.95%	13.92	3.82%	3.22%
30	455.45	3.10%	16.42	4.50%	3.61%
31	292.65	1.99%	6.81	1.87%	2.33%
32	210.78	1.44%	6.20	1.70%	2.94%
33	273.29	1.86%	8.07	2.21%	2.95%
34	307.40	2.09%	9.01	2.47%	2.93%
35	95.74	0.65%	0.81	0.22%	0.85%
36	613.21	4.17%	14.16	3.88%	2.31%
39	264.25	1.80%	5.81	1.59%	2.20%
40	234.65	1.60%	2.53	0.69%	1.08%
41	387.30	2.64%	19.16	5.25%	4.95%
42	461.90	3.14%	16.20	4.44%	3.51%
43	336.69	2.29%	6.24	1.71%	1.85%
44	240.86	1.64%	8.92	2.45%	3.71%
45	156.27	1.06%	2.86	0.78%	1.83%
48	267.59	1.82%	7.98	2.19%	2.98%
49	328.60	2.24%	7.19	1.97%	2.19%
	14687.76		**364.96**		**2.48%**

Figure 5.1: Total energy demand and transmission losses on each section in [kWh] for a simulation without IMC buses. For both total energy and energy losses the total values and percentage values (of full grid) can be found. The final column shows the percentage loss inside each section.

With a total energy transmission loss of 365 [kWh] the percentage of energy lost through transmission is 2.48% for the whole trolleygrid. The second to last column shows the contribution to this total loss of each section. Alternatively, the last column shows the percentage loss of each individual section. The highest contributor to energy losses is section 12. This is a high traffic section which is covered by all six trolleybus lines (see Figure 3.10 and Figure 3.9) also pointed out by having the second highest energy demand of 924 [kWh]. It is also one of the larger sections.

The highest percentage loss inside a section (last column) is found in section 19. This section contains a large loop under which the buses go only in the clockwise direction (see top of Figure 3.10. One cause of the high losses can therefore be explained as the section does not have the regular parallel lines for both sides of the road. This is only the case for sections 6 and 19. This effectively halves the amount of cable over which the current flows. Next to that, section 19 includes the bus line 3 terminus at Burgers' Zoo which is

		With IMC buses				
Section	IMC on section	Total energy	Percent of total energy	Energy loss	Percent of total loss	Percent loss
2	**yes**	802.02	3.60%	39.21	7.17%	4.89%
3	**yes**	797.30	3.58%	24.57	4.50%	3.08%
5	**yes**	5559.66	24.98%	44.55	8.15%	0.80%
6	**yes**	808.84	3.63%	13.02	2.38%	1.61%
8	**yes**	49.78	0.22%	0.06	0.01%	0.12%
9	no	458.34	2.06%	5.38	0.98%	1.17%
12	**yes**	1253.39	5.63%	61.47	11.25%	4.90%
13	no	367.23	1.65%	8.45	1.55%	2.30%
14	**yes**	505.39	2.27%	17.23	3.15%	3.41%
15	no	282.43	1.27%	5.04	0.92%	1.78%
16	**yes**	600.85	2.70%	12.52	2.29%	2.08%
17	**yes**	391.99	1.76%	12.05	2.21%	3.08%
18	**yes**	448.15	2.01%	18.69	3.42%	4.17%
19	no	345.46	1.55%	20.87	3.82%	6.04%
20	no	209.67	0.94%	2.82	0.52%	1.35%
21	no	275.92	1.24%	3.58	0.65%	1.30%
22	**yes**	642.62	2.89%	30.46	5.57%	4.74%
23	**yes**	474.51	2.13%	12.55	2.30%	2.65%
24	**yes**	670.74	3.01%	17.54	3.21%	2.61%
25	**yes**	606.37	2.72%	11.94	2.18%	1.97%
26	no	562.15	2.53%	14.42	2.64%	2.57%
27	no	405.73	1.82%	9.20	1.68%	2.27%
28	no	378.34	1.70%	8.59	1.57%	2.27%
29	no	432.64	1.94%	13.92	2.55%	3.22%
30	no	455.45	2.05%	16.42	3.01%	3.61%
31	no	292.65	1.31%	6.81	1.25%	2.33%
32	no	210.78	0.95%	6.20	1.13%	2.94%
33	no	273.29	1.23%	8.07	1.48%	2.95%
34	no	307.40	1.38%	9.01	1.65%	2.93%
35	no	95.74	0.43%	0.81	0.15%	0.85%
36	no	613.21	2.76%	14.16	2.59%	2.31%
39	no	264.25	1.19%	5.81	1.06%	2.20%
40	no	234.65	1.05%	2.53	0.46%	1.08%
41	no	387.30	1.74%	19.16	3.51%	4.95%
42	no	461.90	2.08%	16.20	2.96%	3.51%
43	no	336.69	1.51%	6.24	1.14%	1.85%
44	no	240.86	1.08%	8.92	1.63%	3.71%
45	no	156.27	0.70%	2.86	0.52%	1.83%
48	no	267.59	1.20%	7.98	1.46%	2.98%
49	no	328.60	1.48%	7.19	1.31%	2.19%
		22256.11		**546.50**		**2.46%**

Figure 5.2: Total energy demand and transmission losses on each section in [kWh] for a simulation with both regular trolleybuses and IMC bus lines. The second column indicates if IMC buses ride on that section. For both total energy and energy losses the total values and percentage values (of full grid) can be found. The final column shows the percentage loss inside each section.

also at the opposite end of the section with the feed-in point sitting at the other side. This means that any energy demand taken while idling at the terminus has to travel a long cable distance which increases losses as well. Similar increases can be found at the sections with other termini at opposite ends of the feed-in point: sections 17 (line 7), 21 (line 3), 24 (line 1), 34 (line 5), 49 (line 7).

With the IMC bus lines added a large increase in total energy can be observed (see Figure 5.2). The total energy increases from 14688 [kWh] to 22256 [kWh] while total losses increase from 365 [kWh] to 547 [kWh]. What stands out is that the percentage loss in total has slightly decreased from 2.48% to 2.46%. This can be explained by considering the large amount of energy that is consumed at section 5. This has gone from 8% of total energy to 25% of total energy and that has to do with bus charging. As all IMC bus lines start at Arnhem CS they spend a considerable amount of time idling at this terminus. While idling the battery is still charging and as such each IMC bus standing there is drawing 100 [kW] of power on top of the HVAC power. The losses stay low as the feed-in point is in close proximity with the trolleybus plaza (i.e. the square at which trolleybuses idle at Arnhem CS).

IMC buses only affect a small portion of all sections. This is because IMC buses do not cover all sections. The

sections covered by IMC lines are indicated in the second column in Figure 5.2. Looking at the percentage loss per section it can be seen that sections 2, 14 and 18 suffer the most from the introduction of IMC buses with losses increasing to more than 1.5x their initial values. In the next section the cause of these increases is further investigated.

5.2. Substation limits

The substations are limited in the amount of power they can provide. This limit is 800 [kW] for all substations. An exception is made for substation 4 (at Arnhem CS) which has extra capacity and can supply 1800 [kW]. By investigating the power demand for different scenarios (i.e. including/excluding IMC bus lines) it can be found whether mitigation of charging powers is a possible solution. This is first done by looking at the effect of IMC bus line 352 specifically.

For this first case a simulation is performed with and without line 352. This bus line runs along the west side of the line 1 bus route. A map of this route can be found in Figure 5.3. While line 1 ends at the tip of the last green section (i.e. section 24) line 352 exits the grid at the intersection where section 24 goes North. The autonomous part of line 352 starts there as it drives to Wageningen and back.

Figure 5.3: Part of the substation and feed-in section map that shows the route that line 352 follows. Its terminus is at section 5 at Arnhem CS and it goes West along all purple, blue and green sections.

The maximum power demand on each substation can be found in Figure 5.4. When only regular trolleybuses are concerned (blue bars) it can be observed that the power demand never exceeds the 800 [kW] limit for any of the 19 substations. However, when considering the addition of line 352 (red bars) sharp increases are found. For substation 4 (at Arnhem CS) this is not a problem as the limit is 1800 [kW]. For substations 1 and 12 these power demands can pose a problem.

By looking at the complete power demand profile of substation 1 (see Figure 5.5) a pattern emerges. There are clear peaks at regular intervals which exceed the 800 [kW] limit. These peaks occur throughout the day but end after the evening rush hour (i.e. around 19:00). The figure shows the power demand both with (blue) and without (orange) battery charging. Here it is already clear that without battery charging the power can be barely contained within the limit.

In Figure 5.6 two peaks are shown in more detail. The first peak, at step 22580 has a value of 1098 [kW] with battery charging. This value is decreased to 874 [kW] without battery charging. The second peak at step 22629 has a value of 850 [kW] with and 693 [kW] without battery charging. Both peaks are examples in which decreasing battery charging on this section would have a positive impact on decreasing the amount of times that the 800 [kW] limit is exceeded.

The power demand of substation 1 can be further split up into power demand of section 2 and section 3 that it feeds. These power demands together with the minimum voltage and maximum current values of the same two peaks can be found in Figure 5.7 (section 2) and Figure 5.8 (section 3). The first peak is a combination of power demands over [500 kW] from both sections. The second peak is from an 850 [kW] peak in section 2 alone. It is interesting to see that, for section 2, the voltage dip is more noticeable at the 500 [kW] peak than at the 850 [kW] peak. The minimum voltages at these peaks are 550 [V] and 669 [V] respectively. This is

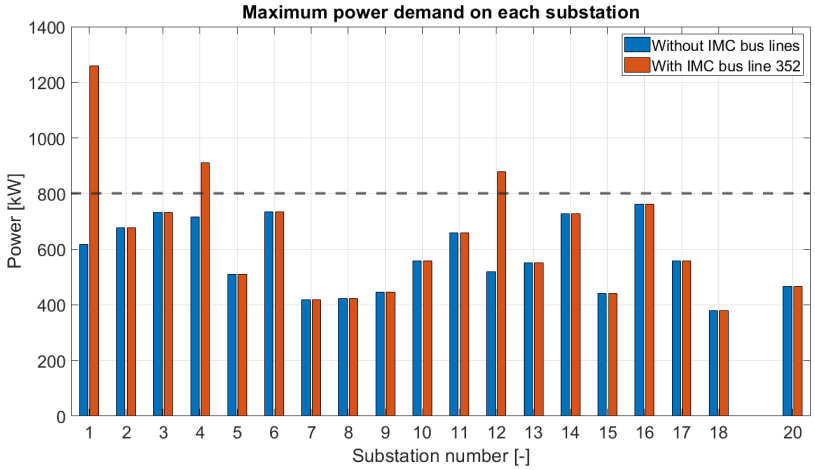

Figure 5.4: Maximum power demand on each substation. The blue bars show power demand without IMC bus lines. The red bars show power demand with IMC bus line 352. An increase in maximum power demand for all relevant substations (i.e. 1, 4 and 12) was found. The black dashed line indicates the 800 [kW] power limit for each substation. Note that this is not true for substation 4 which limit lies at 1800 [kW].

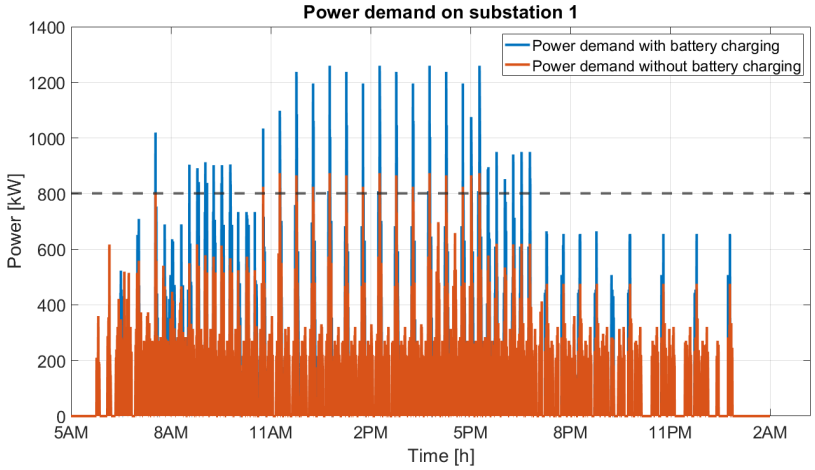

Figure 5.5: Power demand on substation 1 for a full day including IMC bus line 352. It is shown both with (blue) and without (red) battery charging of the IMC buses. The black dashed line indicates the 800 [kW] power limit of the substation.

because the buses are closer to the feed-in point for the second peak so a less steep voltage drop is required. An obvious proportional relation is found between power demand and maximum current for both sections. This is because the maximum current will always occur between the bus nearest to the feed-in point and the feed-in point itself. At this part of the cable all power to buses beyond the first bus also flows.

These results of a detailed look at the effect of substation 1 show that power limits can be breached when adding an IMC bus line. Adding three more IMC bus lines might cause more of these breaches. Therefore in the following section a simulation of the whole trolleygrid including all six regular trolleybus lines and all four IMC bus lines for a full day are considered.

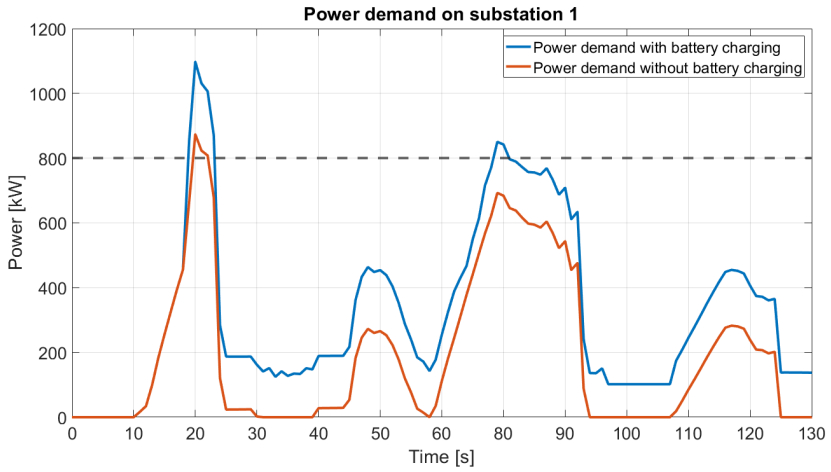

Figure 5.6: Power demand on substation 1 including IMC bus line 352 zoomed in on two peaks. It is shown both with (blue) and without (red) battery charging of the IMC buses. The black dashed line indicates the 800 [kW] power limit of the substation

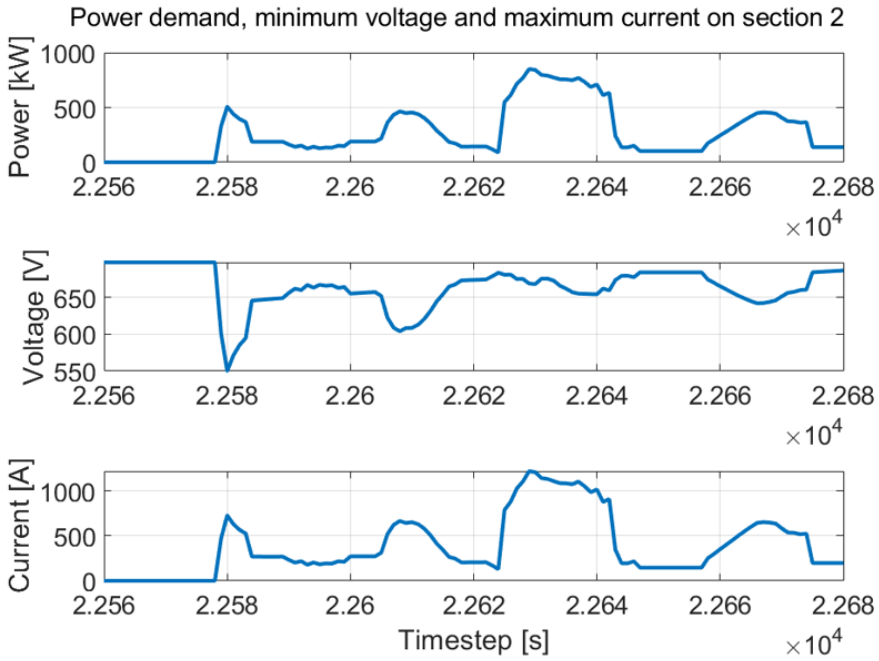

Figure 5.7: Power demand, minimum voltage and maximum current on section 2 zoomed in on two peaks. These are the same peaks as shown in Figure 5.6 but split up into the two separate sections of substation 1.

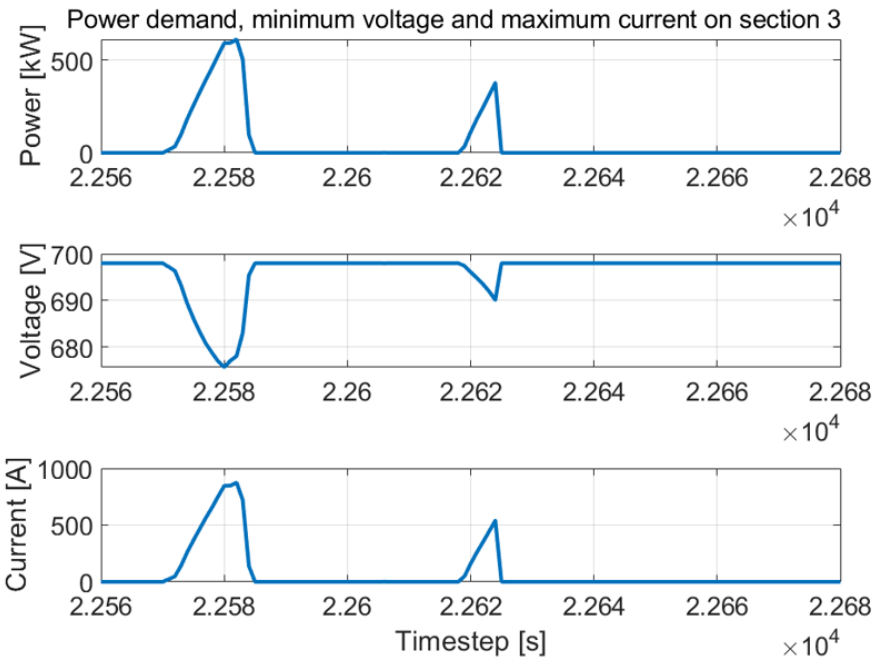

Figure 5.8: Power demand, minimum voltage and maximum current on section 3 zoomed in on two peaks. These are the same peaks as shown in Figure 5.6 but split up into the two separate sections of substation 1.

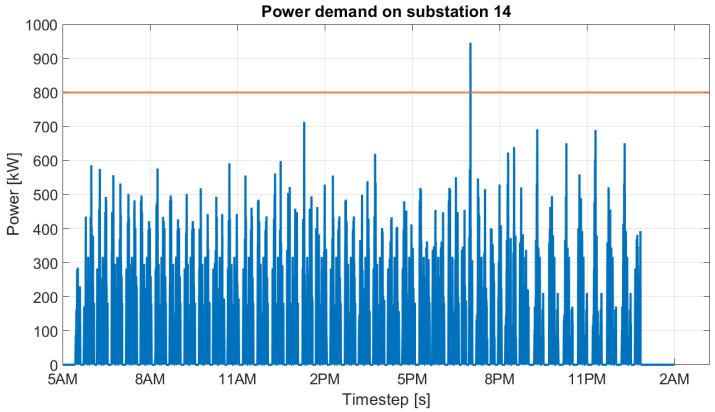

Figure 5.9: Full day power demand of substation 14 for 04-08-2020 without IMC buses. The 800 [kW] limit (orange horizontal line) is exceeded once.

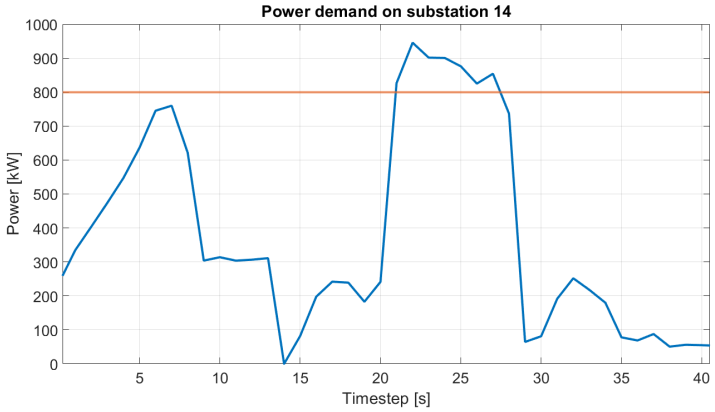

Figure 5.10: Power demand of substation 14 zoomed in at the single peak which exceeds the 800 [kW] limit for 04-08-2020 without IMC buses. The limit is exceeded for 7 [s] and its maximum is 945 [kW].

5.3. Full grid analysis

To see what the effect of adding IMC buses to the Arnhem grid has the current situation is compared to a situation with IMC buses. The two different days 04-08-2020 and 01-09-2020 are analysed. August 4th is a weekday in the Summer Holiday while September 1st is a regular weekday. The number of buses used in simulating a Summer weekday is 36 while a regular weekday has 50 buses. This is because the Summer weekday bus schedule has less trips compared to the regular weekday schedule.

5.3.1. Power demand analysis

First, the power demands on 04-08-2020 on each subsection are analysed. The power demands without and with IMC buses are shown in Figure 5.14 and Figure 5.15 respectively. In both figures it can be noticed that for most substations a peak can be found at 30-40 [kW]. This is because the HVAC draws 38.4 [kW] so whenever a bus stands still with the HVAC running this is the power demand. In substation 4, which is the substation where the main hub Arnhem CS is located, this effect is especially noticeable. Peaks of multiples of this number, as multiple buses will stand still there while HVAC is on, are also visible for substation 4.

If a substation power limit is breached this is indicated by an orange vertical line. The maximum power demand of each substation is indicated by either a green dotted or red dashed line. A green dotted line indicates that the limit is not exceeded. The red dashed lines do exceed the limit. This only happens on substation 14 for 04-08-2020 without IMC buses. Looking at the complete plot for substation 14 in Figure 5.9 it is seen that the limit is exceeded once at timestep 50410. Zooming in on the breach (see Figure 5.10) shows that it exists for 7 [s] and its maximum is 945 [kW] which is 18.1% above the limit. The breach is non-repetitive and only happens once on a day.

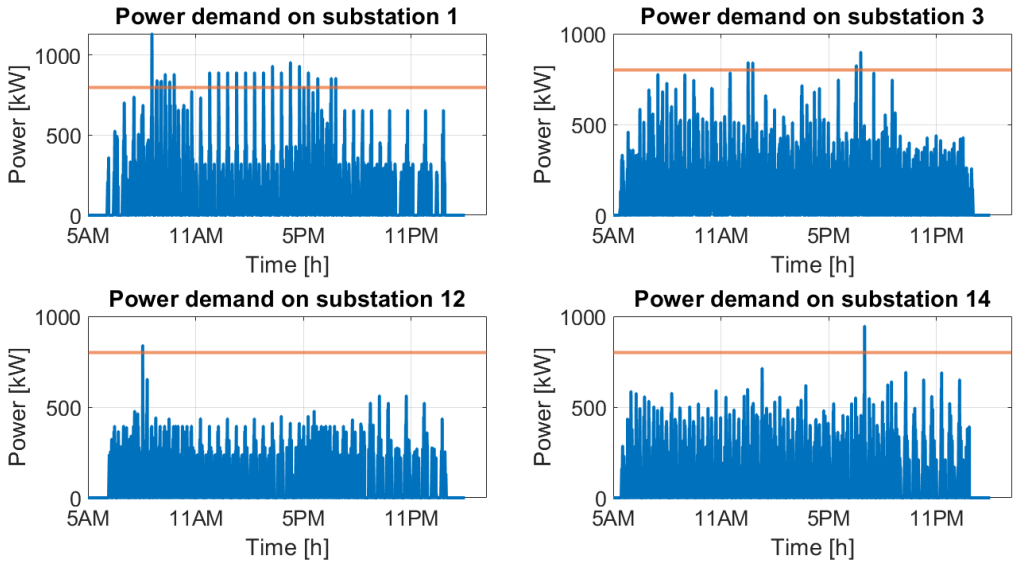

Figure 5.11: Full day power demand of substations 1, 3, 12 and 14 for 04-08-2020 with IMC buses. The 800 [kW] limit (orange horizontal line) is exceeded once or more for these substations. The 'worst offender' is substation 1, breaking the limit 22 times.

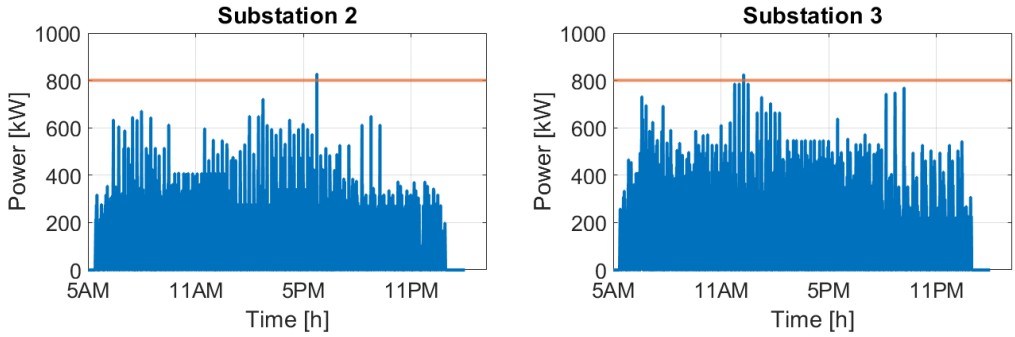

Figure 5.12: Full day power demand of substations 2 and 3 for 01-09-2020 without IMC buses. The 800 [kW] limit (orange horizontal line) is exceeded once on both substations.

Moving on to the simulation of the same day with IMC buses shown in Figure 5.15 more of these limits are exceeded. The red dashed line is visible for substations 1, 3, 12 and (again) 14. The full day power demands of these substations can be found in Figure 5.11. As no IMC bus lines make use of substation 14, the same one instance occurs. Substation 12 has a similar occurrence near the start of the day. Its value is 839 [kW] and it only exceeds the limit for 1 [s]. For substation 3 the limit is exceeded a total of 4 times. All of these peaks have a duration of 1 [s] and the highest peak is 898 [kW]. Again, this is not directly regarded as a reason to consider reinforcement of the section or other measures. However if further research indicates that this happens on a daily basis then a closer investigation to the section's power demand could be advisable.

Breaking the limit happens the most in substation 1. The highest power demand with a value of 1133 [kW] occurs at timestep 12830. The other instances that occur all have a value of around 900 [kW]. Clearly this is a repetitive pattern. It has to do with multiple buses accelerating and charging at the same time. A slight reschedule of one of the bus lines could resolve this issue. Another solution could be to limit the amount of power that can be charged by IMC buses from 8:30 to 19:00 which is the window in which the peaks occur. This can either be done automatically or through driver training.

Just as the analysis was performed for 04-08 it is also performed for 01-09. In Figure 5.16 the power demand of each substation for a simulation without IMC buses is shown. Breaches only occur on substation 2 and 3. The breaches are very small and only occur once as can be seen in Figure 5.12.

When adding IMC buses the power is again exceeded on more substations than before. In Figure 5.17 it can

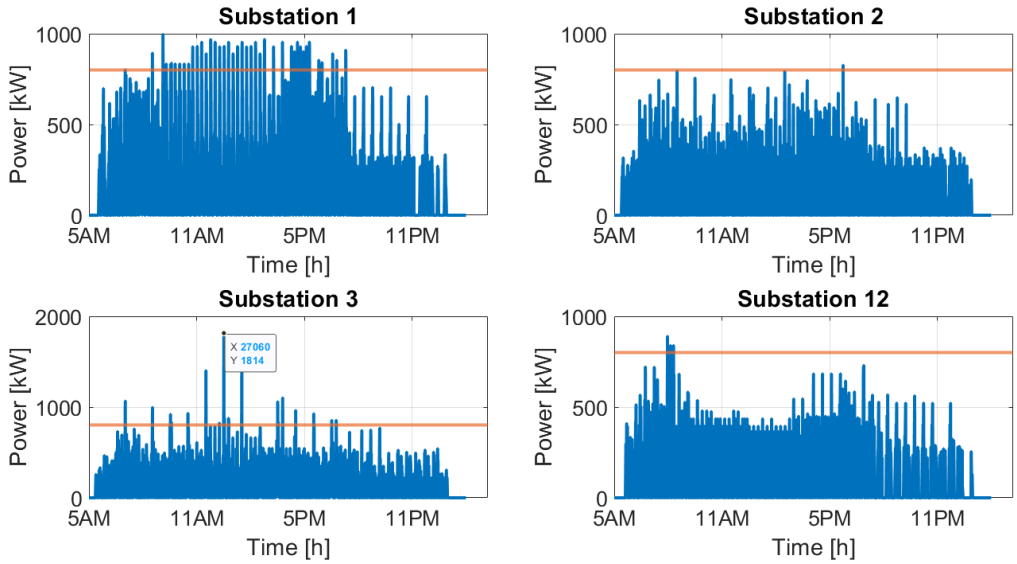

Figure 5.13: Full day power demand of substations 1, 2, 3 and 12 for 01-09-2020 with IMC buses. The 800 [kW] limit (orange horizontal line) is exceeded on all four of these substations. Substations 1 and 3 have high repetitive and very high power demand peaks respectively and require further investigation.

be seen that now four substations have breaches. These are substations 1, 2, 3 and 12. Figure 5.13 shows full day plots of the power demands of these substations. Substations 2 and 12 have small breaches which require no further attention. Substation 1 has a high number of repetitive breaches which average 950 [kW]. These breaches are similar to those on the same substation on 04-08-2020 (see Figure 5.11). Again, this can be avoided by either rescheduling or by limiting charging powers.

There is a very high peak in substation 3. Its breach lasts for 13 seconds and its maximum is 1814 [kW]. This can be caused by a coincidental point in time where multiple buses are accelerating and/or charging. Moments like these can be mitigated by lowering the charging powers temporarily.

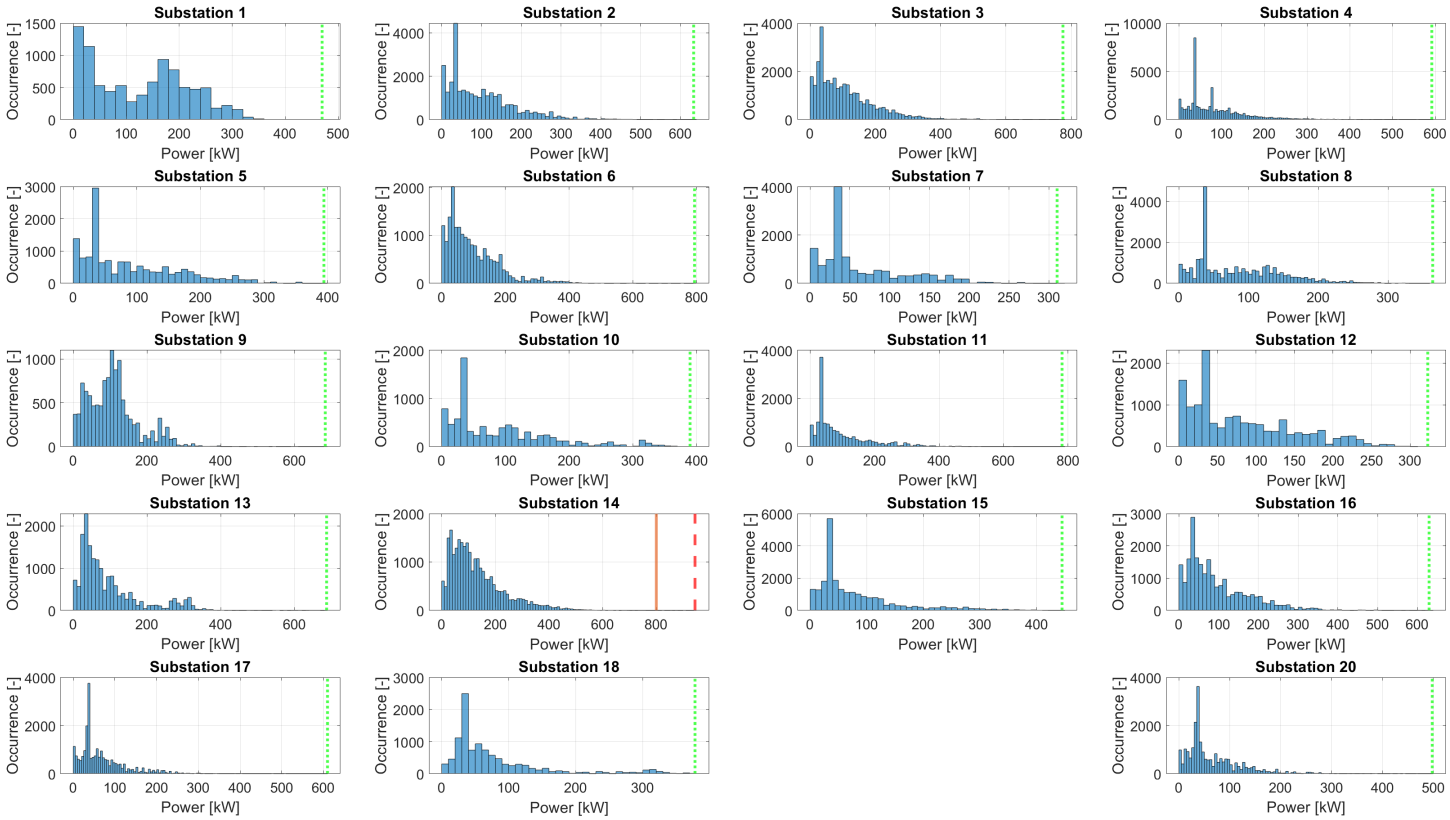

Figure 5.14: Power demands on each substation for 04-08-2020 without IMC buses (i.e. excluding lines 4, 13, 29, and 352). The maximum power demand on each substation is indicated by a vertical dotted or dashed line. A green dotted line indicates that the limit is never exceeded. A red dashed line indicates that the maximum power demand exceeds the limit. When this is the case the substation limit is indicated by the orange vertical line.

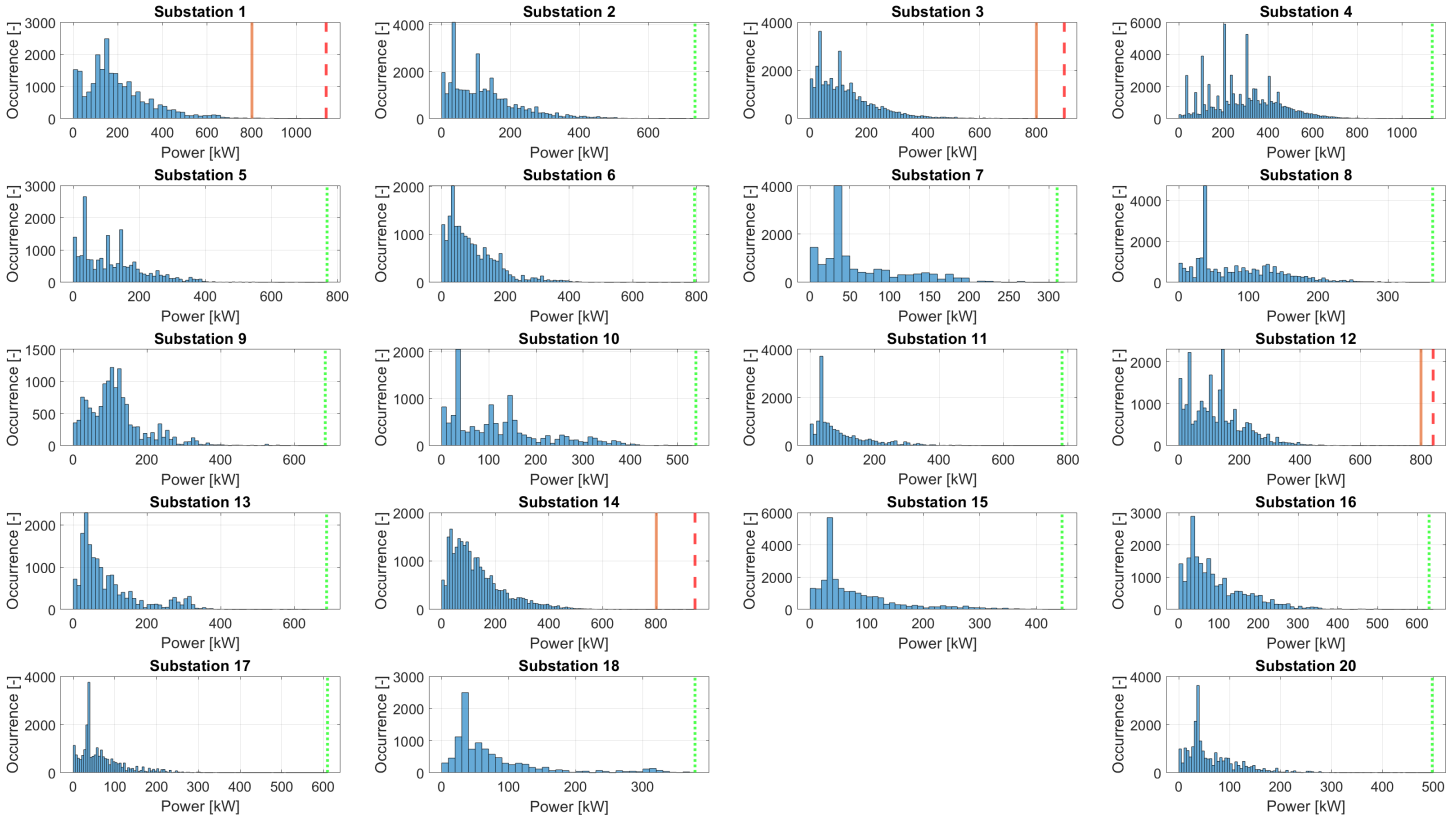

Figure 5.15: Power demands on each substation for 04-08-2020 with IMC buses (i.e. including lines 4, 13, 29, and 352). The maximum power demand on each substation is indicated by a vertical dotted or dashed line. A green dotted line indicates that the limit is never exceeded. A red dashed line indicates that the maximum power demand exceeds the limit. When this is the case the substation limit is indicated by the orange vertical line.

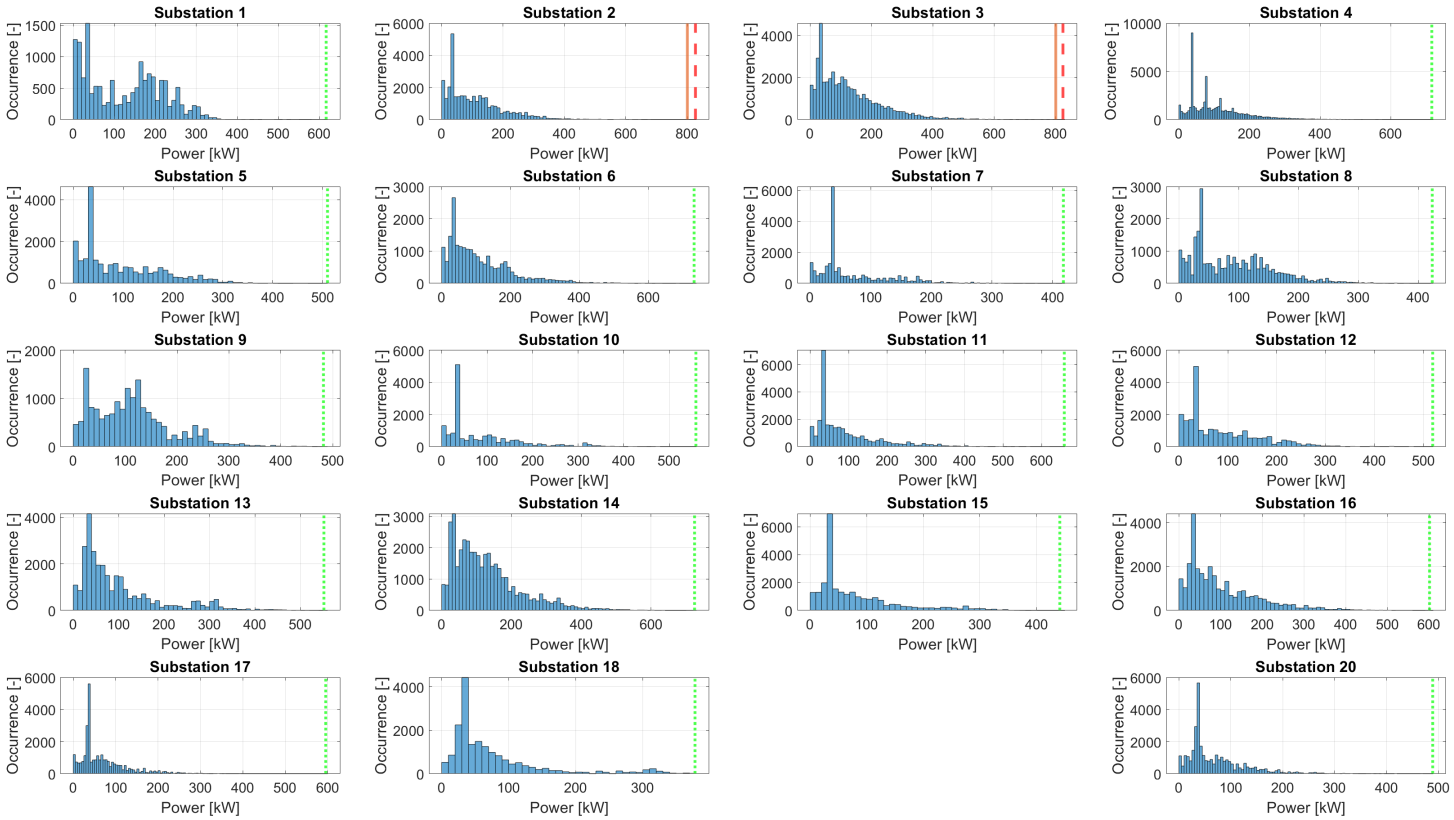

Figure 5.16: Power demands on each substation for 01-09-2020 without IMC buses (i.e. excluding lines 4, 13, 29, and 352). The maximum power demand on each substation is indicated by a vertical dotted or dashed line. A green dotted line indicates that the limit is never exceeded. A red dashed line indicates that the maximum power demand exceeds the limit. When this is the case the substation limit is indicated by the orange vertical line.

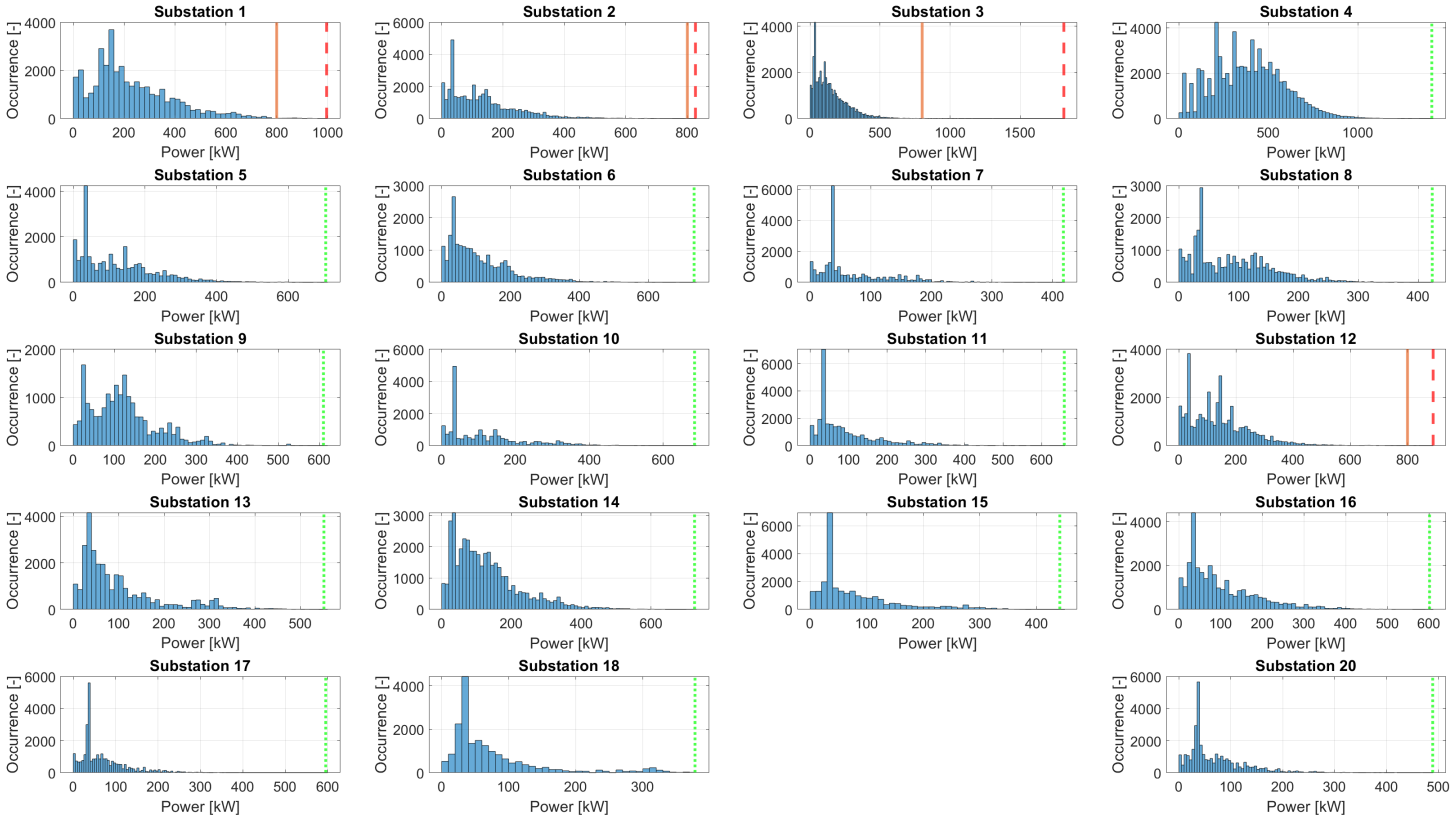

Figure 5.17: Power demands on each substation for 01-09-2020 with IMC buses (i.e. including lines 4, 13, 29, and 352). The maximum power demand on each substation is indicated by a vertical dotted or dashed line. A green dotted line indicates that the limit is never exceeded. A red dashed line indicates that the maximum power demand exceeds the limit. When this is the case the substation limit is indicated by the orange vertical line.

5.3.2. Minimum voltage analysis

In similar fashion as with the power demand the minimum voltage on each section at each timestep can be observed. In a study performed by Liandon in 2012 the voltage limits of the Arnhem trolleybuses is explained [29]. If a trolleybus reaches a low voltage of 500 [V] the power control will intervene. This means that below this limit the bus will not be able to draw the amount of power it is currently demanding. This results in the bus not being able to accelerate the way it is supposed to and can lose its velocity. At 400 [V] this power control completely shuts off the power demand of the bus. The analysis therefore looks at any occurrence of the voltage reaching values below 500 [V].

Again performing a simulation of 04-08-2020 without IMC buses all minimum voltages are shown on each section in Figure 5.18 and Figure 5.19. The sections which have voltages below 500 [V] are sections 12, 26, 29 and 30. Comparing this to a situation with IMC buses does not change a lot. Looking at Figure 5.20 and Figure 5.21 the only big change that can be spotted is that the minimum voltage of section 12 drops even further to below 450 [V]. This section should be further investigated on operation with IMC buses. Only IMC bus line 29 operates on this section.

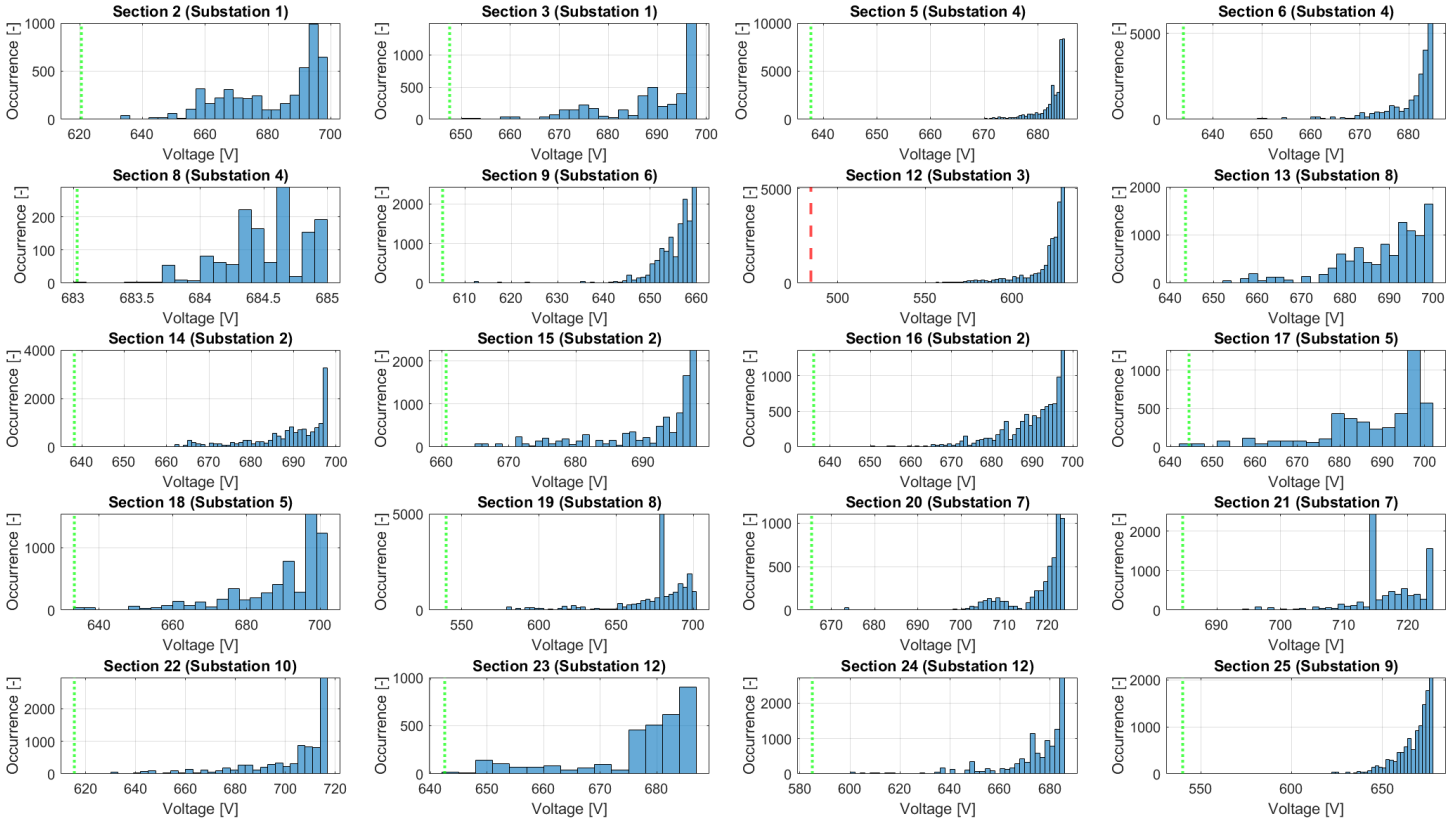

Figure 5.18: Minimum voltages on each section for 04-08-2020 without IMC buses (i.e. excluding lines 4, 13, 29, and 352). (Part 1 of 2)

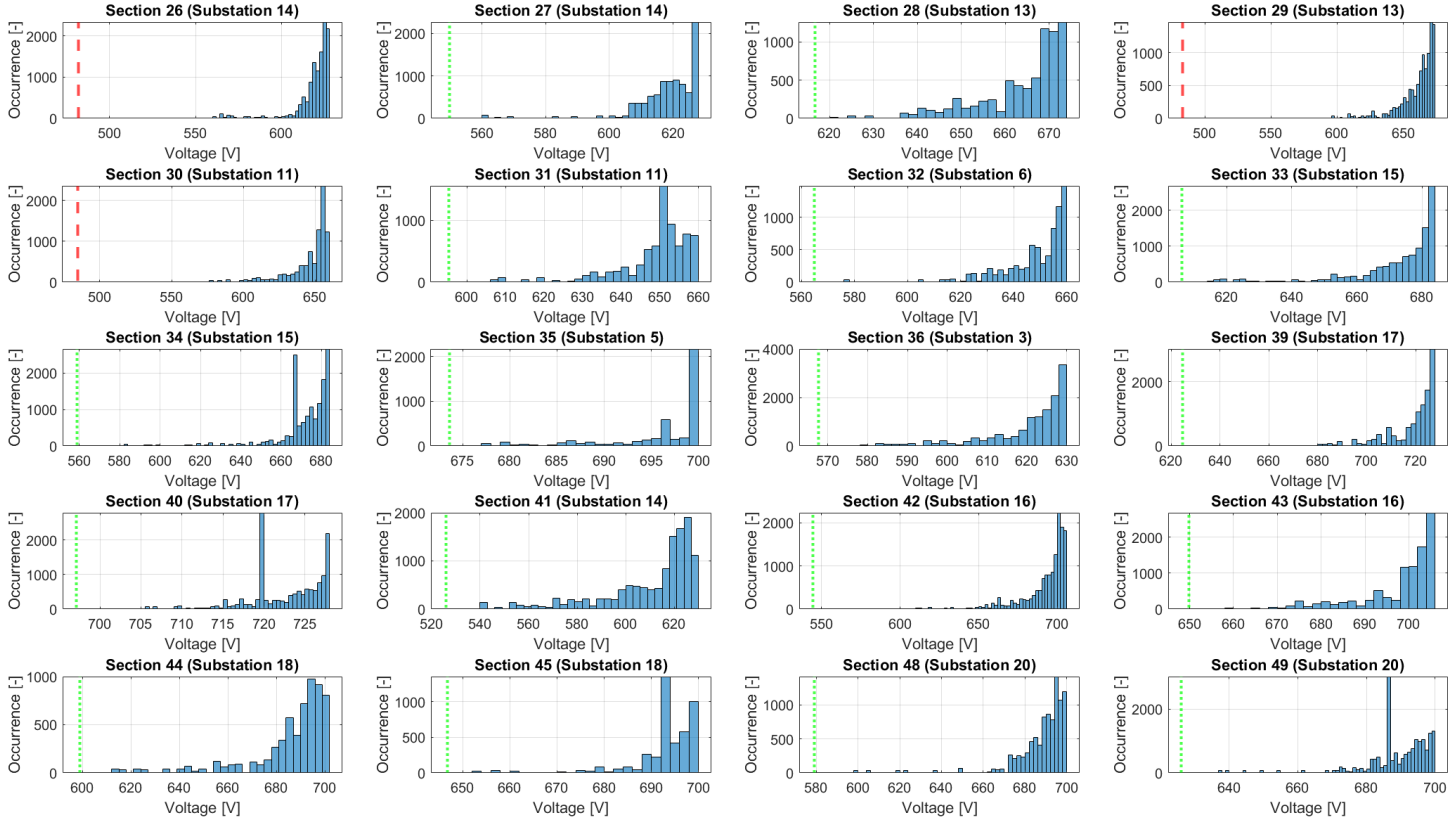

Figure 5.19: Minimum voltages on each section for 04-08-2020 without IMC buses (i.e. excluding lines 4, 13, 29, and 352). (Part 2 of 2)

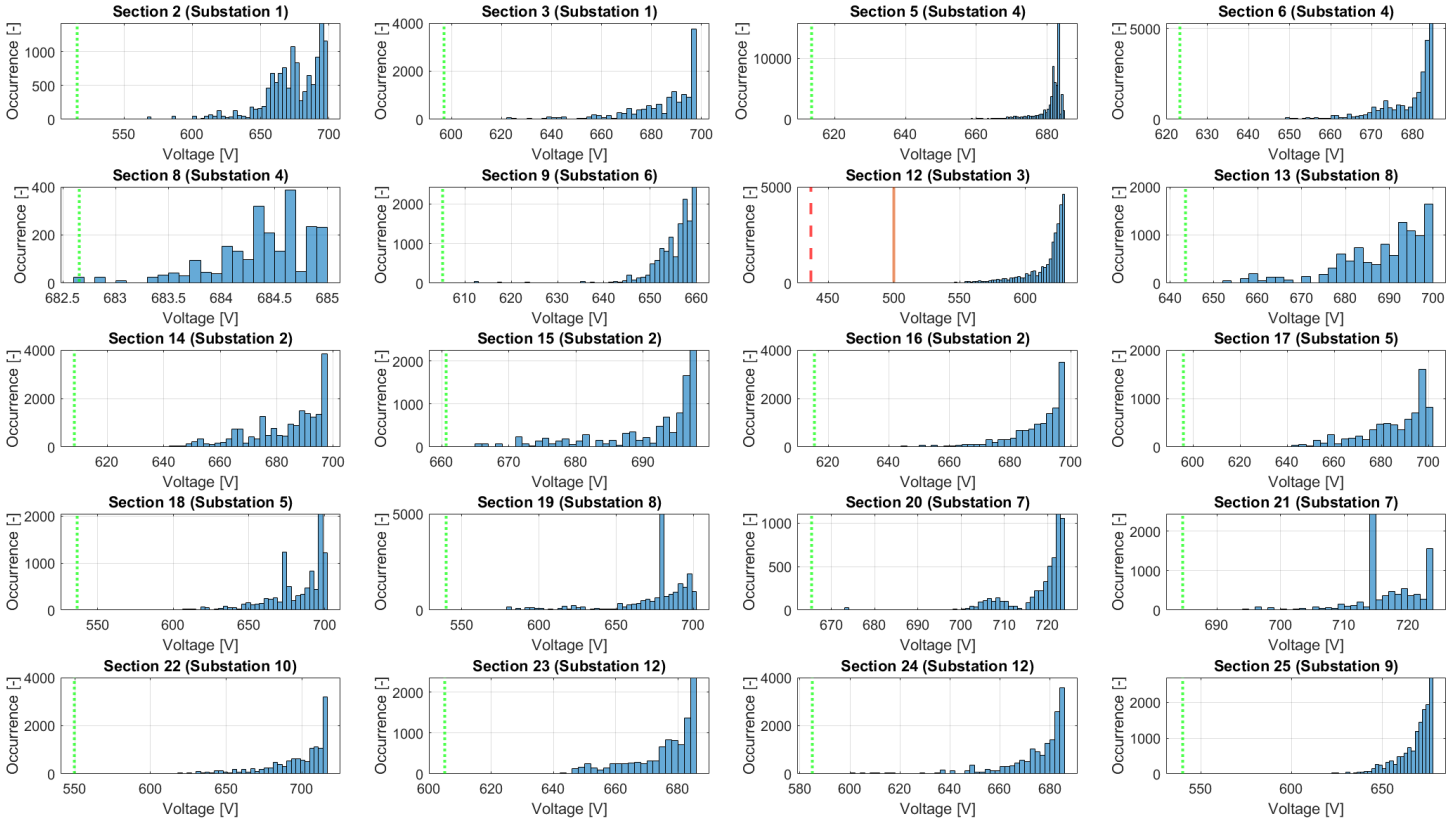

Figure 5.20: Minimum voltages on each section for 04-08-2020 with IMC buses (i.e. including lines 4, 13, 29, and 352). (Part 1 of 2)

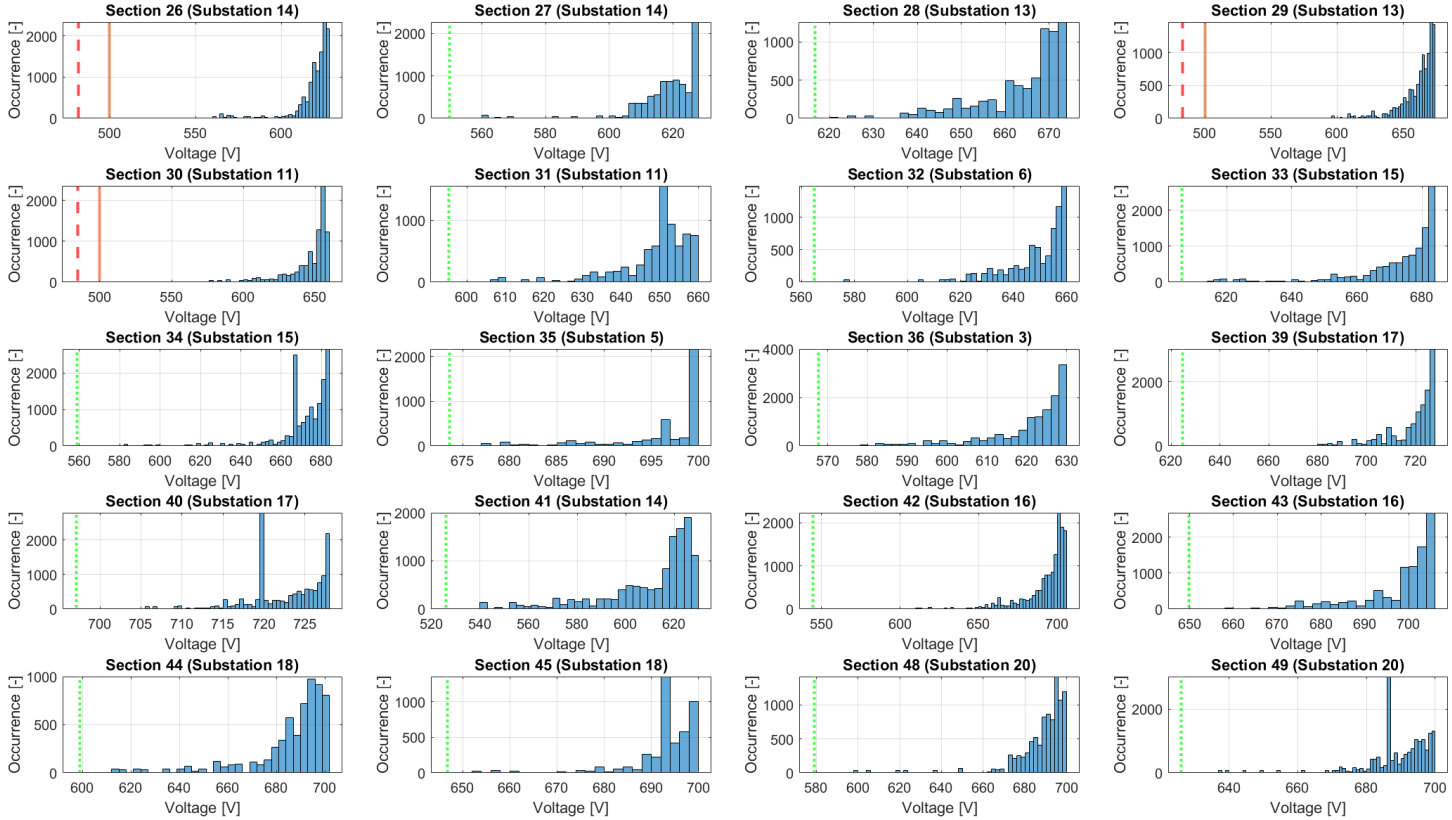

Figure 5.21: Minimum voltages on each section for 04-08-2020 with IMC buses (i.e. including lines 4, 13, 29, and 352). (Part 2 of 2)

Table 5.1: Short circuit currents of each section used in the simulation on the Arnhem trolleygrid [29]. *The values of sections 48 and 49 are based on adjacent section 34 as no information on these sections was available.

Section	Short circuit current	Section	Short circuit current	Section	Short circuit current	Section	Short circuit current
2	1250	16	1350	26	1400	36	1550
3	1400	17	950	27	1400	39	1250
5	1650	18	1000	28	1500	40	4100
6	3950	19	1850	29	1350	41	1050
8	1100	20	2000	30	1300	42	1150
9	2200	21	2700	31	3000	43	1400
12	800	22	1150	32	1200	44	1150
13	1100	23	1300	33	1350	45	1300
14	1300	24	1950	34	1500	48	1400*
15	1550	25	1500	35	1400	49	1400*

5.3.3. Maximum current analysis

Just like with the power demand and minimum voltage the maximum current on each section at each timestep can be found in the results. For each section a certain current value is set as a safety against short circuits Liandon [29]. These values can be found in Table 5.1. Similar to the investigation by Liandon the maximum current during exploitation on each section and 1.5 times this maximum current are considered. Both values will be compared to the short circuit current safety values of each section. The value of 1.5 times the maximum current is used as a rule of thumb which represents the current that could occur during emergencies [29]. As a sidenote: for the full year analysis the maximum current analysis was based on a current-carrying capacity instead.

Taking a first look at the maximum currents on 04-08-2020 without IMC buses some sections which exceed their short circuit safety currents can be found. In Figure 5.22 and Figure 5.23 section 12 has a maximum current of 1009 [A] which exceeds the short circuit of 800 [A]. In all other sections the short circuit current is not exceeded by their maximum currents. However, when looking at the emergency currents which are 1.5x the regular current a high number of sections exceed this short circuit value. It happens for section 12, 25, 26, 29, 30, 32, 39 and 42.

The high number of sections with breaches with the included safety factor of 50% would indicate that the power might be switched off by short circuit protection in case of emergency in those sections. However, the bus operator has mentioned that chances of the current increasing by 50% during emergency are very small [29]. On top of that, as this thesis deals with the effect of IMC buses specifically this is out of the picture completely. IMC buses can preemptively disconnect and drive autonomously when breaches are anticipated.

The breach in section 12 however is of high importance. As mentioned before all regular trolleybus lines run through section 12. Of the IMC bus lines considered line 29 also runs through section 12. It is very important to make sure that the safety mechanism of this section does not trigger during normal operation. This could be resolved by either connecting neighbouring sections to section 12 and/or by dividing section 12 into smaller sections.

When looking at the simulation with IMC buses in Figure 5.24 and Figure 5.25 more breaches can be found. Specifically the two breaching during normal operation in sections 12 and 18. The maximum current in section 12 has increased from 1009 [A] to 1335 [A]. It is clear that bus line 29 has an impact on this as this is the only IMC bus line that is covered by section 12. The same is true for section 18 of which the 1000 [A] limit is breached with a value of 1097 [A].

For both these sections it will have to be investigated whether the high currents are due to the amount of buses on the section or due to the distance of buses from the feed-in point. A combination of both is also possible. If mostly distance is the issue then it could be considered to add one or two feed-in points at the other end of the section. A deeper investigation on this can be found in section 5.5.

This concludes the simulations performed on two specific weekdays. Based on power demand, minimum voltage and maximum current it was found that some substations and/or sections breach their limits when IMC buses are included. For a more thorough analysis the next section will expand the simulations to include

days of a whole year. This was done to make sure that all types of schedules and regular weather patterns are covered.

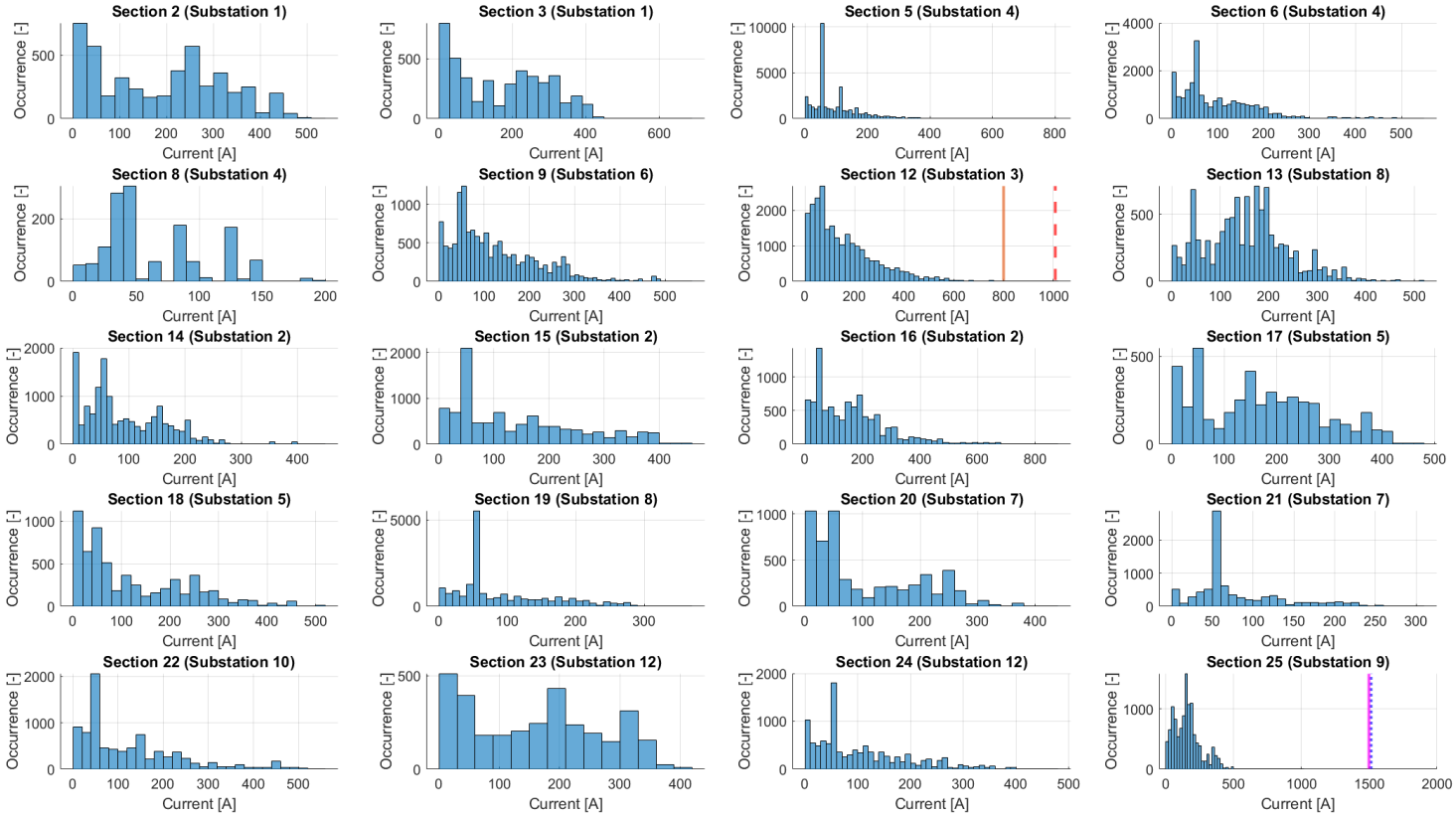

Figure 5.22: Maximum currents on each section for 04-08-2020 without IMC buses (i.e. excluding lines 4, 13, 29, and 352). If the maximum current of the day exceeds the short circuit current (orange vertical line) the maximum current is indicated by a red dashed line. If 1.5x the maximum current exceeds it then this is indicated by a magenta and dotted blue line. (Part 1 of 2)

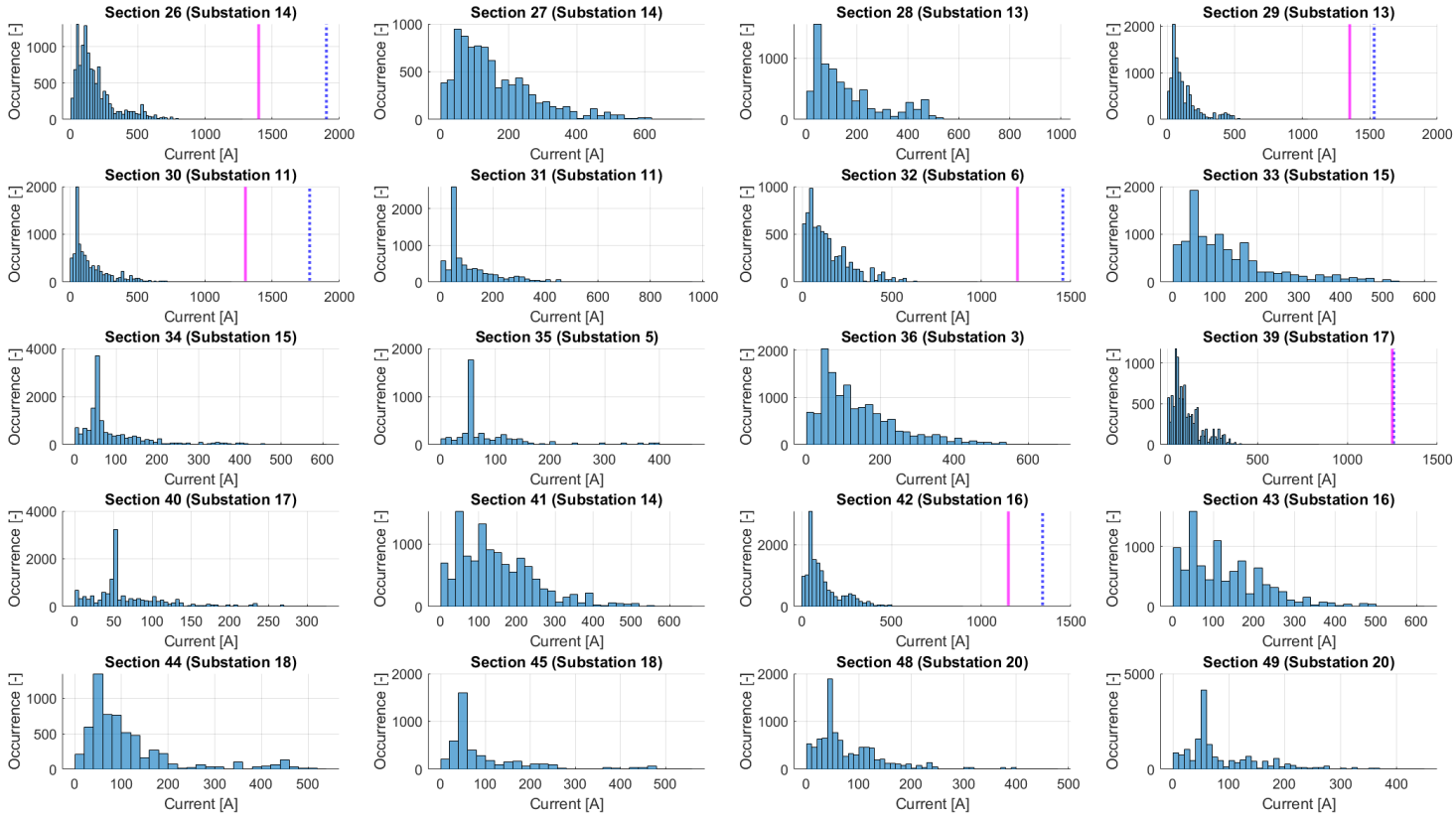

Figure 5.23: Maximum currents on each section for 04-08-2020 without IMC buses (i.e. excluding lines 4, 13, 29, and 352). If the maximum current of the day exceeds the short circuit current (orange vertical line) the maximum current is indicated by a red dashed line. If 1.5x the maximum current exceeds it then this is indicated by a magenta and dotted blue line. (Part 2 of 2)

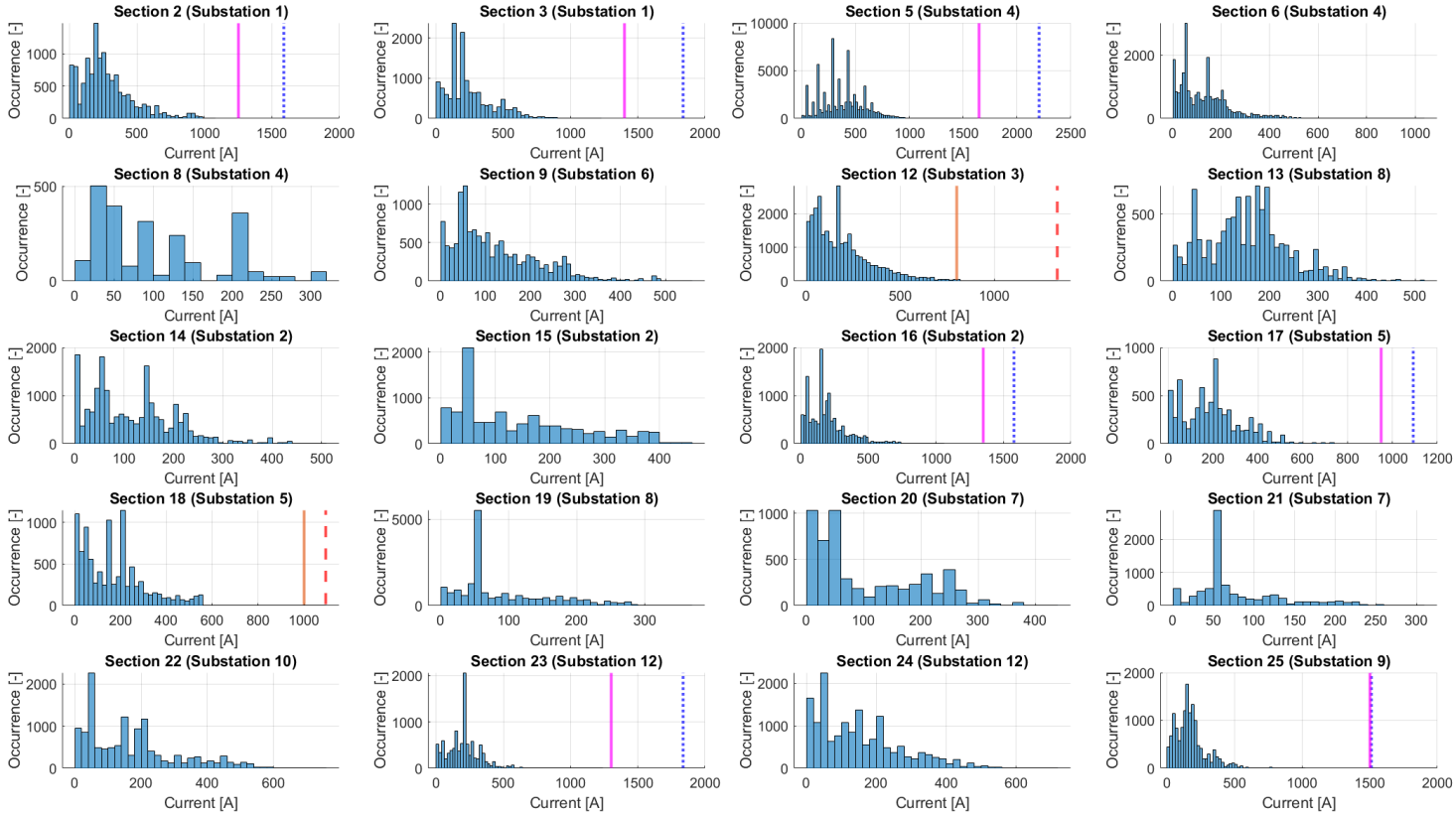

Figure 5.24: Maximum currents on each section for 04-08-2020 with IMC buses (i.e. including lines 4, 13, 29, and 352). If the maximum current of the day exceeds the short circuit current (orange vertical line) the maximum current is indicated by a red dashed line. If 1.5x the maximum current exceeds it then this is indicated by a magenta and dotted blue line. (Part 1 of 2)

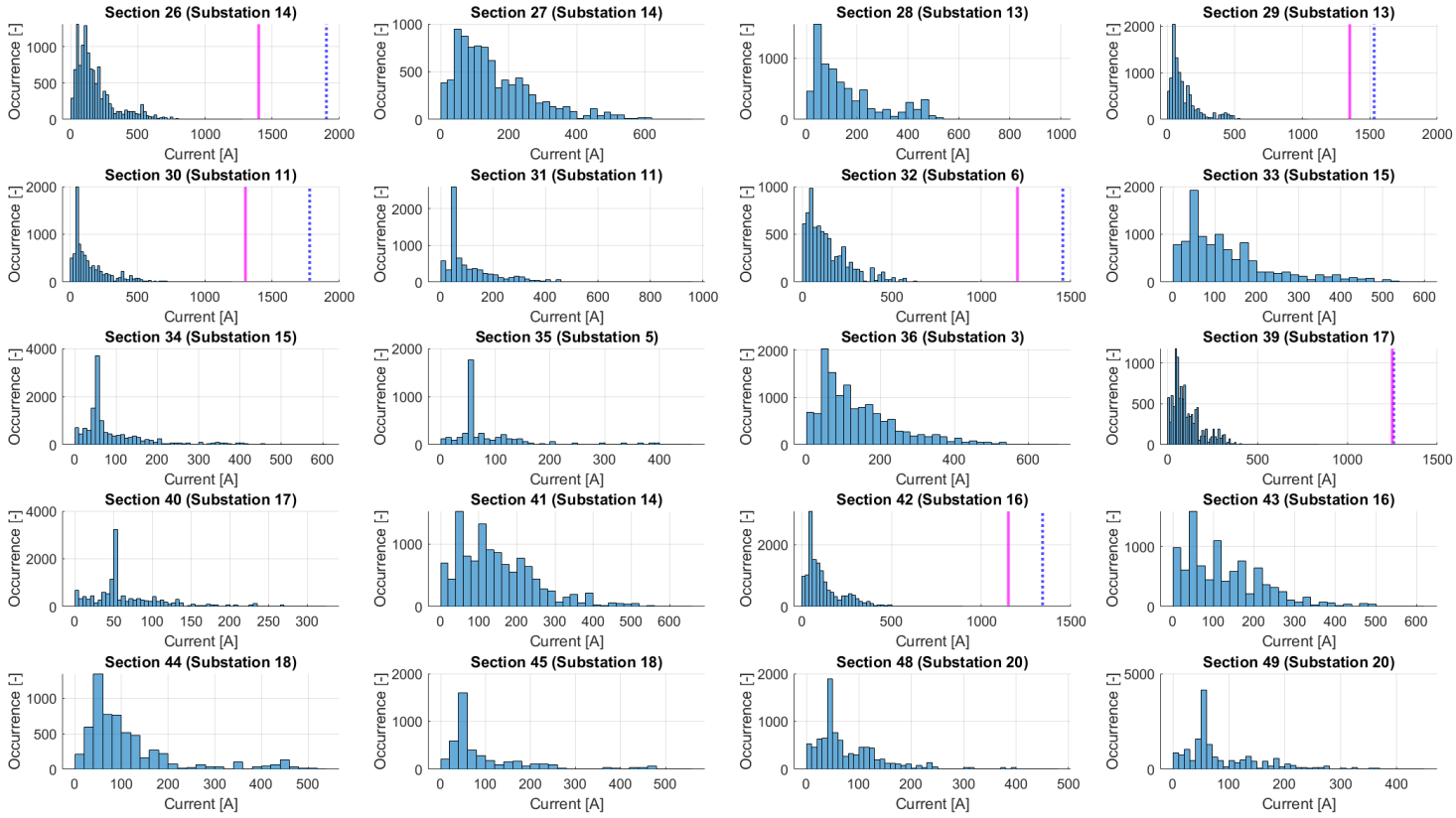

Figure 5.25: Maximum currents on each section for 04-08-2020 with IMC buses (i.e. including lines 4, 13, 29, and 352). If the maximum current of the day exceeds the short circuit current (orange vertical line) the maximum current is indicated by a red dashed line. If 1.5x the maximum current exceeds it then this is indicated by a magenta and dotted blue line. (Part 2 of 2)

5.4. Full grid analysis for a whole year

In the last section it was found that limit breaches occurred on some sections/substations of the grid when IMC buses are implemented. The scope was limited to two specific days (i.e. 04-08-2020 and 01-09-2020). For a more thorough approach this scope is broadened to a full year. This way all different schedule types and regular weather patters (i.e. ambient temperatures) are considered. The full year 2020 is analysed.

5.4.1. Whole year power demand analysis

By looking at the power demands per substation for a whole year in histograms an idea can be developed of the power demand pattern. By doing this for both a simulation without and with IMC buses the effect that the addition of IMC bus lines has on the trolleygrid is shown. What is most interesting is whether or not the power limit of each substation is breached. This power limit of 800 [kW] (1800 [kW] for substation 4) is what the substations are built for. By further analysing the consistency and nature of the power breach it might become clear whether or not the substation should be upgraded when the discussed IMC bus lines are to be added.

The power demands without and with IMC buses are shown in Figure 5.26 and Figure 5.27 respectively. In both figures it can be noticed that for most substations a peak can be found at 30-40 [kW]. This is because the HVAC draws 38.4 [kW] so whenever a bus stands still with the HVAC running this is the power demand. In substation 4, which is the substation where the main hub Arnhem CS is located, this effect is especially noticeable. Peaks of multiples of this number, as multiple buses will stand still there while HVAC is on, are also visible for substation 4.

If a substation power limit is breached this is indicated by an orange vertical line (which represents the substation power limit). The maximum power demand of each substation is indicated by either a green dotted or red dashed line. A green dotted line indicates that the limit is not exceeded. The red dashed lines do exceed the limit. For the simulation without IMC buses this happens in substations 2, 3, 6, 11, 14 and 16. By looking at histograms of just the breaches the severity for each substation can be assessed.

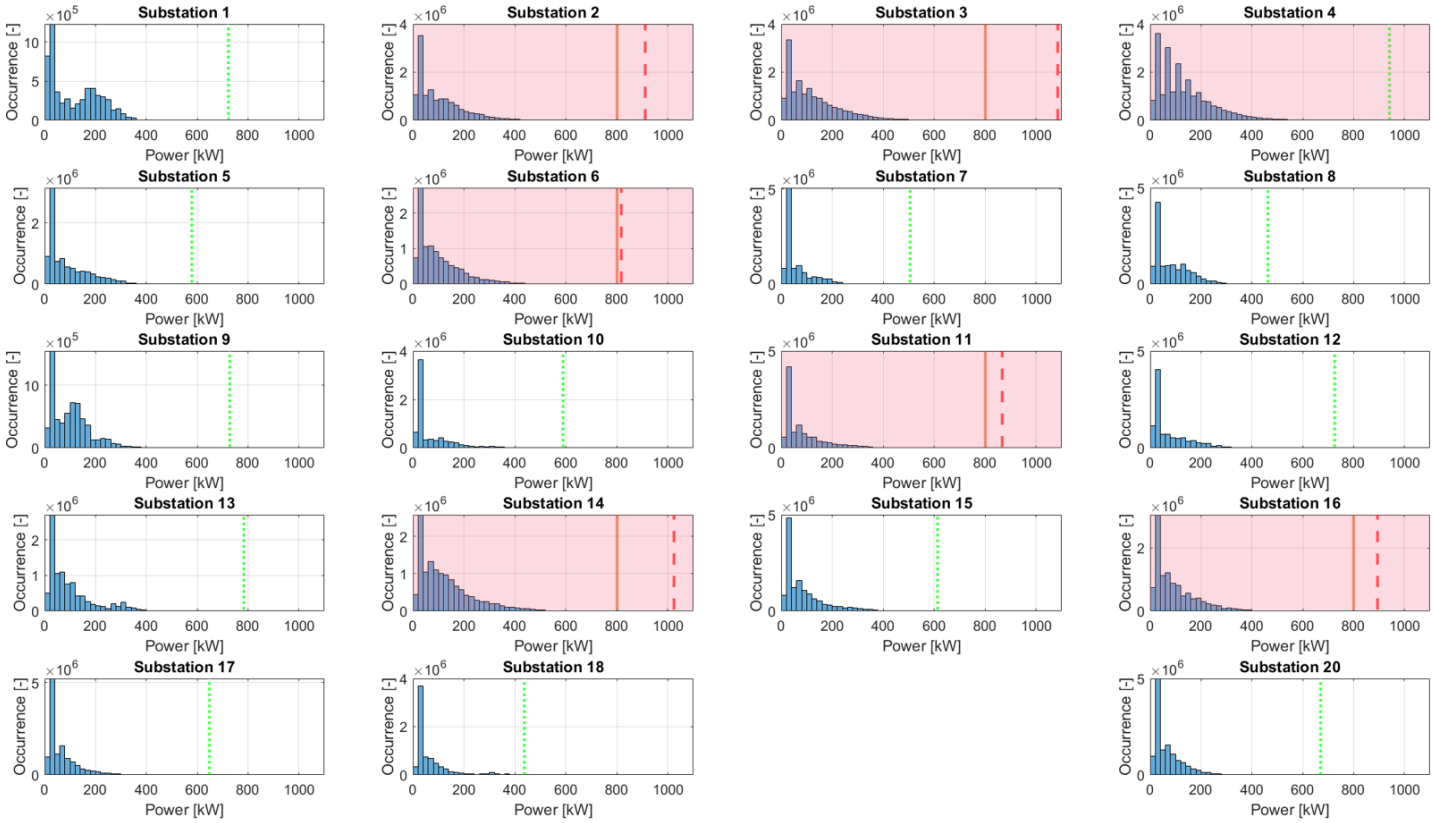

Figure 5.26: Power demands on each substation for the year 2020 without IMC buses (i.e. excluding lines 4, 13, 29, and 352). The maximum power demand on each substation is indicated by a vertical dotted or dashed line. A green dotted line indicates that the limit is never exceeded. A red dashed line indicates that the maximum power demand exceeds the limit. When this is the case the substation limit is indicated by the orange vertical line.

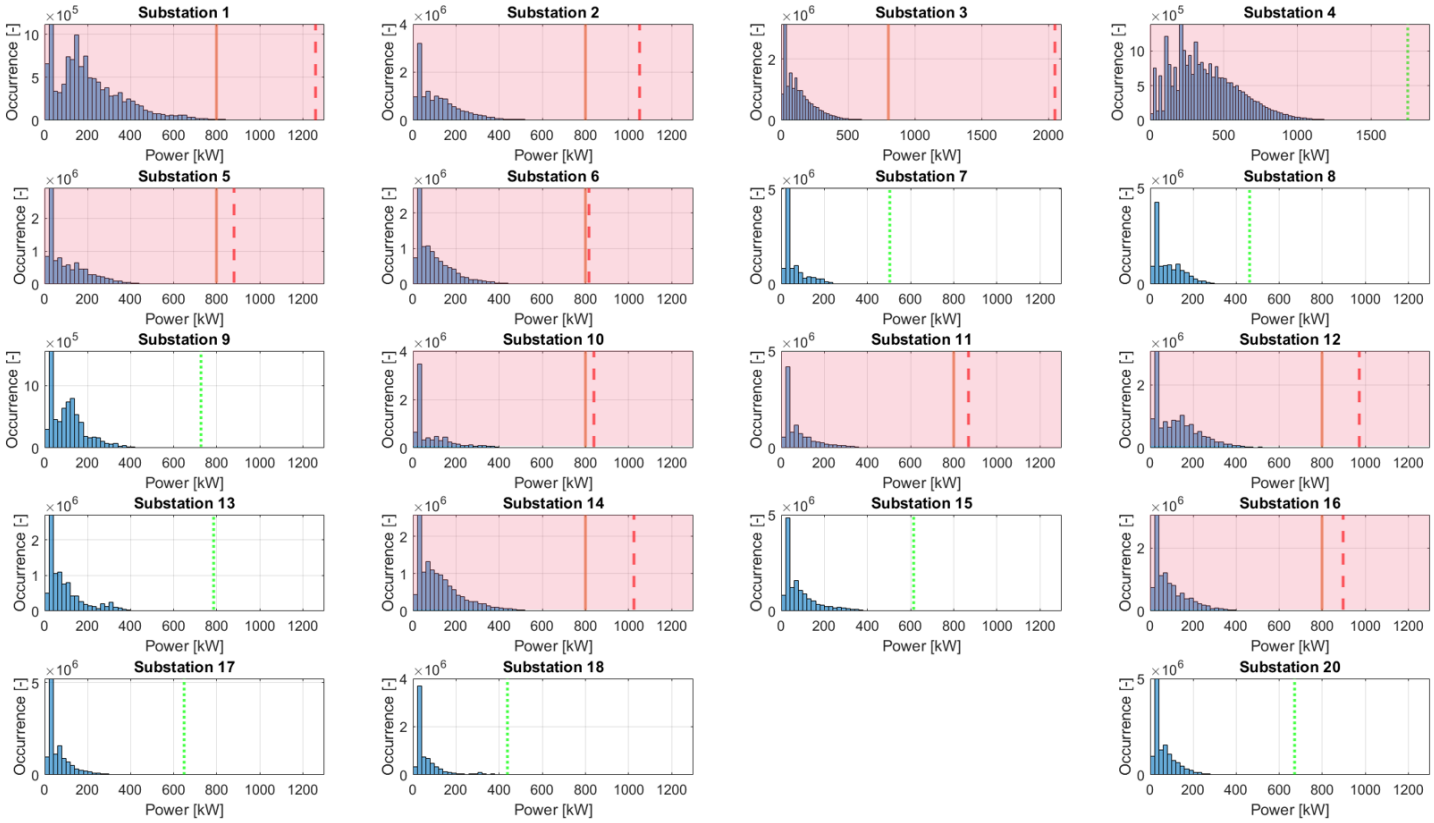

Figure 5.27: Power demands on each substation for the year 2020 with IMC buses (i.e. including lines 4, 13, 29, and 352). The maximum power demand on each substation is indicated by a vertical dotted or dashed line. A green dotted line indicates that the limit is never exceeded. A red dashed line indicates that the maximum power demand exceeds the limit. When this is the case the substation limit is indicated by the orange vertical line.

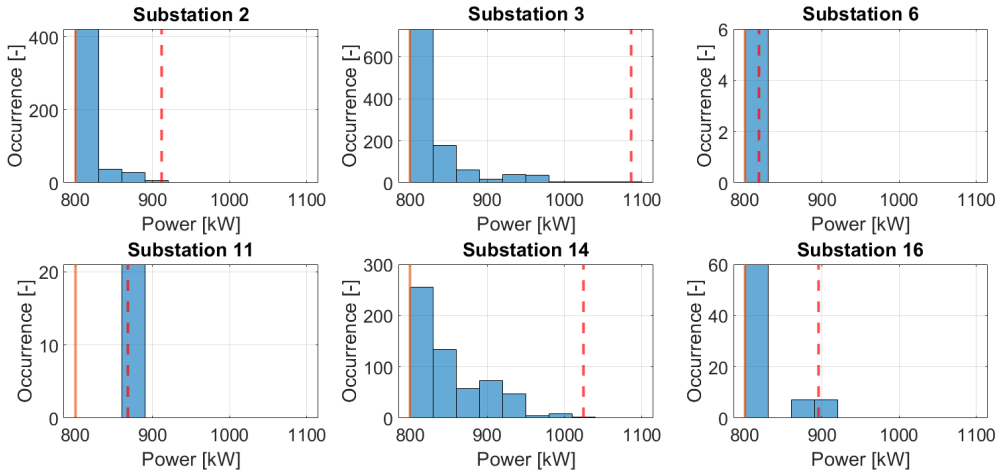

Figure 5.28: Breaches of power demands on substations 2, 3, 6, 11, 14 and 16 for the full year 2020 without IMC buses. The power limit is indicated by the orange vertical line. The maximum power demand on each substation is indicated by a red dashed line.

These breaches are shown in Figure 5.28. Again, the limit is indicated with an orange vertical line while the maximum power demand on each substation is indicated be a red dashed line. The severity of breaches for each of the substations can be gauged by looking at both the amount of occurrences of the breaches in seconds in a year (y-axis) and the size [kW] of the breach (x-axis). The occurrences for substations 6, 11 and 16 do not exceed 100 per year with 6, 21 and 74 seconds respectively. In addition to this the maximum power demand of these substations never exceeds 900 [kW]. These breaches can be categorised as incidental. Coincidentally these three substations do not supply power to sections on which the IMC bus lines operate. These substations are outside the scope of this thesis. Although the amount of occurrences (583 seconds) and size of breaches (maximum of 1025 [kW]) are relatively severe for substation 14, this substation too is outside the scope of the thesis as it does not supply power to IMC buses.

However, the severity of the breaches on substation 14 should be noted. Together with the severity of breaches in substations 2 and 3 these breaches can be seen as an example of relatively low severity. Furthermore, in reality the Arnhem trolleygrid employs bilateral connections for the relevant sections while these simulations are based on unilateral models of the sections. These breaches might therefore not occur in reality. Without IMC buses substation 2 has power limit breaches occurring 493 seconds with a maximum breach of 912 [kW]. For substation 3 these numbers are 1087 times and 1086 [kW] respectively. By using these numbers as a baseline and comparing this to the situation with IMC buses the extra strain that IMC buses put on the system can be evaluated.

Moving on to power demand breaches in a simulation with IMC buses which are illustrated in Figure 5.29. Substations 5 and 10 show very small breaches in relatively low numbers. These two substations will need no further investigation. Compared to the simulation without IMC buses substation 2 shows a slight increase in both breach occurrence and maximum power demand. The severity of breaches for both substations 2 and 12 can be considered as low to moderate. The two glaring outliers can be found in the remaining two histograms. The occurrence of breaches in substation 1 (53015 seconds) and the maximum power demand on substation 3 of 2048 [kW] are severe.

The breaches on substations 1 and 3 will be further investigated. This will be done by looking at the actual power profiles of the substations and the underlying sections. Substation 1 supplies its power to sections 2 and 3. Substation 3 supplies its power to sections 12 and 36.

5.4.2. Whole year minimum voltage analysis

In similar fashion as with the power demand the minimum voltage on each section at each timestep can be observed. In a study performed by Liandon in 2012 the voltage limits of the Arnhem trolleybuses is explained [29]. If a trolleybus reaches a low voltage of 500 [V] the power control will intervene. This means that below this limit the bus will not be able to draw the amount of power it is currently demanding. This results in the bus not being able to accelerate the way it is supposed to and can lose its velocity. At 400 [V] this power

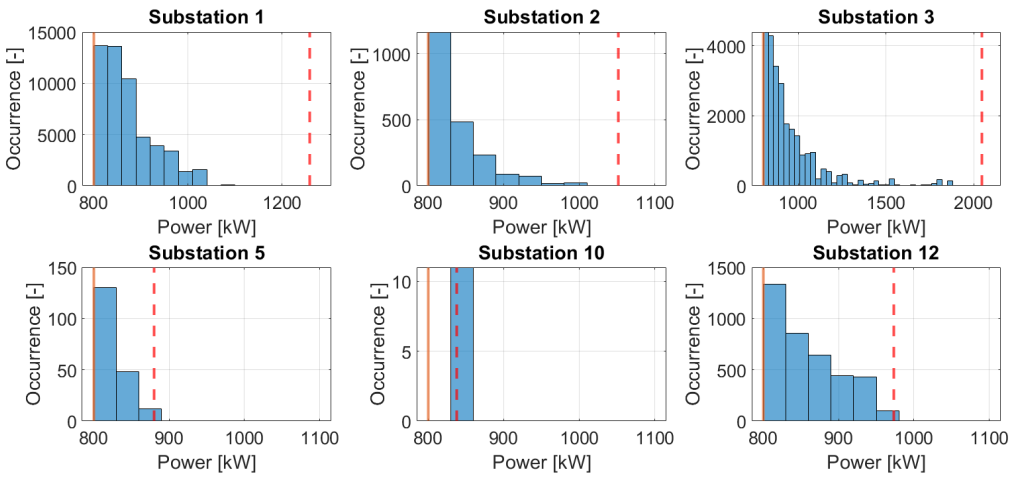

Figure 5.29: Breaches of power demands on substations 1, 2, 3, 5, 6, 10, 11, 12, 14 and 16 for the full year 2020 with IMC buses. The power limit is indicated by the orange vertical line. The maximum power demand on each substation is indicated by a red dashed line.

control completely shuts off the power demand of the bus. For this analysis any occurrence of the voltage reaching values below 500 [V] is looked at.

Minimum voltages on each section for the simulation without IMC buses can be found in Figure 5.30 and Figure 5.31. The sections which have voltages below 500 [V] are sections 12, 19, 26, 29, 30, 41 and 42. Of these sections section 12 has the lowest voltage instance with a voltage of 443 [V]. Coincidentally this is the only section with a voltage below 500 [V] on which one of the four IMC bus lines (i.e. line 29) operates. This section has already proven to be problematic when considering the maximum power.

Comparing this to a situation with IMC buses (see Figure 5.32) and it can be noticed that sections 2 and 22 now also have small voltage drops below 500 [V]. The minimum voltage of section 12 drops even further to the minimum of 400 [V]. This value and section should be further investigated on operation with IMC buses. Although all regular trolleybus lines operate on it, only IMC bus line 29 operates on this section.

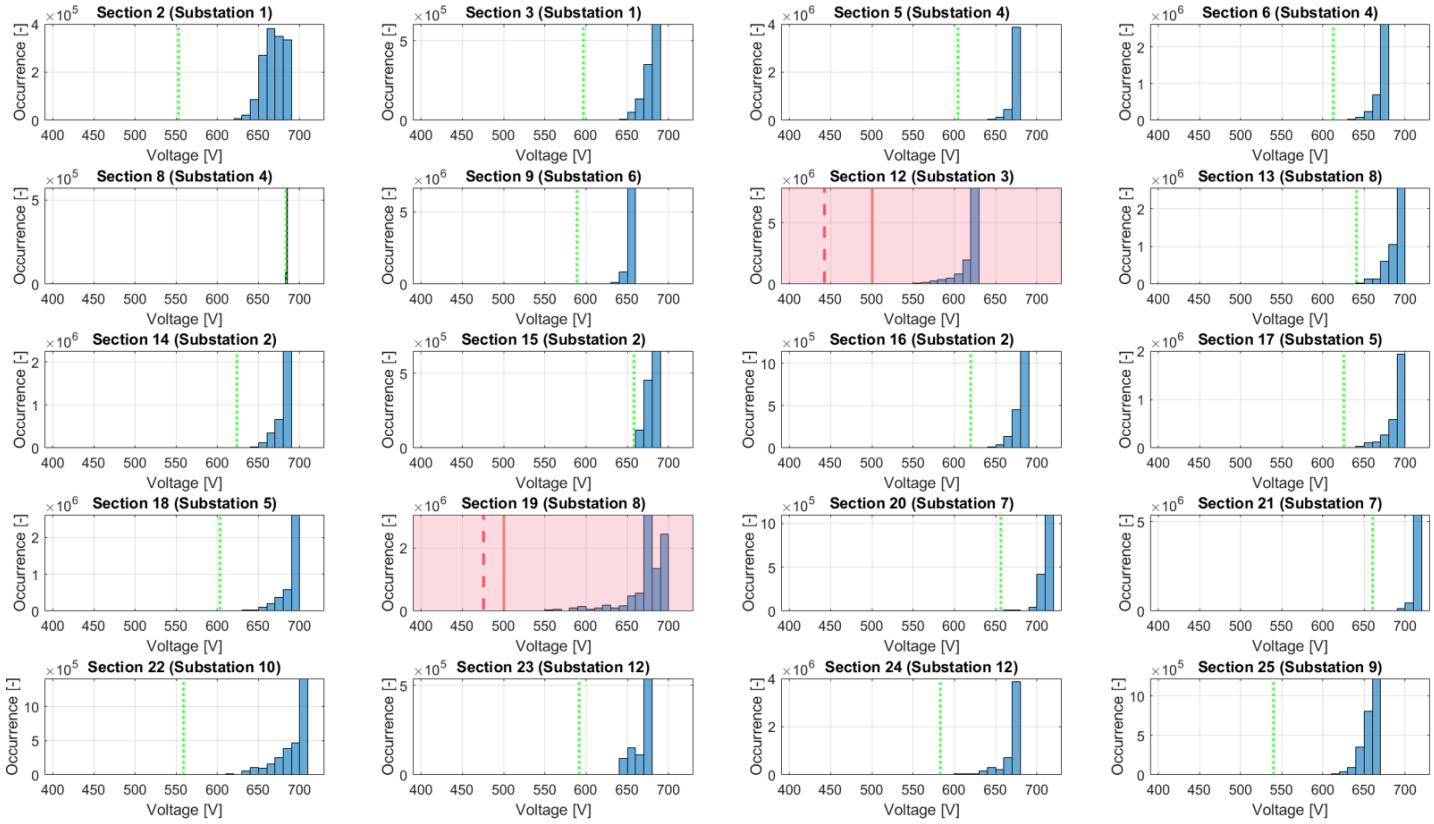

Figure 5.30: Minimum voltages on each section for the year 2020 without IMC buses (i.e. excluding lines 4, 13, 29, and 352). If the lowest voltage is below the 500 [V] limit (orange vertical line) this lowest voltage is indicated by a red dashed line. Otherwise the lowest voltage is indicated by a green dotted line. (Part 1 of 2)

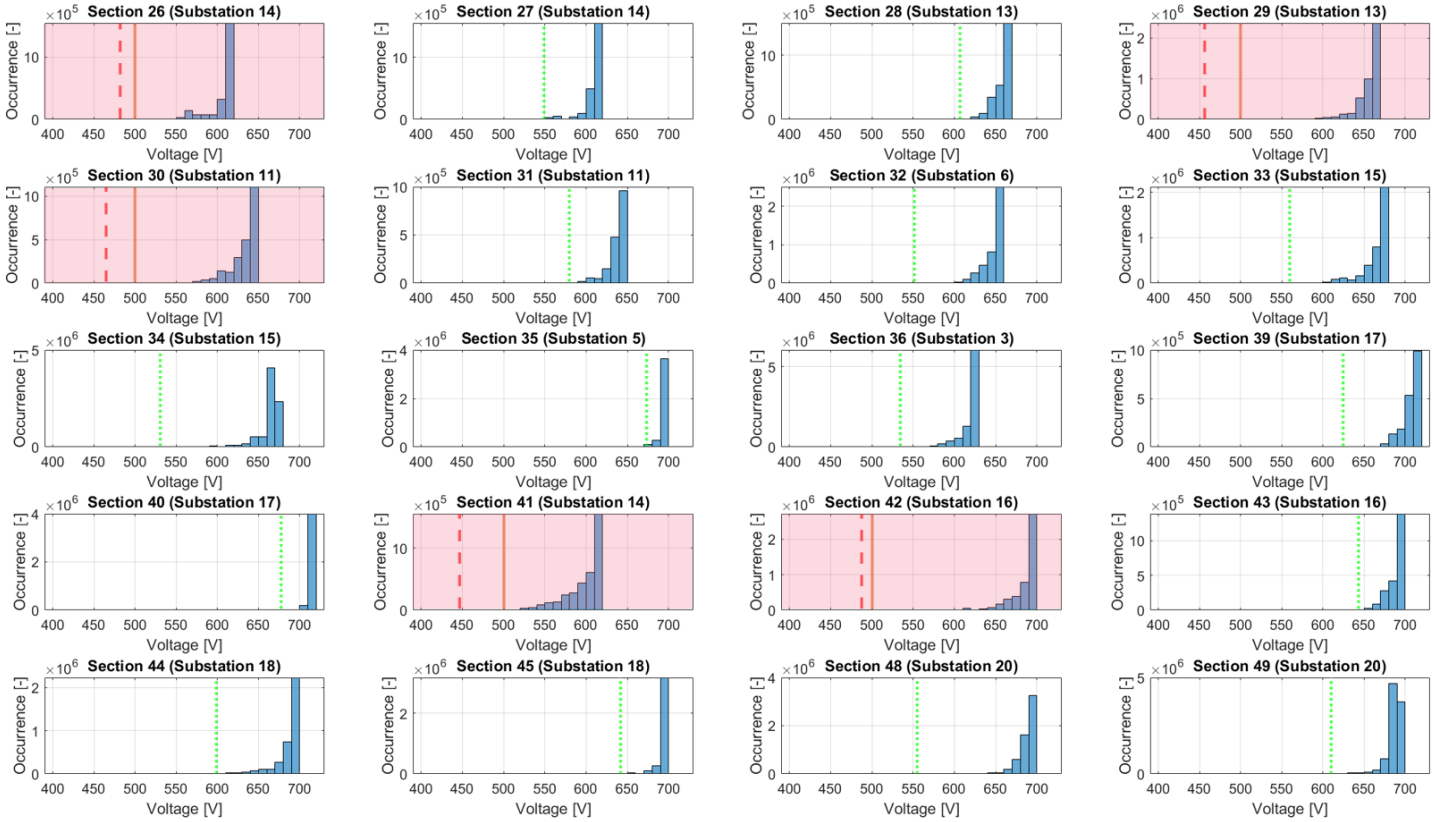

Figure 5.31: Minimum voltages on each section for the year 2020 without IMC buses (i.e. excluding lines 4, 13, 29, and 352). If the lowest voltage is below the 500 [V] limit (orange vertical line) this lowest voltage is indicated by a red dashed line. Otherwise the lowest voltage is indicated by a green dotted line. (Part 2 of 2)

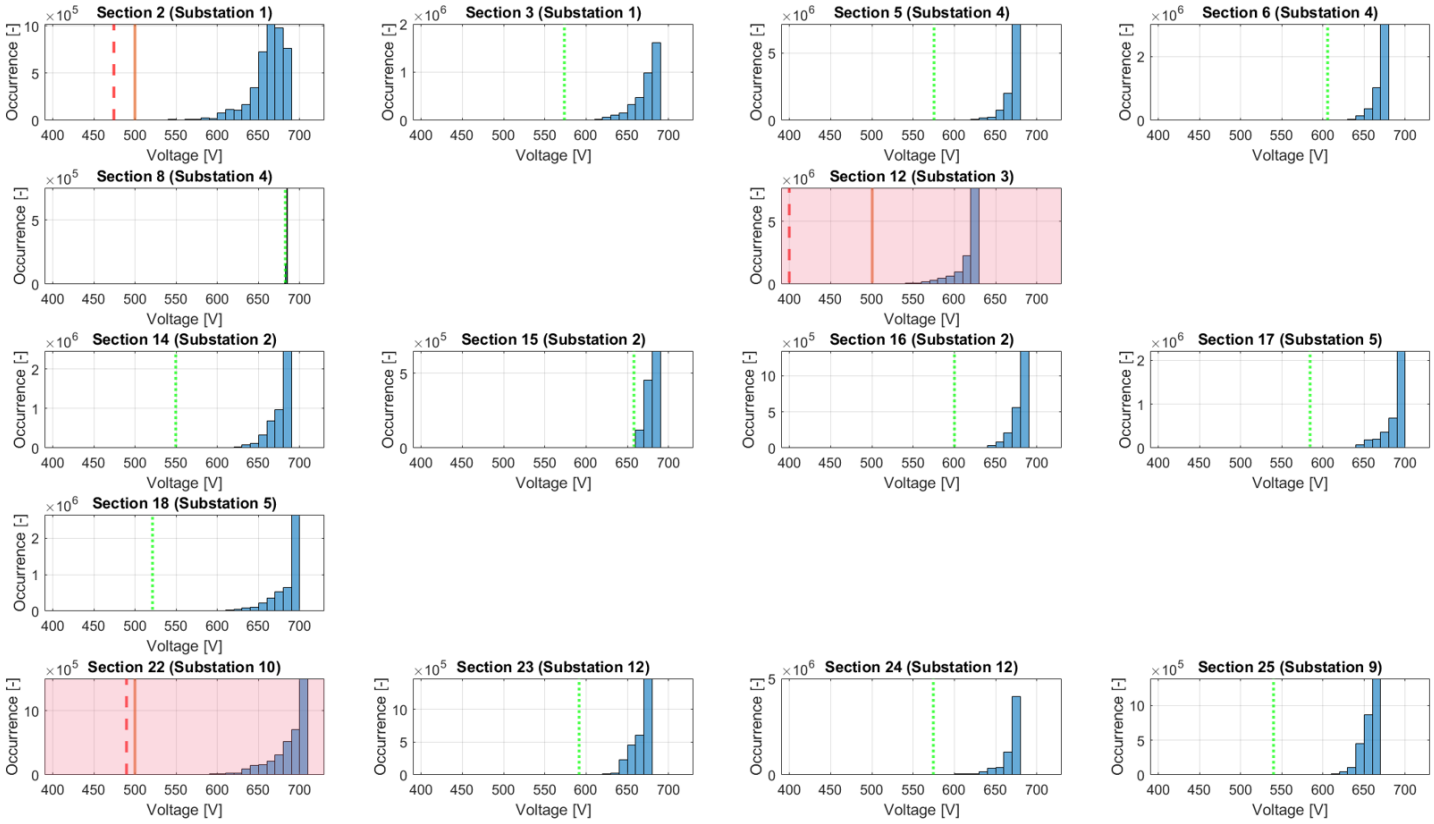

Figure 5.32: Minimum voltages on each relevant section (i.e. sections where no IMC bus operates are excluded) for the year 2020 with IMC buses (i.e. including lines 4, 13, 29, and 352). If the lowest voltage is below the 500 [V] limit (orange vertical line) this lowest voltage is indicated by a red dashed line. Otherwise the lowest voltage is indicated by a green dotted line.

5.4.3. Whole year maximum current analysis

Just like with the power demand and minimum voltage the maximum current on each section at each timestep can be found in the results. This maximum current can be evaluated by comparing it to the current-carrying capacity of the wire. This is the current value at which the wire can carry a constant current while still staying under its temperature rating. A continuous current that exceeds this value can damage the wire permanently.

The substations can supply 800 [kW] of power which the parallel wires should be able to transport to the buses safely. 500 [V] is considered a critical voltage as at that point buses will reduce their power demand. The current needed to transport 800 [kW] at that voltage is 1600 [A]. As the wires should not fail under any circumstances this current value can be considered as an upper limit. 1600 [A] is therefore used as the current-carrying capacity that the results are compared to. As sections 6 and 19 do not have parallel lines this value is halved to 800 [A] for those two sections. It should be noted that this is an approximation. In reality the current is split between wires based on relative length.

The results of the comparison of maximum current on each section with this current-carrying capacity can be found in Figure 5.33 and Figure 5.34 for the simulation without IMC buses. The first thing that can be noticed from these figures is that the current-carrying capacity is exceeded only on section 6. This is one of two sections with no parallel lines. It does appear however, based on the lack of occurrences above the limit, that the currents do not exceed the current-carrying capacity for long periods of time. This indicates that, when no IMC buses are present, the currents on the overhead lines stay within safe limits.

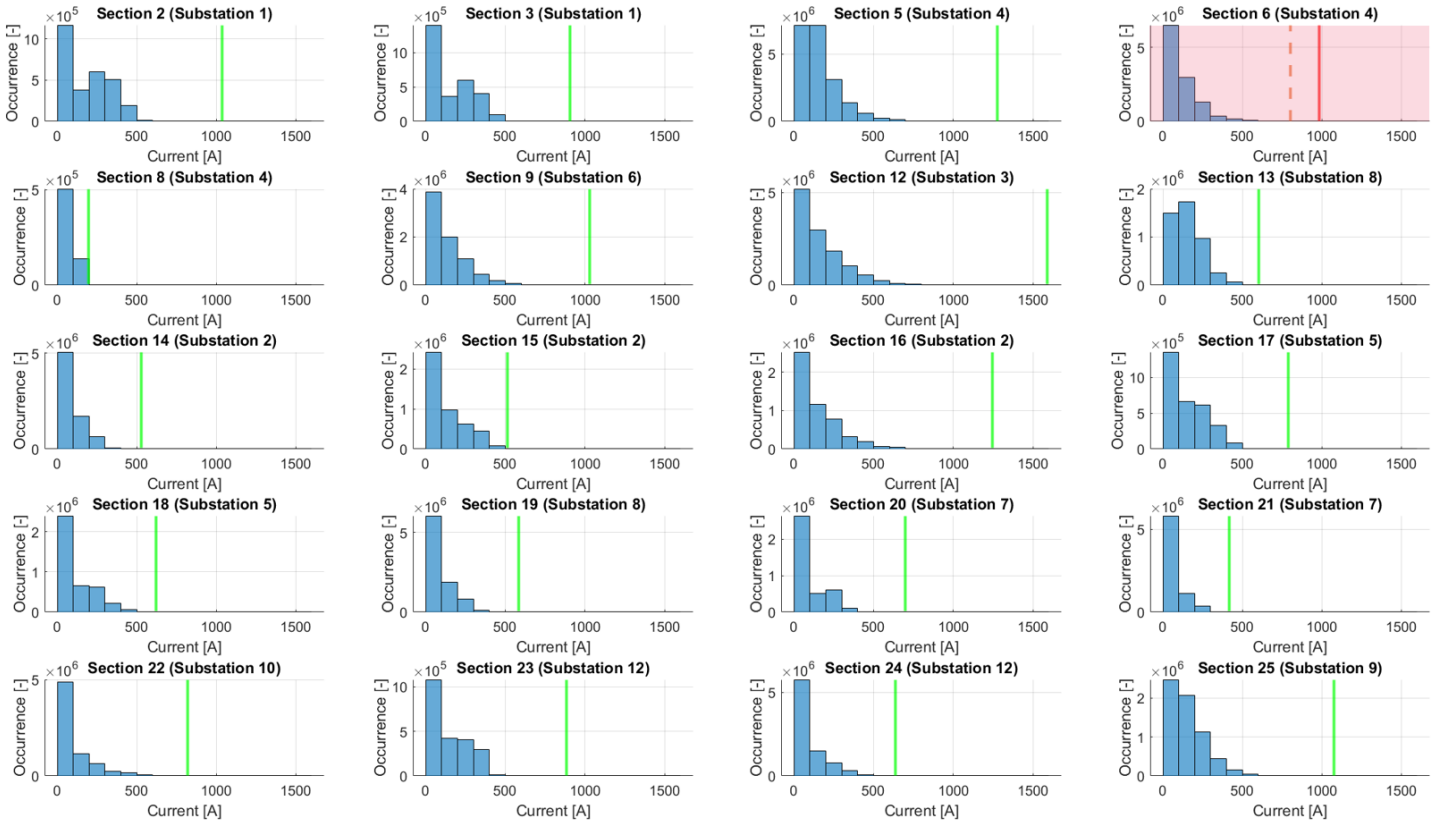

Figure 5.33: Maximum currents on each section for the year 2020 without IMC buses (i.e. excluding lines 4, 13, 29, and 352). If the highest current exceeds the current-carrying capacity (orange dashed line) this highest current is indicated by a red line. A green line indicates that the maximum current is below the current-carrying capacity. (Part 1 of 2)

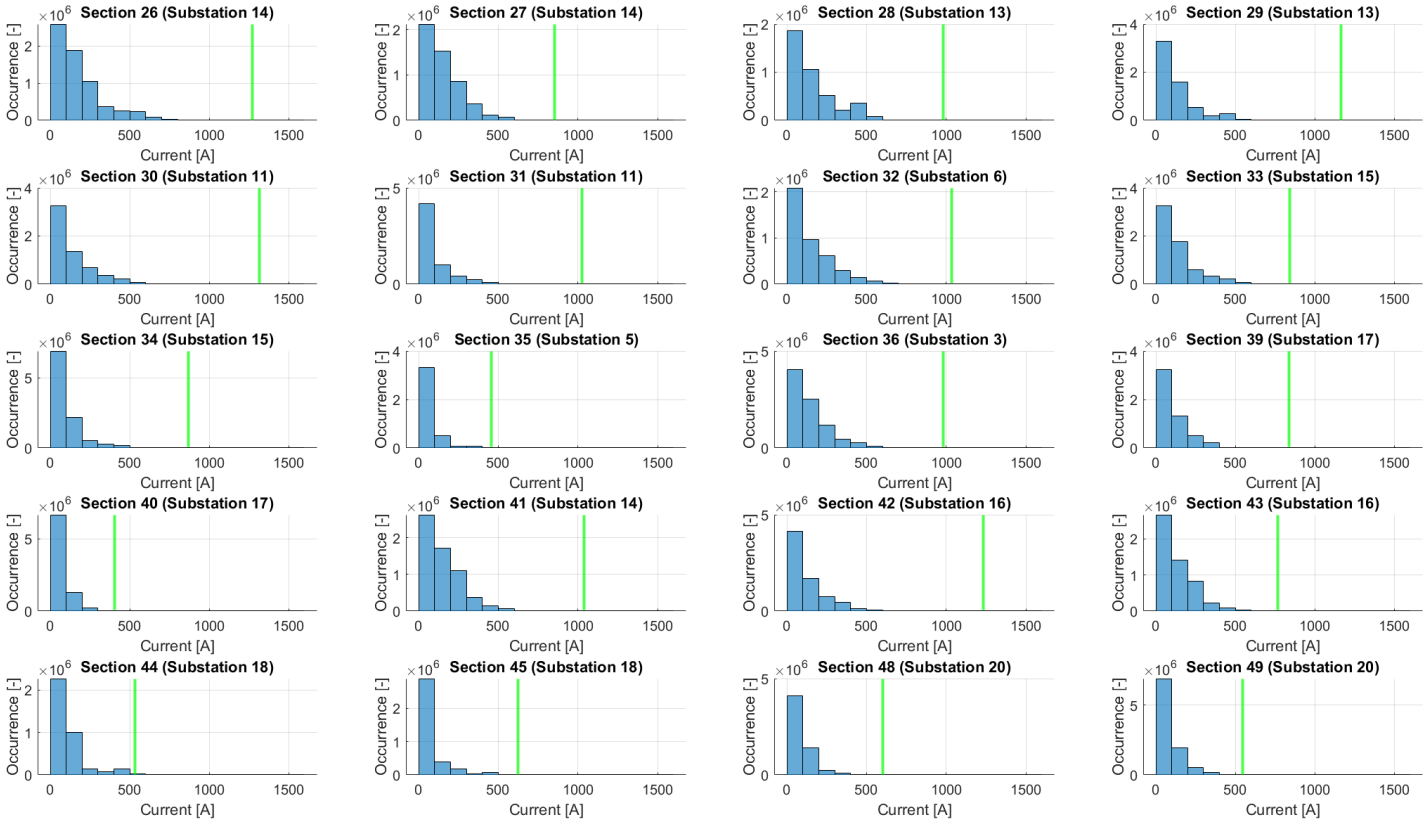

Figure 5.34: Maximum currents on each section for the year 2020 without IMC buses (i.e. excluding lines 4, 13, 29, and 352). If the highest current exceeds the current-carrying capacity (orange dashed line) this highest current is indicated by a red line. A green line indicates that the maximum current is below the current-carrying capacity. (Part 2 of 2)

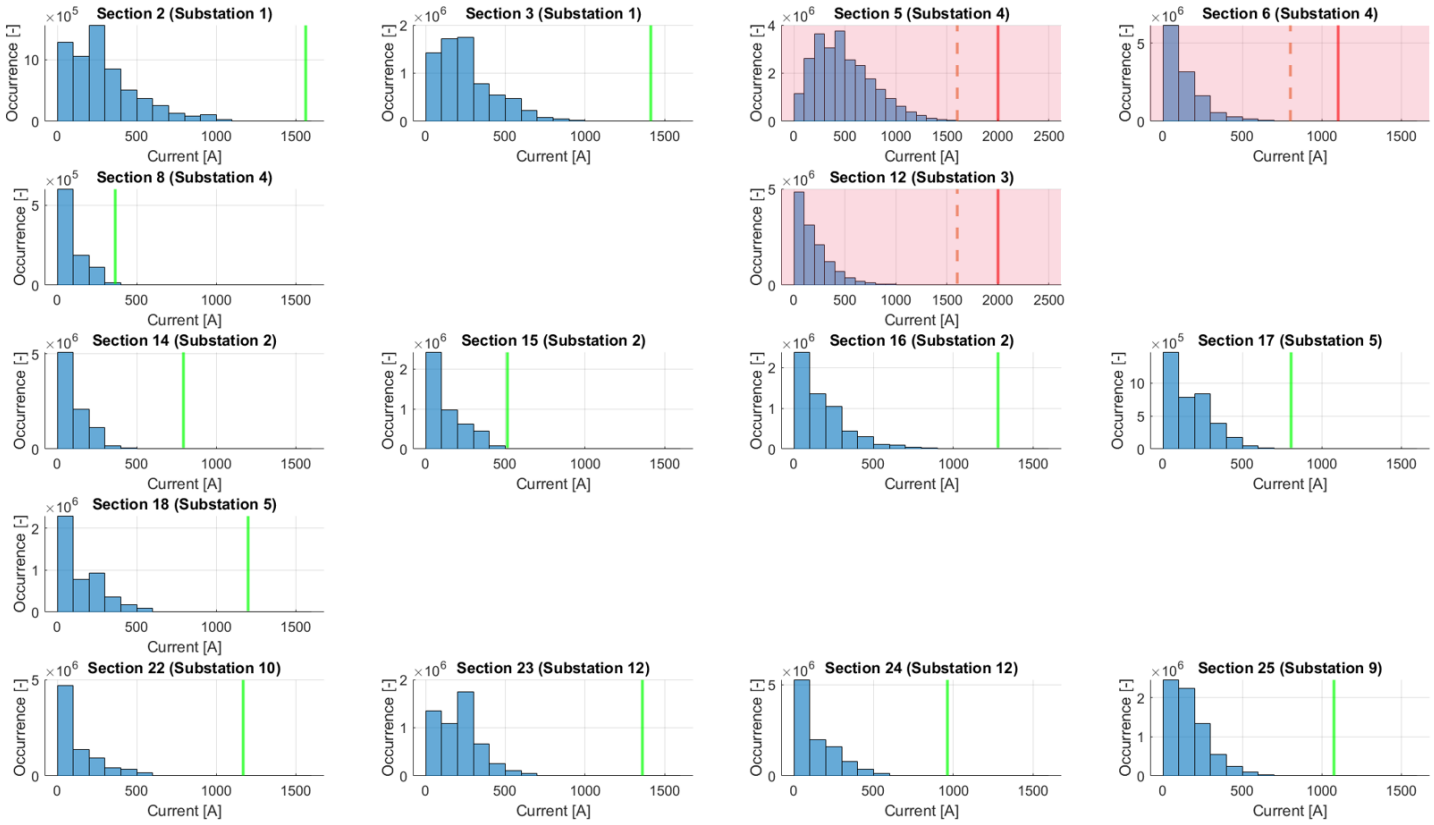

Figure 5.35: Maximum currents on each relevant section (i.e. sections where no IMC bus operates are excluded) for the year 2020 with IMC buses (i.e. including lines 4, 13, 29, and 352). If the highest current exceeds the current-carrying capacity (orange dashed line) this highest current is indicated by a red line. A green line indicates that the maximum current is below the current-carrying capacity.

The results for the simulation with IMC buses can be found in Figure 5.35. In the results of sections 5, 6 and 12 there are occurrences of currents above the current-carrying capacity. The shear amount of high currents is especially noticeable in section 5. This is most likely because in that section lies the trolleybus plaza at Arnhem CS where a high number of buses stop for a long time.

In Figure 5.36 the maximum currents on section 5 simulated for a regular weekday (1-4-2020) are shown. The plot shows the currents for two cases in which the IMC buses are included. The difference between the blue line and the red line is the exclusion/inclusion of battery charging respectively. A charging power of 100 [kW] while stopped and 150 [kW] while moving was applied. By looking at the red line it can be seen that the high amount of IMC buses stopped at the trolleybus plaza drastically increase the current on the section. This increase should not be overlooked.

When considering the addition of IMC buses one option would be to replace the overhead lines at the trolleybus plaza by thicker wires. A less expensive option would be to look into mitigation of battery charging to other sections and/or dynamic charging. This mitigation is discussed in section 5.6. First, in the next section the substations and sections that were found to pose the most problems through this whole year analysis will be investigated more thoroughly.

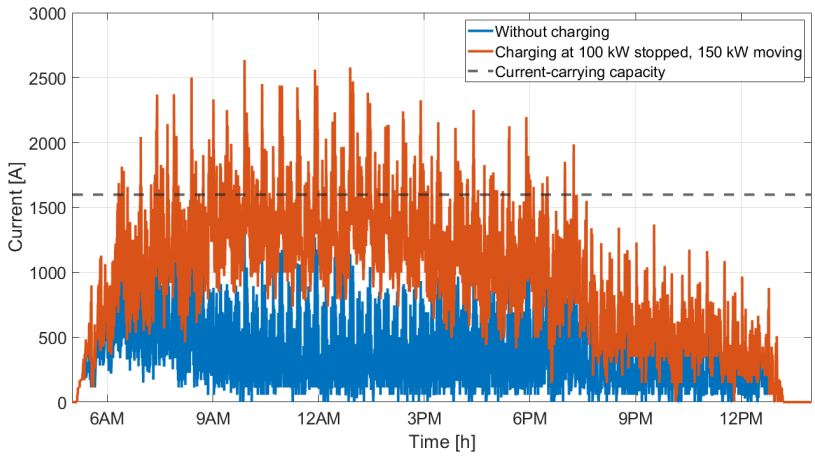

Figure 5.36: Maximum current on section 5 with IMC buses for a regular weekday schedule. Without charging (blue) and with charging (red) with a battery charging power of 100 [kW] while stopped and 150 [kW] while moving. A dashed black line indicates the current-carrying capacity of 1600 [A].

5.5. Detail analysis on critical sections/substations

By looking at histograms for power demand, minimum voltage and maximum current the problematic substations and sections can be identified. Through a full year analysis of 2020 it was found that most problems occurred on substation 1 (with sections 2 and 3) and substation 3 (with sections 12 and 36). No IMC buses operate on section 36 but its power demand can interfere with section 12 and it is therefore included in these deeper investigations.

Instead of looking at the full year power, voltage and current profiles six days will be considered. Each of these days is representative for one of the six types of bus schedules. The day numbers and corresponding dates for each of the schedules can be found in Table 5.2. The first four representative days were chosen by taking the day with the lowest temperature. For the two Summer schedules the days with the highest temperatures were taken. In both cases this was done to show the days with the highest HVAC energy demand.

Substations 1 and 3 will be discussed separately in the next sections. This will be done by again taking a look at the histograms for these specific days as well as specific instances on which breaches occur. By finding the nature and cause of these breaches specific advice can be offered on how to remedy the problems.

5.5.1. Substation 1 (sections 2 and 3)

Substation 1 is situated to the West of Arnhem CS. It supplies power to feed-in point 2 and 3 which are on the route of regular trolleybus line 1 and IMC bus line 352. Figure 5.29 has shown that substation 1 has a

Table 5.2: The six day numbers and dates of the representative days. For the first four schedule types the day with the lowest temperature was used. For the Summer schedules the days with the highest temperature was used.

Type of schedule	min/max temperature [°C]	day number	date
Regular weekday	-5.6	92	1-4-2020
Regular Saturday	-1.9	67	7-3-2020
School Holiday weekday	-1.3	366	31-12-2020
Sun- and special holiday	-5.0	334	29-11-2020
Summer weekday	35.2	224	11-8-2020
Summer Saturday	35.3	221	8-8-2020

high number of power limit breaches. Breaches occur on four of the six schedule types in the histograms for different schedule types in Figure 5.37.

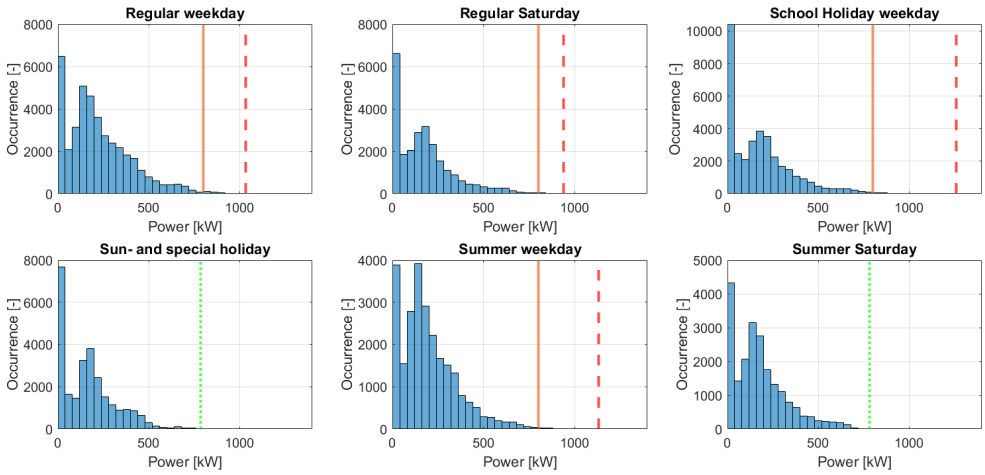

Figure 5.37: Power demands on substation 1 for each type of bus schedule with IMC buses. The maximum power demand on each substation is indicated by a vertical dotted or dashed line. A green dotted line indicates that the limit is never exceeded. A red dashed line indicates that the maximum power demand exceeds the limit. When this is the case the substation limit is indicated by the orange vertical line.

In Figure 5.38 full day plots instead of histograms of the four schedule types with breaches are shown. It can be seen that for every one of these schedule types repetitive breaches occur during daytime (i.e. 6AM-7PM). As the breaches have a maximum of around 1000 [kW] a 'simple' solution to this problem would be to increase the substation capacity to 1000 [kW].

However, when charging (which was set to 100 [kW] while stopped/150 [kW] while moving) is excluded just a single breach in all four schedule types occurs. This breach is shown in Figure 5.39. It occurs around 9AM on the School Holiday weekday schedule. What can be concluded from this is that temporarily restricting charging power for IMC buses connected to this substation can be a viable strategy to stay within substation power limits.

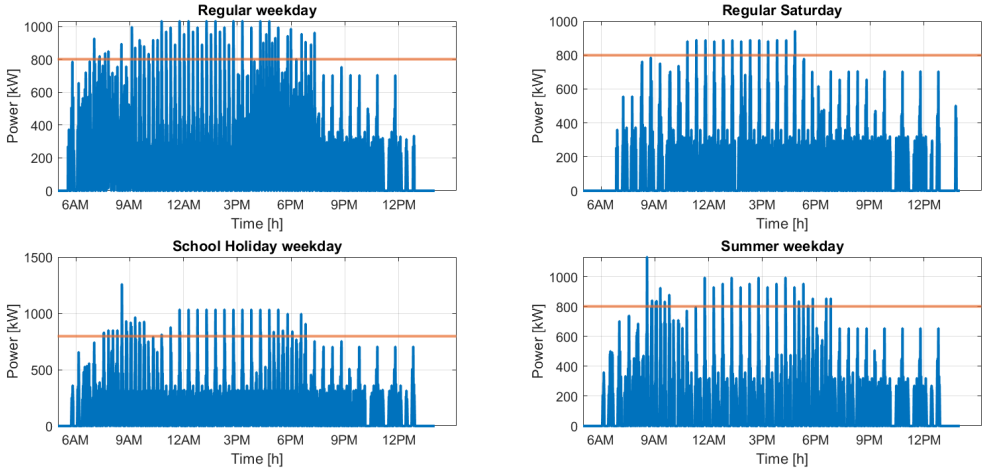

Figure 5.38: Full day power demand of substation 1 for four different bus schedule types with IMC buses. The 800 [kW] limit (orange horizontal line) is exceeded more than once for these schedule types.

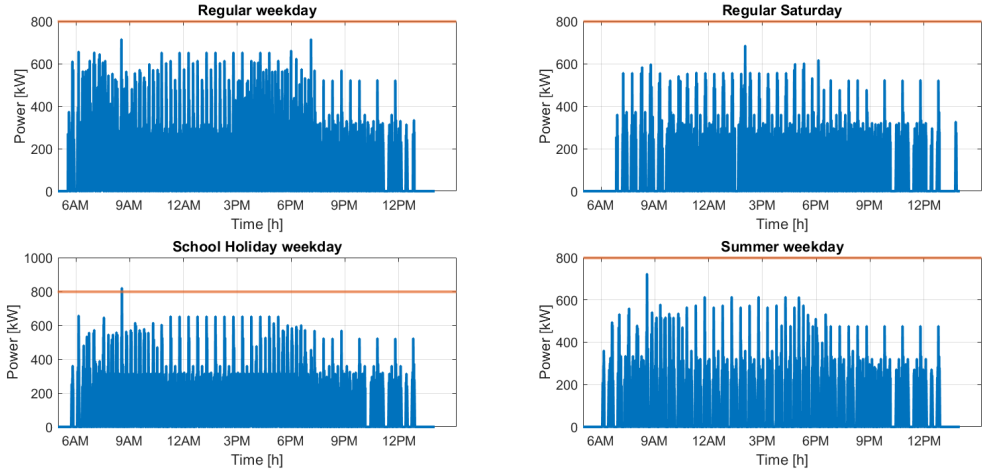

Figure 5.39: Full day power demand of substation 1 for four different bus schedule types with IMC buses without charging. Without charging the 800 [kW] limit (orange horizontal line) is exceeded just once and it happens on the School Holiday weekday schedule.

5.5.2. Substation 3 (sections 12 and 36)

Substation 3 supplies power to sections 12 and 36. The two sections are relatively far apart with section 12 at the North side of the river Rijn and section 36 on the South side. The substation itself is placed next to the bus depot on the North side of the river. Section 36 covers the route of bus lines 2 and 3 while section 12 covers the route of all six regular trolleybus lines and IMC bus line 29. Similar to what was done for substation 1 the histograms of the power demand for all six different schedule types for substation 3 are considered.

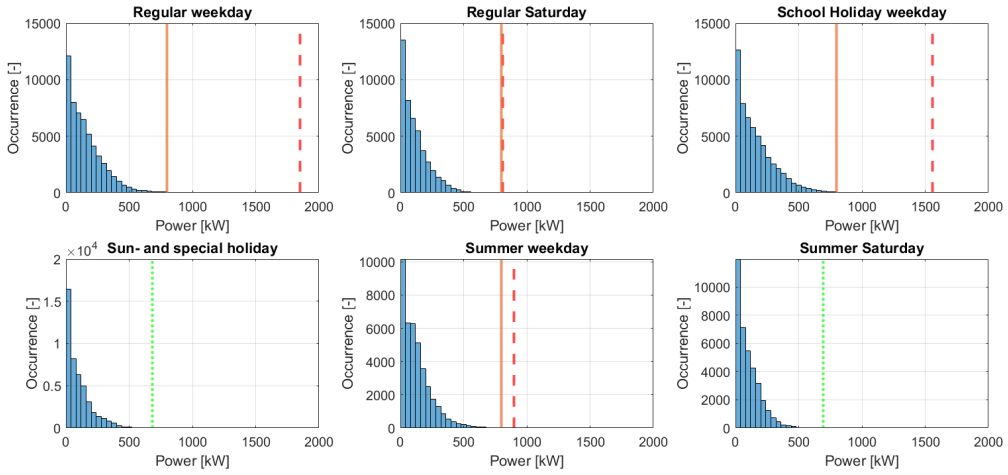

Figure 5.40: Power demands on substation 3 for each type of bus schedule with IMC buses. The maximum power demand on each substation is indicated by a vertical dotted or dashed line. A green dotted line indicates that the limit is never exceeded. A red dashed line indicates that the maximum power demand exceeds the limit. When this is the case the substation limit is indicated by the orange vertical line.

Histograms of the power demand of substation 3 for the different schedule types can be found in Figure 5.40. Again both sun- and special holiday and Summer Saturday schedules do not have power demand issues. The issues occur in the four other schedule types. The full day power demands with IMC buses and charging of these schedule types are shown in Figure 5.41.

Compared to the full day power demands of substation 1 it seems that the there is a relatively low occurrence of breaches. The size of the breaches in some cases is however very large. These high peaks only occur on regular weekday and school Holiday weekday schedules. The breaches on a regular Saturday and Summer weekday are tame in comparison. It would not be reasonable to resize the substation for these high peaks as the highest peak is more than twice the size of the current power limit of 800 [kW].

Again, the effect of excluding the charging power on the relevant section is considered. In Figure 5.42 the highest peaks from Figure 5.41 do disappear. What is left however is a handful of breaches that exceed 1000 [kW]. The highest peak left occurs on a School Holiday weekday and has a value of 1370 [kW]. Where temporary charging power restriction on substation 1 seems like a suitable solution, here on substation 3 this solution does not entirely satisfy.

5.6. Substation power demand for different charging powers

In the full grid analysis for a whole year maximum power demands that exceeded the substation power limit came to light. This was caused by the power demand increase due to the addition of IMC bus lines. It was suggested that limiting battery charging on substations where power breaches occur could be mitigated by increasing the battery charging power on other substations (i.e. peak shaving).

By looking at the results of five different simulations of the power demand on substations where IMC buses drive it can be found if this peak shaving is feasible for the four IMC bus lines considered. The five different simulations are, in order:

- Without IMC buses but with all six regular trolleybus lines.
- IMC bus lines are included but batteries are not charged on the section.

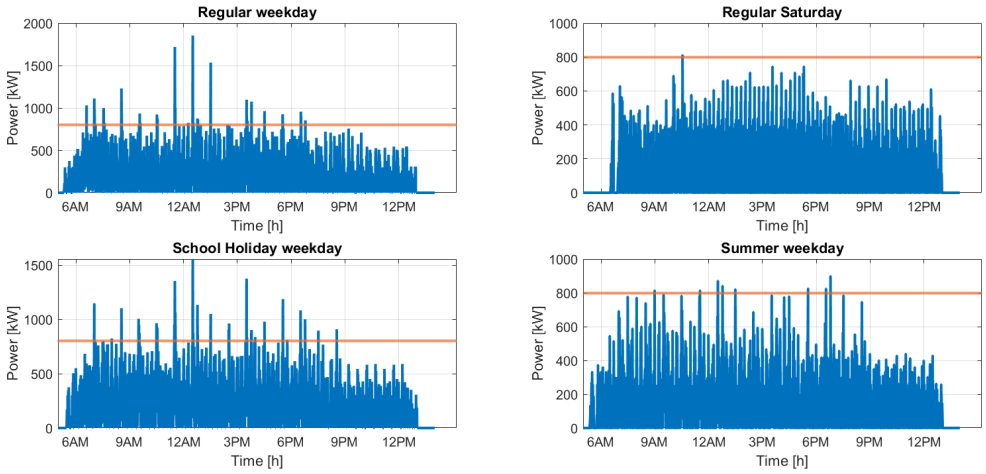

Figure 5.41: Full day power demand of substation 3 for four different bus schedule types with IMC buses. The 800 [kW] limit (orange horizontal line) is exceeded more than once for these schedule types.

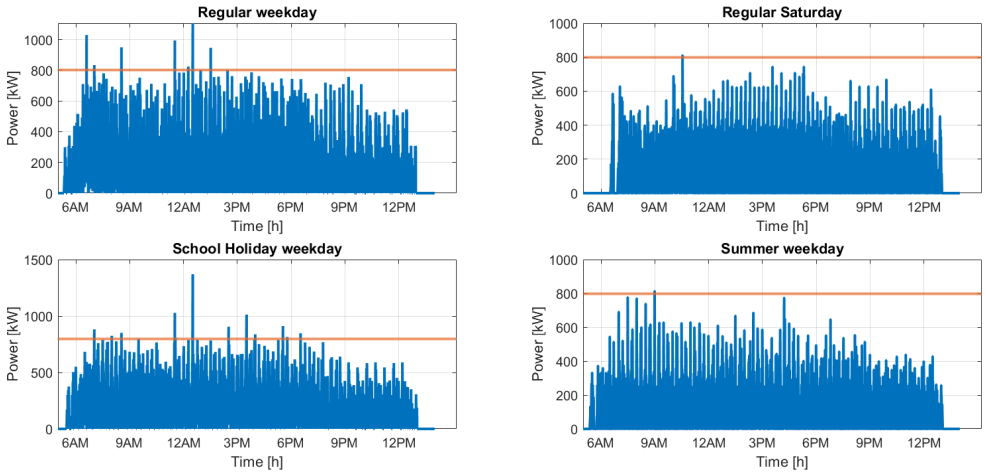

Figure 5.42: Full day power demand of substation 3 for four different bus schedule types with IMC buses without charging. Without charging the 800 [kW] limit (orange horizontal line) is exceeded just once and it happens on the School Holiday weekday schedule.

- All bus lines included and battery charging at 100 [kW] while stopped and 150 [kW] while moving. These are values currently in use Gdynia.
- All bus lines included and battery charging at 200 [kW] while stopped and 300 [kW] while moving. These are values currently in use in Solingen.
- All bus lines included and battery charging at 200 [kW] while stopped and 500 [kW] while moving. These are the values used in Solingen but with an increased maximum of 500 [kW] while moving which takes into account the maximum demand of Kiepe IMC-500 technology.

The results of these simulations can be found in Figure 5.43 and Figure 5.44. Power demand throughout the day is shown in blue while the substation limit (i.e. 800 [kW] for all substations except substation 4 which is set to 1800 [kW]) is indicated with an orange dashed line. The substations (i.e. 1 to 5, 9, 10 and 12) are the eight substations which deliver power to the four IMC bus lines (i.e. 4, 13, 29 and 352) considered in this thesis.

Across the board an increase in power demand can be observed when looking from left to right. For substations 2, 9 and 10 this power demand increase is relatively small. On the opposite end we have substations 1 and 4 which show drastic increases. Battery charging of IMC buses waiting for their next trip at Arnhem CS

even cause the power demand for substation 4 to constantly be above zero from early in the morning to at least 7PM. Substations 3, 5 and 12 show power demands that do increase quite a lot but this mostly shows up as short peaks instead of a constant increase.

This indicates that substations 2, 9 and 10 could supply to buses with a higher charging power to compensate for a decrease in charging power on other sections. It is therefore good to know if each of the four IMC bus lines makes use of both types of substations (i.e. substations that need their power demand decreased and substations that can take a higher charging power). Combinations of the relevant substations will be considered for each of the IMC bus lines.

The first IMC bus line considered is bus line 4. It makes use of substations 4 and 9. It can be seen that substation 9 can even take charging powers of 500 [kW] without exceeding the power demand limit too much. For substation 4 this is not the case. Charging powers on substation 4 should not be increased above the 100 [kW] / 150 [kW] combination. If needed bus line 4 can mitigate battery charging from substation 4 to 9.

Bus line 13 makes use of substations 2 and 4. The results indicate that substation 2 can take charging power at the 200 [kW] / 300 [kW] combination safely while one step above that the power breaches become severe. If needed bus line 13 can mitigate battery charging from substation 4 to 2.

Bus line 29 makes use of substations 2, 3, 4, 5 and 10. The large peaks that can be found for simulations with battery charging for substations 3 and 5 should be mitigated. Both substations 2 and 10 offer this possibility at the 200 [kW] / 300 [kW] charging power combination.

Bus line 352 makes use of substations 1, 4 and 12. As substation 1 shows power limit breaches even at low charging powers the charging power should potentially be mitigated to another section. However, both substations 4 and 12 also show power limit breaches with battery charging. For this IMC bus line it might be difficult to find a good way to mitigate charging powers.

In these observations it became obvious that for three of the four IMC bus lines there is a clear potential for mitigation battery charging from one substation to another in order to decrease power demand breaches. This promise could be further investigated by looking into dynamic charging in future works.

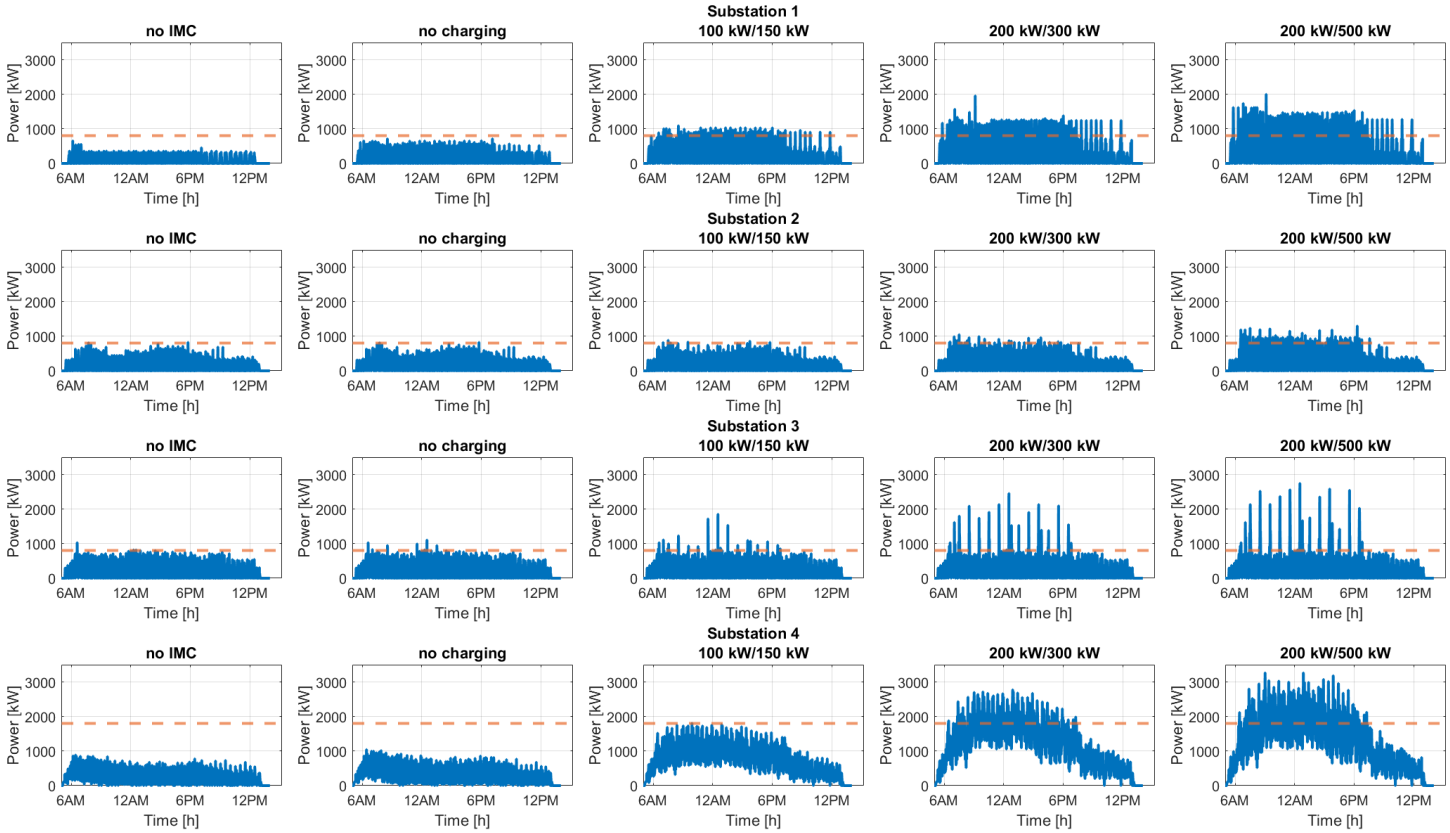

Figure 5.43: Power demand on substations 1, 2, 3 and 4 on a regular weekday for five different simulations. The left most simulation is with only regular trolleybuses (i.e. no IMC buses). Second from the left is with all buses but no battery charging. The other three simulations are with charging, but at different levels. These levels are 100/150 [kW], 200/300 [kW] and 200/500 [kW] for stopped/moving respectively.

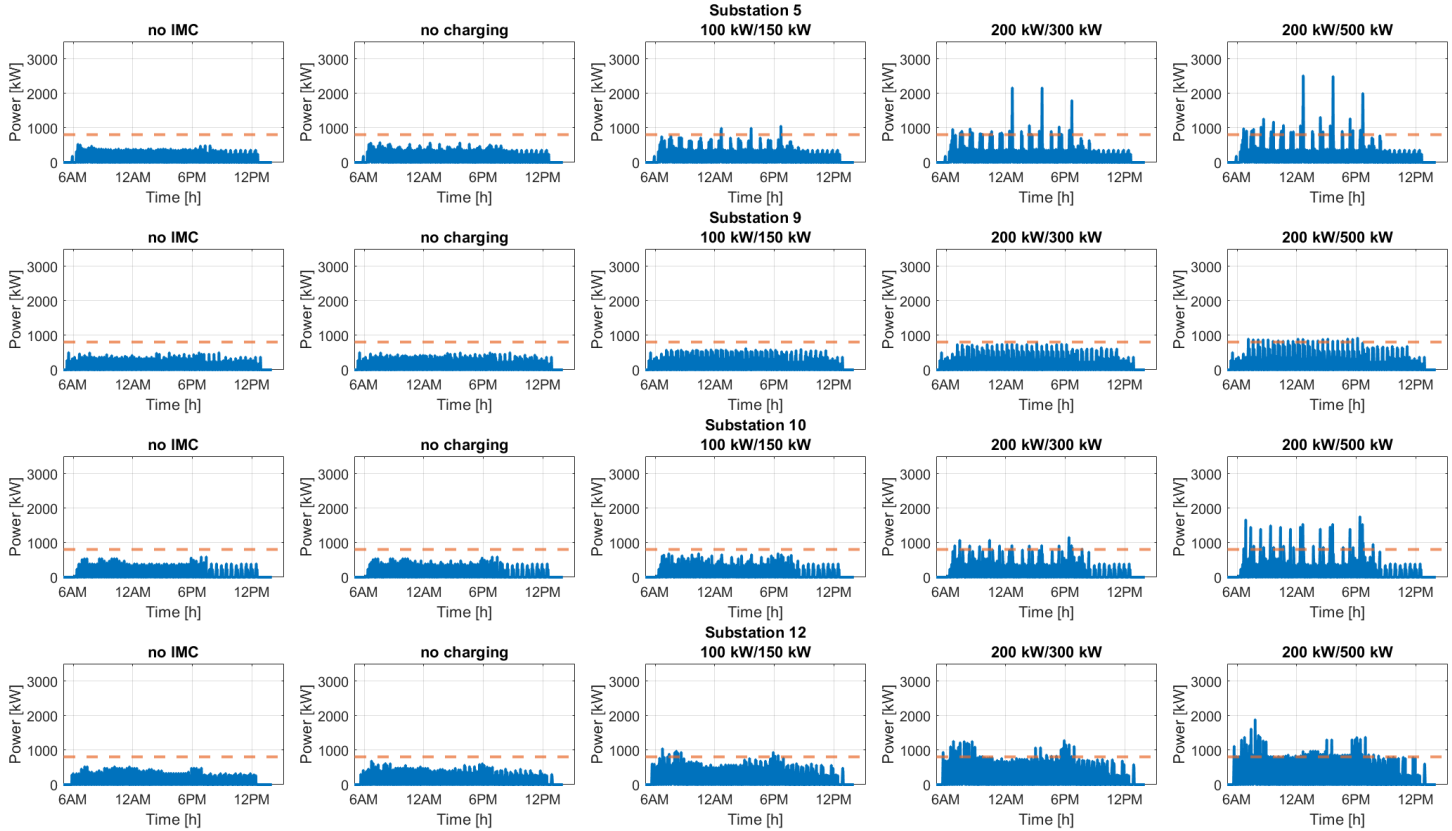

Figure 5.44: Power demand on substations 5, 9, 10 and 12 on a regular weekday for five different simulations. The left most simulation is with only regular trolleybuses (i.e. no IMC buses). Second from the left is with all buses but no battery charging. The other three simulations are with charging, but at different levels. These levels are 100/150 [kW], 200/300 [kW] and 200/500 [kW] for stopped/moving respectively.

6

Conclusion and future works

This chapter summarises the thesis and the conclusions. Next, recommendations on future works are offered which can be used to elaborate on the work performed in this thesis.

6.1. Conclusion: energy approach

By varying the mass parameter in the trolleybus model provided by HAN trips performed by buses with different masses could be simulated. This was done specifically to find the traction energy increase needed for IMC buses as the on-board traction battery resulted in a higher mass. It was found that the addition of a traction battery to a regular trolleybus can result in an increase of traction energy of up to 10%. This number was found for the addition of a 500 [kWh] traction battery.

Regenerative braking energy generation was also investigated. Studying the measurement data of 24 trips of Arnhem trolleybuses resulted in finding that the electric motors of the bus generate on average 0.53 [kWh] for every kilometre driven. This was compared to the average traction energy consumption of 1.68 [kWh/km]. Simplifying this it can be said that on average for every 1 [kWh] the bus needs for traction it also generates 0.3 [kWh] by regenerative braking.

The preceding points added up indicate that an IMC bus can be more energy efficient compared to a regular trolleybus even when taking into account the increase in traction power needed because of slightly higher mass because of the traction battery. For this conclusion it should be assumed that IMC buses can make near-optimal use of regenerative braking, while most braking energy of regular trolleybuses is lost. This is especially the case in low traffic sections where regenerative braking is not shared between trolleybuses and would be wasted instead. Further research could prove that it would be beneficial to overall energy efficiency to convert all current trolleybus lines to IMC buses.

The next topic that was discussed in the energy approach of the research was about the picked up energy of IMC buses. It was found that traffic density can have a large effect on this picked up energy. If a bus has to come to a halt often it will be able to pick up more energy. An IMC bus moving through a charging corridor too quickly because of low traffic might not pick up enough energy for its next round trip.

In other words, the effect of average velocity on picked up energy should not be assessed without taking into account the move-to-stop ratio. This means that, for a certain given route, it is not possible to define a coverage length ratio without defining the position of the charging corridor. A corridor with low traffic/high velocity will be less suited for charging than vice versa.

6.2. Conclusion: Arnhem case study

The Arnhem case study started with looking at the total energy demand on a typical day for a simulation without and with IMC buses. A more than 50% increase of total energy consumption did not come as a surprise. Comparison of the amount of transmission losses in both cases was more interesting as it was shown that in both cases these losses accounted for 2.5% on average.

This contradicted the hypothesis that the relative contribution to total energy demand of transmission losses would be higher when introducing IMC buses to the model. This was predicted both because the IMC buses

are concentrated on fourteen of the 40 sections and because IMC buses have a higher average power demand resulting in higher peak power demands. Instead what was found is that because a lot of the charging occurs relatively close to feed-in points (i.e. while buses are stopped at bus stops) the losses were kept low. This positive outcome led to the advice that in order to keep transmission losses low, feed-in points should be close to important stops, most importantly the trolleybus plaza at Arnhem CS, when IMC buses are implemented.

The remainder of the Arnhem case study went into the limits of the trolleygrid. The first limit discussed was the maximum power demand which was 800 [kW] for each substation. A first analysis of power demand by including/excluding IMC bus line 352 showed that in the case without IMC buses the power demands stayed within limits. Introducing IMC buses resulted in periodic peaks of up to 1200 [kW] in substation 1. Running the simulation with IMC line 352 but without battery charging on substation 1 it was found that these peaks could be decreased to a little over 800 [kW]. This showed the potential for smart charging for peak shaving. By in some way anticipating peaks in power demand and temporarily stopping the battery charging of buses on the underlying sections these peaks can be mitigated.

Further power demand analysis showed that substations 1, 2, 3 and 12 have breaches in the substation power limits when als IMC bus lines are added. This means that on all those substations and underlying sections some alterations or mitigations are necessary in order to successfully implement the range extension IMC buses. It is suggested that either the capacity of substations is increased, schedules are adjusted to one another to avoid peaks and/or the charging power of IMC buses is limited on those sections during heavy traffic hours.

Based on minimum voltage analysis section 12, 26, 29 and 30 were found to drop below the 500 [V] voltage threshold during normal IMC operation. At this point the safety mechanism inside the buses will activate which makes the buses unable to draw their required power. The most worrisome results were found in section 12. Even without IMC buses a minimum was found of 443 [V].

Introducing IMC buses made it so that at some points in time this value dropped to 400 [V]. This is the lowest value that can occur as a safety mechanism in the bus will shut off the power connection at that point. On the one side this indicated that action should be taken on section 12 specifically. Another way to look at this is that the practicality of IMC buses is beneficial to this situation. These buses make it possible to quickly switch to autonomous (i.e. battery mode) operation in order to temporarily alleviate the trolleygrid whenever a heavy traffic situation occurs on one of the sections.

Current analysis was performed by comparing the maximum currents on each section to the current-carrying capacity of the overhead wires. Sections 5 and 12 showed values above the 1600 [A] limit because of IMC bus addition. Section 12 was found to be problematic in the voltage analysis as well. For this section it can be especially important to limit charging powers at times with high traffic.

Section 5 is the section where most buses stop for longer periods of time as it contains the trolleybus plaza at Arnhem CS. IMC buses that stop here will draw high power continuously in order to charge their batteries. Excluding battery charging in the simulation showed that this completely solves this problem as current levels again stay within limits. However, as buses can typically have 15 minutes of wait time there, excluding battery charging there can heavily decrease the amount of energy picked up. This decreases the viability of IMC implementation. A further investigation on the limitations of IMC bus battery charging on section 5 in particular could be necessary.

Another current analysis was done by looking at short circuit protection values. Based on this short circuit current protection analysis it was found that sections 12, 18, 25, 26, 29, 30, 32, 39 and 42 do not meet the safety requirement that is asked for during emergencies when IMC buses are added. However, the bus operator has stated that this safety requirement is one that is not expected to be an issue [29]. On top of that, IMC buses are especially suited to disconnect from the trolleygrid and not draw power from it in case of emergency.

Based on maximum current analysis it was found that the maximum currents in sections 12 and 18 exceed the short circuit safety limits during normal operation with IMC buses. Without resolution this would mean that the safety mechanism might be falsely triggered. A costly way to resolve this is by adding feed-in points to the supply sections and/or dividing the sections into smaller sections.

6.3. Recommendations on future works

As mentioned in the conclusion of the energy approach it could be interesting to, instead of adding 'converted' CNG buses as IMC buses to the simulated Arnhem trolleygrid, convert all regular trolleybuses in the

simulation to IMC buses. By comparing this new situation to the regular situation proof can be found of the hypothesis that a complete conversion of the trolleybus fleet to IMC buses will result in a significant energy reduction.

The research performed in this thesis was based on a set of fixed velocity profiles. Therefore parameters that could be further investigated are the bus velocity and stop times. Playing around with these two parameters can provide further understanding of the cause of high variability in amount of energy picked up by an IMC bus.

The Arnhem case study was performed with a grid model with unilateral sections. Most sections of the Arnhem trolleygrid are connected to a neighbouring section which results in a bilateral supply. So in order to more closely approximate reality the same simulations could be performed with a bilateral supply grid model.

By looking at substation power demand for increasing values of charging power it was found that some substations can supply high amounts of charging power on top of other power demands. The opposite is true for other substations as some are already reaching power supply limits without IMC bus implementation. Setting a fixed amount of maximum charging power for all IMC buses on the grid is therefore not optimal. Instead, further works could investigate the possibility of dynamic charging and employing different charging powers for each substation. Dynamic charging could for instance mean that IMC buses will vary their battery charging power based on their voltage. Different charging powers for each substation could be based on the amount of traffic on each of the corresponding sections (i.e. lowering charging powers on high traffic sections and vice versa).

A

Arnhem trolleybus measurements

HAN University has performed measurements on all six trolleybus lines in Arnhem in the period from 13-12-2018 to 22-01-2019. We received a total of 24 measurement data files from HAN University of this to use for research purposes. This includes four data files for each of the six lines, two for each direction of which one has the measurement with the lowest energy consumption for that line and direction and the other with the highest energy consumption for that line and direction. Table A.1 Contains an overview of the general information of these trips and energy consumptions.

With the new IMC bus two more sets of measurements were taken. The first set was measured on March 4th 2019 and started with a trip from Oosterbeek to Velp in trolleymode (i.e. connected to the grid) and a return trip in batterymode right after. The second set of measurements was performed on March 6th 2019 which started with a trip from Schuytgraaf to Presikhaaf in batterymode and a return trip in trolleymode after this. General information on these trips and energy consumptions can be found in Table A.2.

Table A.1: General information and energy consumption values obtained from measurement data of all six Arnhem trolleybus lines [35]

			V_{av} [m/s]	d_{trip} [km]	t_{trip} [s]	e_{trac} [kWh/km]	e_{aux} [kWh/km]	e_{comb} [kWh/km]	e_{total} [kWh/km]
line 1	O2V	min	4.909	11.86	2414	1.0791	1.0377	2.1168	2.1265
		max	4.4723	11.60	2592	1.2819	1.7672	3.049	3.0596
	V2O	min	4.5071	11.76	2608	1.3005	1.051	2.3515	2.3615
		max	4.7685	11.54	2419	1.6169	1.6825	3.2994	3.3091
line 2	AC2DLW	min	6.1214	8.56	1398	0.9329	1.0303	1.9633	1.9707
		max	5.1892	8.49	1635	1.2102	1.3977	2.6079	2.6172
	DLW2AC	min	6.0349	8.34	1381	0.985	1.0951	2.0801	2.0883
		max	5.494	8.31	1511	1.1946	1.7777	2.9723	2.9814
line 3	BZ2HD	min	4.4987	10.37	2304	0.6857	1.1661	1.8519	1.8622
		max	4.5902	10.47	2279	1.1649	1.3471	2.512	2.522
	HD2BZ	min	4.1902	9.92	2366	1.276	1.2103	2.4864	2.4967
		max	4.563	9.98	2187	1.4289	1.8123	3.2412	3.2532
line 5	DZ2P	min	5.8909	14.14	2399	1.0967	0.6752	1.7719	1.7791
		max	5.2009	14.32	2753	1.0632	1.4948	2.558	2.5676
	P2DZ	min	6.4503	13.95	2161	0.9387	0.9626	1.9013	1.909
		max	4.2962	15.14	3524	1.2115	1.5695	2.781	2.792
line 6	DLW2HAN	min	5.9896	11.99	2001	1.2619	0.9791	2.2411	2.2487
		max	5.9489	11.92	2002	1.3694	1.236	2.6054	2.613
	HAN2DLW	min	5.6489	12.33	2182	0.981	1.2114	2.1924	2.2006
		max	4.7329	11.89	2511	1.0308	1.5532	2.584	2.5938
line 7	G2R	min	5.2446	12.36	2356	0.6868	1.4083	2.095	2.1037
		max	4.2656	12.42	2910	0.9013	1.7295	2.6308	2.6413
	R2G	min	4.9329	12.71	2575	1.2286	1.4588	2.6873	2.6972
		max	4.6821	12.71	2714	1.5623	1.5443	3.1067	3.1172

Table A.2: General information and energy consumption values obtained from measurement data of two sets of test trips with IMC buses in Arnhem [35]

		V_{av} [m/s]	d_{trip} [km]	t_{trip} [s]	e_{trac} [kWh/km]	e_{aux} [kWh/km]	e_{comb} [kWh/km]	e_{total} [kWh/km]
line 1	O2V (trolley)	6.4196	9.41	1465	0.9379	1.4076	2.3455	2.381
	V2O (battery)	7.6079	11.72	1540	1.1079	0.1356	1.2435	1.2491
line 5	P2DZ (trolley)	6.8858	14.03	2037	0.9015	1.1287	2.0303	3.2893
	DZ2P (battery)	8.059	15.08	1870	0.8894	0.1202	1.0096	1.0156

B

Arnhem trolleybus fleet

The trolleybus fleet in Arnhem comprises 40 single-articulated buses. All vehicles were manufactured by Hess while the electric components were manufactured and supplied by Vossloh Kiepe. Nine of the vehicles are older Swisstrolley 3 (ST3) models which were put into service in 2009. The other 31 buses are Swisstrolley 4 (ST4) models and were put into service over several years from 2013 to 2017. Two of those were repurposed into IMC buses by replacing the diesel APU with a 30 kWh traction battery. All of these vehicles are single-articulated buses with a length of 18m. The electrical equipment of the vehicles was manufactured by Kiepe Electric GmbH. The older models (ST3) have two driven axles with an 160 kW engine each and one diesel APU of 50/80 kW in the back of the bus. The newer ST4 has a single driven axle with a 240 kW engine and a 50 kW diesel APU in the back. A complete overview of the buses can be found in Table B.1.

Table B.1: Information on all buses in the Arnhem trolleybus fleet. Most information was found in [36] and [37]. Mass was found on OVI [2].

serial number	manufacturer	type	designation	license plate	start of service	passengers			empty mass	traction power
						seated	standing	wheelchair		
5234	Hess	Swisstrolley 3	BGT-N2C	BX-DT-41	16-10-2009	46+2	90	2	18010	Two driven axles, 2x 160 kW engine, 50 or 80 kW APU (?)
5235				BX-FN-38	16-10-2009					
5236				BX-FN-39	6-11-2009					
5237				BX-FP-72	3-11-2009					
5238				BX-FP-73	16-10-2009					
5239				BX-FP-74	27-10-2009					
5240				BX-FT-74	30-10-2009					
5241				BX-FT-75	21-11-2009					
5242				BX-FT-76	2-11-2009					
5243		Swisstrolley 4	BGT-N1D	07-BBX-3	27-6-2013	45+2	86		18270	Single driven axle, 240 kW engine, 50 kW APU
5244				08-BBX-3	27-6-2013					
5245				09-BBX-3	27-6-2013					
5246				11-BBX-3	27-6-2013					
5247				12-BBX-3	27-6-2013					
5248				13-BBX-3	1-7-2013					
5249				16-BBX-3	1-7-2013					
5250				19-BBX-5	8-7-2013					
5251				18-BBX-5	8-7-2013					
5252				17-BBX-5	7-7-2013					
5253				16-BBX-5	11-7-2013					
5254				50-BGJ-7	26-9-2015	44+2	88			
5255				52-BGJ-7	26-9-2015					
5256				54-BGJ-7	26-9-2015					
5257				55-BGJ-7	3-10-2015					
5258				60-BGJ-7	7-10-2015					
5259				82-BGX-2	23-3-2016					
5260				81-BGX-2	24-3-2016					
5261				83-BGX-2	30-3-2016					
5262				84-BGX-2	2-4-2016					
5263				85-BGX-2	7-4-2016					
5264				41-BJG-6	21-3-2017					
5265				47-BJG-6	21-3-2017					
5266				47-BJH-4	25-3-2017					
5267				89-BJJ-3	8-4-2017					
5268				90-BJJ-3	7-4-2017					
5269				48-BJK-2	15-4-2017					
5270				58-BJK-2	15-4-2017					
5271				60-BJK-2	22-4-2017					
5272		Swisstrolley 4*		41-BJK-8	*26-4-2017	42+2	86		18665	No diesel APU but 30 kWh battery
5273				43-BJK-8	*26-4-2017					

C

Drive cycle

C.1. Drive cycle construction

Initial demand for creation of drive cycles that match certain criteria stems from the desire to test motor vehicle emission levels [22]. To test for these emission limits test cycles have to be performed that are both reproducible and representative of real-world driving. The drive cycle should also be fully controlled and be practical in the sense that it should be long enough to include all types of operating conditions but not too long to preserve costs. It is also important to keep in mind that vehicles within the intended vehicle category should be able to perform the cycle pattern. All these criteria are put in place to be sure that the actual emissions and power/energy consumption of a vehicle is accurately predicted before it is put onto the road. For conventional ICE vehicles this includes both cold starting and hot starting as emissions might be different for those cases. It should also include representative parts of acceleration, deceleration, cruise and idling sections. Different driving schedules like urban, sub-urban and extra-urban should also be included.

Two distinct types of synthetic drive cycles can be constructed: modal and transient. Modal cycles can be defined by a sequence of driving modes (i.e. accelerating, decelerating, cruising, idling in some order). Visually such a velocity profile is shaped like a (set of) trapeziums as a constant acceleration and deceleration form the sides while the top of the trapezium is formed by a constant cruise speed. This is the type of driving cycle that first emerged for motor vehicle certifying purposes. The discrepancy between power/energy consumption of this type of drive cycle and real-world drive cycles is relatively high (e.g. a real-world drive cycle has more and steeper accelerations and no extended periods of constant cruise speed).

The transient cycle, with its more realistic curvature, was quickly deemed as superior for realistic emission results. Emissions are found to be especially high during transient behaviour and the instantaneous acceleration change in modal cycles does not show this [22]. The same lack of similarity can be found in traction power demand. Figure C.1 visualises the differences between a modal and transient drive cycle.

The construction of a realistic drive cycle can be done through different methodologies . The four commonly used methodologies in recent times are: micro-trip cycle construction, segment-based cycle construction, cycle construction based on pattern classification and stochastic modal cycle construction.

Micro-trip cycle construction as seen in [12, 43] is a method in which micro-trips are stitched together to form a complete cycle. A micro-trip is a trip between two idle phases. These micro-trips is gathered from relevant measured drive cycles to ensure realism.

Segment-based cycle construction like in [21] stitches together segments instead of micro-trips. In this context trip segments are defined by certain characteristics like traffic conditions or type of road. By putting together different types of segments a cycle can be produced that represents a multitude of realistic situations.

Cycle construction based on pattern classification as seen in [4, 30] makes use of kinematic sequences. These sequences, which are snippets of real drive cycles, are first classified into classes that can be described based on classes (e.g. mean and standard deviation of velocity and acceleration). Stitching kinematic sequences from desired classes in a random order results in a unique drive cycle that represents those classes.

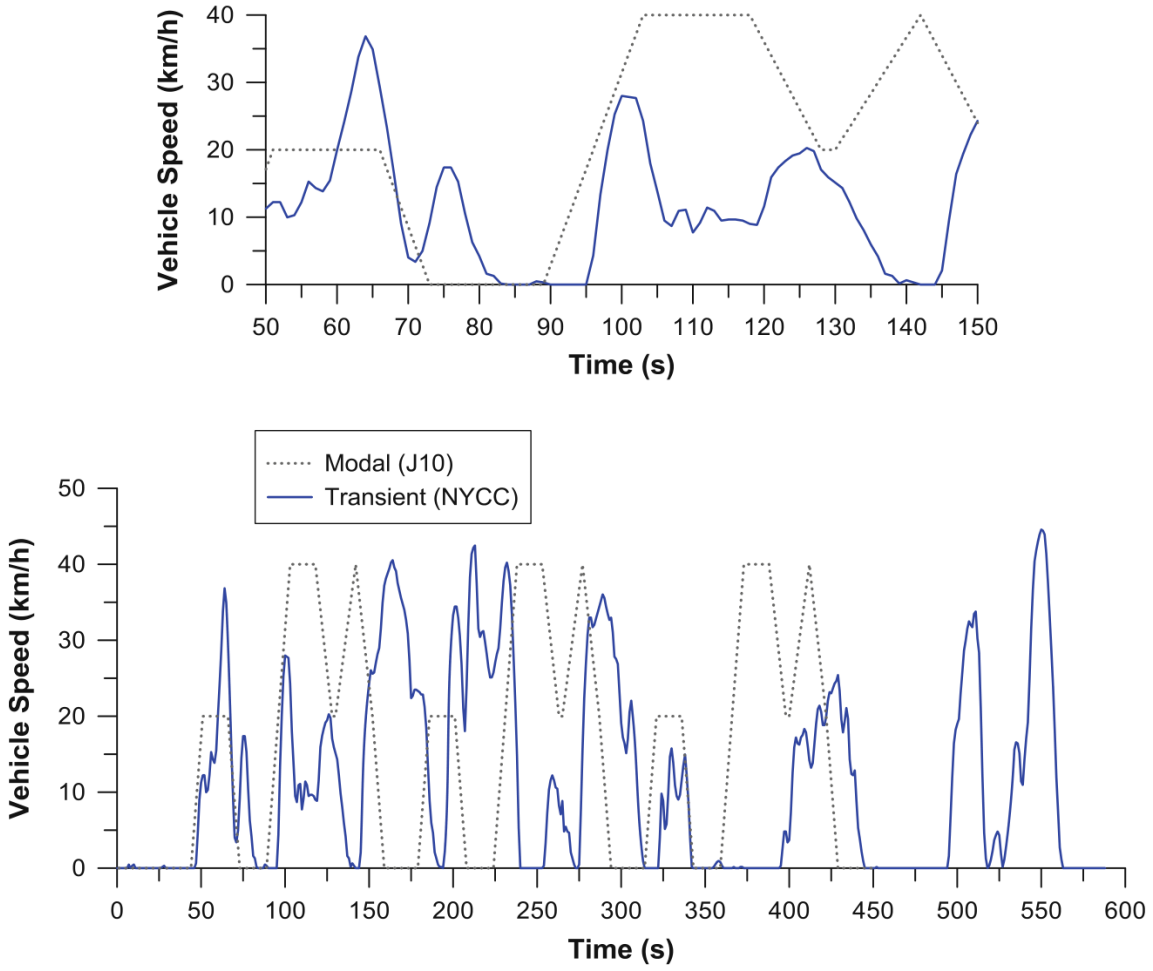

Figure C.1: Comparison between a modal (dotted line) and transient (solid line) drive cycle. The bottom graph shows three repetitions of the short J10 modal cycle and the NYCC transient cycle. The top graph zooms in on 50-150 seconds [22].

Stochastic modal cycle construction like in [5, 24, 27] is performed in four steps. Measured drive cycles are again divided in snippets but this time based on driving modes (i.e. cruising, idling, accelerating, decelerating). The modes are further partitioned by for instance defining different speeds (e.g. 0-5, 5-15, 15-30, 30+ km/h) and different acceleration rates (e.g. 0-.15, .15-.60, .60-1.0, 1.0+ m/s²). Next, a transition matrix is created that defines the likelihood of succession from one mode to the other. By applying Markov chain a complete drive cycle can then be stitched together from these snippets.

The resulting synthetic drive cycles from all four of these methodologies are of the transient type and represent realistic driving of the sourced drive cycles. When instead the drive cycle should satisfy certain (combinations of) criteria (e.g. a specific acceleration or percentage time spent in cruise) then the cycle can be engineered for that specific purpose. This type of cycle is called an engineering cycle [22]. It can be used to force specific conditions and can be created without the use of a measured drive cycle database and modal-type cycle (i.e. simple straight-line construction) can be used.

C.2. Drive cycle assessment

A synthetic drive cycle can be assessed for similarity to the source real-world drive cycles by comparing drive cycle metrics. Some common metrics used for comparison are [22]:

- Trip duration
- Trip distance
- Average/maximum velocity
- Average/maximum acceleration
- Standard deviation of velocity and acceleration
- Speed acceleration (frequency) distribution (SAFD)
- Idling
- Percentage of time spent in different driving modes
- Relative positive acceleration (RPA)
- Positive kinetic energy (PKE)
- Vehicle specific power (VSP)

The above list starts off simple with the total time and distance of a trip. Velocity and acceleration throughout a trip can be defined through both averages and maximums. The distribution of these metrics is further identified by the standard deviation from the average. A more thorough visualisation of this distribution is done through the speed acceleration (frequency) distribution (e.g. a histogram that shows the distribution of acceleration occurrence). Idling is an especially important metric for public transit buses and can be defined in a number of ways (e.g. stops per km, total number of stops, stop duration). The same can be said for percentage of time spent in the different driving modes (i.e. acceleration, deceleration, idle, (fast) cruise, coast/slow cruise).

The last three metrics are relatively complex properties of the drive cycle. These metrics give an indication of the traction power demand. RPA and PKE are closely related as both indicate how harsh the cycle is (i.e. a high amount of velocity changes and high acceleration values). RPA [ms^{-2}] is given by Equation C.1,

$$RPA = \frac{1}{d_{\text{trip}}} \int_0^{t_{\text{trip}}} V_{\text{bus}} \cdot a_{\text{bus}} \, dt \tag{C.1}$$

Where, d_{trip} [m] is the trip distance and t_{trip} [s] is the trip duration. V_{bus} [m/s] is the bus velocity and a_{bus} [ms^{-2}] is the acceleration. In the integration only the time steps should be used in which positive acceleration occurs. Low values of RPA indicate that accelerations are few and/or moderate while high values of RPA indicate that accelerations occur often and/or are steep in nature. This also means that modal cycles will

generally have lower RPA values than transient cycles. Values of 0 to 0.10 are considered low, while a value of 0.20 is on the high side for modal cycles. For transient cycles values

Positive kinetic energy is a metric of similar nature as RPA. It indicates the amount of acceleration work that is performed throughout the drive cycle. PKE [ms^{-2}] is given by Equation C.2,

$$PKE = \frac{1}{d_{\text{trip}}} \sum_{i}^{t_{\text{trip}}} ({V_{\text{bus},i}}^2 - {V_{\text{bus},i-1}}^2) \tag{C.2}$$

Where again, d_{trip} [m] is the trip distance, t_{trip} [s] is the trip duration and V_{bus} [m/s] is vehicle velocity. Only instances of time steps where $V_{\text{bus},i} > V_{\text{bus},i-1}$ are to be included to get to the positive kinetic energy which is why it is similar to RPA. PKE therefore is an indication of the required acceleration work.

Vehicle specific power is a vector that indicates how high the traction power of a vehicle that runs the drive cycle is throughout the trip. This is different from RPA and PKE which is just one value for a drive cycle. VSP is given by Equation C.3,

$$VSP = \frac{P_{\text{traction}}}{M_{\text{bus}}} = \frac{(F_{\text{roll}} + F_{\text{aero}} + F_{\text{gradient}} + F_{\text{inertia}}) \cdot V_{\text{bus}}}{M_{\text{bus}}} \tag{C.3}$$

Where, P_{traction} [kW] is the traction power at a certain point in time and M_{bus} [kg] is the vehicle mass. The traction power is composed of four forces on the vehicle (i.e. rolling, aerodynamic, gradient and inertia forces) which are multiplied with velocity (V_{bus}) to get power. By dividing it by the vehicle mass we get VSP [kW/kg]. A positive VSP means that the engine should provide power while a negative VSP indicates that either mechanical brakes or regenerative braking should be applied.

Bibliography

[1] GVB neemt eerste elektrische bus op in dienstregeling | OVPro.nl. URL https://www.ovpro.nl/bus/2020/04/03/gvb-neemt-eerste-elektrische-bus-op-in-dienstregeling/.

[2] OVI: RDW Kentekencheck. URL https://ovi.rdw.nl/default.aspx.

[3] StatLine - Verkeersprestaties bussen; kilometers, leeftijdsklasse, grondgebied. URL https://opendata.cbs.nl/statline/#/CBS/nl/dataset/80589ned/table?fromstatweb.

[4] Michel André. The ARTEMIS European driving cycles for measuring car pollutant emissions. *Science of the Total Environment*, 334-335:73–84, 2004. ISSN 00489697. doi: 10.1016/j.scitotenv.2004.04.070.

[5] Ali Ashtari, Eric Bibeau, and Soheil Shahidinejad. Using large driving record samples and a stochastic approach for real-world driving cycle construction: Winnipeg driving cycle. *Transportation Science*, 48 (2):170–183, 2014. ISSN 15265447. doi: 10.1287/trsc.1120.0447.

[6] Barnimer Busgesellschaft. Barnimer Busgesellschaft, 2020. URL https://bbg-eberswalde.de/.

[7] Mikołaj Bartłomiejczyk. Practical application of in motion charging: Trolleybuses service on bus lines. In *Proceedings of the 2017 18th International Scientific Conference on Electric Power Engineering, EPE 2017*. Institute of Electrical and Electronics Engineers Inc., 6 2017. ISBN 9781509064052. doi: 10.1109/EPE.2017.7967239.

[8] Mikołaj Bartłomiejczyk. Bilateral power supply of the traction network as a first stage of Smart Grid technology implementation in electric traction. *MATEC Web of Conferences*, 180, 2018. ISSN 2261236X. doi: 10.1051/matecconf/201818002003.

[9] Mikołaj Bartłomiejczyk. Dynamic charging of electric buses. *Dynamic charging of electric buses*, 2018. doi: 10.2478/9783110645088.

[10] Mikołaj Bartłomiejczyk and Marcin Połom. Spatial aspects of tram and trolleybus supply system. *Proceedings of the 8th International Scientific Symposium on Electrical Power Engineering, ELEKTROENERGETIKA 2015*, pages 211–215, 2015.

[11] Roger Bedell. A practical, 70-90% electric bus without overhead wires. *24th International Battery, Hybrid and Fuel Cell Electric Vehicle Symposium and Exhibition 2009, EVS 24*, 3:1543–1549, 2009.

[12] Lorenzo Berzi, Massimo Delogu, and Marco Pierini. Development of driving cycles for electric vehicles in the context of the city of Florence. *Transportation Research Part D: Transport and Environment*, 47: 299–322, 2016. ISSN 13619209. doi: 10.1016/j.trd.2016.05.010.

[13] BRENG. Arnhem bus timetables, 2020. URL https://www.breng.nl/nl/resultaten/dienstregeling.

[14] Les Brunton. The trolleybus story. *IEE Review*, 38(2):57, 1992. ISSN 09535683. doi: 10.1049/ir:19920024.

[15] Les Brunton. Why not the trolleybus? *IEE Colloquium (Digest)*, (50):25–32, 2000. ISSN 09633308. doi: 10.1049/ic:20000265.

[16] Martyn Z Chymera, Alasdair C Renfrew, Mike Barnes, and John Holden. Modeling Electrified Transit Systems. *IEEE Transactions on Vehicular Technology*, 59(6):2748–2756, 7 2010. ISSN 0018-9545. doi: 10.1109/TVT.2010.2050220. URL http://ieeexplore.ieee.org/document/5464260/.

[17] Connexxion. Schakelschema bovenleiding trolleygrid Arnhem, 1999.

[18] Electric Mobility Europe. Trolley:2.0 leaflet: New developments of modern trolleybus systems for smart cities, 2018. URL https://www.trolleymotion.eu/trolley2-0/.

[19] European Commission. Proposal for A Directive of the European Parliament and of the Council amending Directive 2009/33/EC on the promotion of clean and energy-efficient road transport vehicles. pages 1–76, 2017. URL https://eur-lex.europa.eu/legal-content/EN/TXT/?uri=CELEX%3A52017PC0653.

[20] evopro. evopro Group, 2020. URL http://www.evopro.hu/en.

[21] Uditha Galgamuwa, Loshaka Perera, and Saman Bandara. A Representative Driving Cycle for the Southern Expressway Compared to Existing Driving Cycles. *Transportation in Developing Economies*, 2(2), 2016. ISSN 2199-9287. doi: 10.1007/s40890-016-0027-4.

[22] Evangelos G. Giakoumis. *Driving and engine cycles*. 2016. ISBN 9783319490342. doi: 10.1007/978-3-319-49034-2.

[23] Bernd Heid, Matthias Kässer, Thibaut Müller, and Simon Pautmeier. The urban electric bus market | McKinsey, 2020. URL https://www.mckinsey.com/industries/automotive-and-assembly/our-insights/fast-transit-why-urban-e-buses-lead-electric-vehicle-growth.

[24] Kobus Hereijgers, Emilia Silvas, Theo Hofman, and Maarten Steinbuch. Effects of using Synthesized Driving Cycles on Vehicle Fuel Consumption. *IFAC-PapersOnLine*, 50(1):7505–7510, 2017. ISSN 24058963. doi: 10.1016/j.ifacol.2017.08.1183.

[25] Seungmin Jeong, Young Jae Jang, and Dongsuk Kum. Economic Analysis of the Dynamic Charging Electric Vehicle. *IEEE Transactions on Power Electronics*, 30(11):6368–6377, 2015. ISSN 08858993. doi: 10.1109/TPEL.2015.2424712.

[26] Hamide Keskin. *The cost-effectiveness analysis of transition from brt system to bi-articulated trolleybus system in Istanbul*. PhD thesis, 2019.

[27] Klaus Kivekäs, Antti Lajunen, Jari Vepsäläinen, and Kari Tammi. City bus powertrain comparison: Driving cycle variation and passenger load sensitivity analysis. *Energies*, 11(7), 2018. ISSN 19961073. doi: 10.3390/en11071755.

[28] R. Kuhne. Electric buses – An energy efficient urban transportation means. *Energy*, 35(12):4510–4513, 2010.

[29] Liandon. Connexxion - Arnhems trolleybusnet Onderzoek bovenleidingnet. Technical report, 2012.

[30] Bingjiao Liu, Qin Shi, Lin He, and Duoyang Qiu. A study on the construction of Hefei urban driving cycle for passenger vehicle. *IFAC-PapersOnLine*, 51(31):854–858, 2018. ISSN 24058963. doi: 10.1016/j.ifacol.2018.10.100.

[31] Samuel Rodman Oprešnik, Tine Seljak, Rok Vihar, Marko Gerbec, and Tomaž Katrašnik. Real-world fuel consumption, fuel cost and exhaust emissions of different bus powertrain technologies. *Energies*, 11(8):2160, 8 2018. ISSN 19961073. doi: 10.3390/en11082160. URL http://www.mdpi.com/1996-1073/11/8/2160.

[32] PRE. Power Research Electronics BV, 2020. URL http://www.pr-electronics.nl/en/.

[33] Bram Scheurwater. *The potential of renewable energy sources for powering of trolleybus grids - An Arnhem case-study*. PhD thesis, 2020.

[34] Szegedi Közlekedési Társaság. Szegedi Közlekedési Társaság, 2020. URL http://szkt.hu/.

[35] Abhishek Singh Tomar, Bram P A Veenhuizen, Lejo Buning, and Ben Pyman. Viability of traction battery for battery-hybrid trolleybus. *EVS32 Symposium*, pages 1–12, 2019.

[36] Trolleyclub NL. Trolleybus Arnhem serie 5234-5242, . URL https://www.trolleyclub.nl/docs/s15-5234-5242.pdf.

[37] Trolleyclub NL. Trolleybus Arnhem serie 5243-5253 / 5254-5258 / 5259-5265 / 5264-5273, . URL https://www.trolleyclub.nl/docs/s16-5243-5273.pdf.

[38] trolley:motion. trolley:motion, 2020. URL https://www.trolleymotion.eu/.

[39] TU Delft. TU Delft, 2020. URL https://www.tudelft.nl/.

[40] TU Dresden. TU Dresden, 2020. URL https://tu-dresden.de/.

[41] University of Gdansk. University of Gdansk, 2020. URL https://pg.edu.pl/.

[42] University of Szeged. University of Szeged, 2020. URL https://u-szeged.hu/english.

[43] Peng Yuhui, Zhuang Yuan, and Yang Huibao. Development of a representative driving cycle for urban buses based on the K-means cluster method. *Cluster Computing*, 22:6871–6880, 2019. ISSN 15737543. doi: 10.1007/s10586-017-1673-y.